Diatoms as indicators of water quality change from drought to flood conditions in the Kruger National Park

RCJ Koen

orcid.org/0000-0002-1583-2972

Dissertation accepted in fulfilment of the requirements for the degree *Master of Science in Environmental Sciences* at the North-West University

Supervisor: Prof JC Taylor

Graduation May 2023

26004534

Declaration

I, (Ruan Koen) hereby declare that all the research done for my master's dissertation titled 'Diatoms as indicators of water quality change from drought to flood conditions in the Kruger National Park' is my own. All the relevant sources have been cited in a complete reference list.

Acknowledgements

Firstly, I want to thank God for giving me the necessary strength, patience and persistence. For without Him, there is little purpose.

I also want to thank the following people for their invaluable contribution:

My Family for their unconditional love and support, for my accomplishments are theirs as well.

Prof. Jonathan Taylor, for the countless hours of meaningful discussions and conversation, for his aspiring mentorship and friendship. You have taught me many things for which I am sincerely grateful.

My colleagues and friends for their support and assistance.

The staff of the Kruger National Park who has made my journey an amazing unforgettable experience. Your stories and wisdom will always be held near my heart.

Abstract

Water as a resource is important for all living organisms and forms the very basis of life. The transportation of water, around the globe, forms the hydrologic cycle. This cycle includes precipitation, evaporation, and transpiration. Anthropogenic accelerated global warming and climate change have altered the timing, magnitude, and frequency by which these elements occur, thereby causing instability in the hydrologic cycle. Natural events such as droughts and floods can occur more frequently with more devastating impact.

South Africa is a water-stressed country that frequently experiences drought due to the low annual precipitation across most of its interior. The country is considered semi-arid and has a growing human population, which places stress on water as a resource for South Africa, since its quality must be suitable for human consumption and use. This limited amount of water is unfortunately subject to anthropogenic pollution and heavy exploitation. Also, there are virtually no natural lentic systems and so our rivers are used for abstraction, by impounding them along their flow direction to improve yield. Rivers and their impoundments therefore serve as major contributors to freshwater for personal consumption as well as for irrigation and industry, and thus, the state of these rivers in terms of water quantity and quality is important with regard to water security.

Changes in seasonal rainfall intensity and duration can also alter the discharge of rivers by changing the contribution to surface water or runoff. Low seasonal rainfall decreases the contribution of surface runoff to discharge, while higher seasonal rainfall increases the surface runoff. El Niño Southern Oscillation (ENSO) influences the amount of seasonal rainfall for the greater interior of South Africa. During El Niño years, South Africa is prone to lower-than-normal summer rainfall and consequently at risk of drought. La Niña in turn creates higher than normal rainfall for South Africa and can increase the risk of floods.

Seasonal rainfall patterns, the ENSO effect, flow regulation, and water abstraction are drivers of riverine flow regime changes. Additionally, wastewater discharge, stormwater discharge and agricultural discharge increase streamflow through a higher contribution of surface water, especially during dry seasons. When the water quantity of a river decreases, there are consequent changes in the water quality as well. Periods of prolonged low streamflow can lead to eutrophic conditions, where surface water temperatures increase, dissolved oxygen concentration decrease, and nutrients and/or pollutants are further increased in concentration

due to less dilution. A prolonged period of increased discharge can also alter water quality by increasing nutrient flux from surrounding agricultural areas. Large amounts of water flowing downstream can also remove much sediment, which holds elements including nutrients, pollutants and/or toxicants. Natural seasonal flooding generally improves water quality by removing toxicants that have been retained in the sediment, thereby ‘flushing’ the system. Habitat scouring can also alter the biotope composition consequently altering ecosystem resilience through niche occupancy. These conditions further complicate the effect of flooding on water quality.

Aquatic biota have proven to be the preferred method for monitoring integrated water quality changes within rivers over time, rather than using once-off chemical and physical analysis. Within aquatic biomonitoring, bioindicator organisms are used to infer the water quality of aquatic ecosystems, in the present study diatoms were used. Diatoms have many advantages as bioindicators, they respond reliably and predictably to a range of pollutants and toxicants. Their short generation time allows for cross-generation studies. Collecting diatoms are also quick and relatively cheap due to their ubiquitous nature, however, the analysis of diatom samples requires specialised equipment and training, and this can add cost to the process due to the time-comsuming nature of the analysis, thereby prohibiting diatoms from being implemented on a greater scale.

The Kruger National Park (KNP) has experienced many years of drought throughout its history, many of which had devastating effects. From 2016 to 2019 the park was still experiencing the devastating effect of a recent drought. From 2020, however, an increase in the annual summer rainfall, due to La Niña was evident, alleviating to a large extent the impact of the drought experienced. La Niña still prevails during 2022, and will likely persist into 2023, thereafter a short return to neutral conditions is expected. The KNP has therefore seen a steady increase in average annual seasonal rainfall from 2018 to 2021 due to the phase shift of El Niño and La Niña. This provides an invaluable opportunity to use diatoms as an inference of water quality change during this period. The use of diatoms in the park is further important since it is on the cusp of entering the biomonitoring arsenal of the park, and this will only increase its efficacy as bioindicator.

Many diatom indices have been developed of which the Indice de Polluosensibilité Spécifique (IPS) was used in the present study, based on previous studies from the same region. The parameter values used for the IPS are based on the autecological preferences of diatom taxa to

ionic composition and organic pollution. Increased levels of nutrients increase the ionic load of water, and consequently also aids in the increase in primary production of a system, leading to eutrophication – also an important component of the IPS calculation.

The IPS index was used to indicate water quality change from 2018 to 2022 within five large perennial rivers within the KNP in terms of ionic composition (electrical conductivity), trophic status and organic pollution. Sites sampled were selected as part of the park's internal monitoring program and most sites were sampled across the entire period.

Most rivers sampled experienced a temporal improvement in water quality from 2018 to 2022, except the Olifants River which experienced a deterioration in water quality over time, possibly due to an increased nutrient load from diffuse sources and/or an increase in point-pollution from the Palabora mining company. Spatially, the water quality for the Sabie River increased with distance downstream, however, from the second last site to the last, water quality severely decreased, although it did improve over time. The Crocodile, Sabie, Letaba and Olifants rivers all exhibited spatial increases in water quality with flow direction, while the Luvuvhu River experienced a decrease in water quality with flow direction.

The IPS index indicated an increase in water quality in terms of ionic composition, trophic state and organic pollution temporally and spatially for the Crocodile, Sabie and Letaba rivers due to the increase in average annual seasonal precipitation across the entire park. The Luvuvhu River exhibited a temporal increase and spatial decrease in water quality, while the Olifants River exhibited a temporal decrease and spatial increase in water quality. These rivers did not respond in a similar fashion to other rivers toward the increase in seasonal rainfall and may suggest the influence of other sources of pollution.

Diatoms were therefore successfully implemented to indicate water quality change in response to increased seasonal rainfall, by using the IPS index. This index was not expressly designed for the purpose of determining water quality changes in response to water quantity changes as a result of rainfall, nevertheless it was successful in this regard. The use of diatoms as indicator organisms is therefore highly recommended within the KNP. The implementation thereof would increase the ease of sampling, and decrease the overall cost of monitoring. It is well established that diatom communities are correlated with water quality variables and, therefore, the further use of physico-chemical analysis in addition to diatom analysis in the park is redundant, unnecessary and costly. Diatoms can, therefore, form part of the biomonitoring tools used in the

KNP, however, as always, it is recommended that multiple bioindicators be used to infer water quality when possible to improve the accuracy of results.

Keywords: Drought, Floods, Diatoms, Water quality, Kruger National Park.

Table of Contents

List of tables

List of figures

List of abbreviations

°C	Degrees Celsius
AMD	Acid Mine Drainage
BDI	Biological Diatom Index
CCA	Canonical Correspondence Analysis
CEC	Council for European Communities index
Cl^-	Chloride
CSIR	Council for Scientific and Industrial Research
DAIpo	Diatom Assemblage Index of Organic Water Pollution
DCA	Detrended Correspondence Analysis
DES	Descy's Method
DIC	Differential Interference Contrast

DO	Dissolved Oxygen
DWAF	Department of Water Affairs and Forestry
DWS	Department of Water and Sanitation
EC	Electrical Conductivity
ECI	Extreme Climate index
ENSO	El Niño Southern Oscillation
GDI	Generic Diatom Index
H_2O_2	Hydrogen peroxide
HCl	Hydrochloric Acid
IPS	Indice de Polluosensibilité Spécifique
$KMnO_4$	Potassium permanganate
KNP	Kruger National Park
L	Litre
LM	Light Microscopy
Na^+	Sodium
NAEHMP	National Aquatic Ecosystem Health Monitoring Programme
NaCl	Sodium chloride
$NaNO_3$	Sodium nitrate
NH_4Cl	Ammonium chloride
NO_3^-	Nitrate
NOAA	National Oceanic and Atmospheric Administration
NWA	National Water Act
PCA	Principle Component Analysis
PO_4^{3-}	Orthophosphate
RDA	Redundancy Analysis
REMP	River Eco-status Monitoring Programme

RHP	River Health Programme
SANParks	South African National Parks
SiO_2	Silicon dioxide
SLA	Slàdeček's index
SO_4^{2-}	Sulphate
SPI	Standard Precipitation Index
SRP	Soluble Reactive Phosphate
SST	Sea Surface Temperature
TDI	Trophic Diatom Index
TDS	Total Dissolved Solids
TSS	Total Suspended Solids
WRC	Water Research Commission

Chapter 1: Introduction

1.1 Global climate change and the hydrologic cycle

Planet Earth, in terms of habitability, is regulated by a number of forces or processes that include, among others, the global hydrologic cycle, also called the water cycle. This cycle is one of the main components of the planetary system that regulate animal, plant and human life (Loaiciga *et al*., 1996; Sohoulande & Singh, 2015). The stability of this cycle is of utmost importance since it regulates other cycles including the nitrogen and carbon cycles, thus, it is absolutely necessary to maintain the stability of the hydrologic cycle for the sustainability of human populations and natural ecosystems (Sohoulande & Singh, 2015). The stability of the hydrologic cycle is threatened by climate change as well as by anthropogenic impact (Loaiciga *et al*., 1996).

The hydrologic cycle governs the movement of water, through all of its phases, around the globe. Components of this cycle, that include precipitation, evaporation and evapotranspiration, among others, are responsible for the phase shifting of water (Kundzewicz, 2008). Water is the most valuable resource on Earth and forms the very basis of all life (Chaplin, 2001). The amount of surface water available may seem abundant, however, only 0.3% of this surface water is considered freshwater and consequently usable (Khatri & Tyagi, 2014).

Climate change can be defined as the persistent alteration in the global weather patterns due to anthropogenic activities such as industrialisation, which entails the burning of fossil fuels (Aizebeokhai, 2009; Sohoulande & Singh, 2015). The burning of fossil fuels has undoubtedly increased the amount of greenhouse gasses in the atmosphere. They include methane, carbon dioxide and ozone among others (Loaiciga *et al*., 1996). These gasses, in their unnaturally high abundance, have created a so called blanket around Earth that blocks radiation from leaving Earth's atmosphere (Aizebeokhai, 2009). This energy, which would normally dissipate into space, remains on Earth and contributes significantly to global warming. It is important to know that the greenhouse effect is a natural phenomenon that creates habitable conditions on Earth by blocking some solar radiation from leaving the atmosphere (Loaiciga *et al*., 1996).

Climate change is, however, a natural process that occurs over the span of thousands of years through changes in its components, including precipitation, temperature and wind movements among others. (Sohoulande & Singh, 2015). From the start of Earth's existence until now, the climate of the planet has changed significantly, however, this took place over thousands of

years through Earth's geological time periods. Anthropogenic influence has accelerated the intensity of the greenhouse effect and increases the residual radiation on Earth (Loaiciga *et al*., 1996; Sohoulande & Singh, 2015).

The effects of global climate change have manifested in various natural phenomena by altering the frequency and intensity thereof. Events such as floods and droughts are becoming increasingly unpredictable in their timing and magnitude (Parry *et al*., 2007). This calls for evaluation of the effects of these natural phenomena to increase our understanding thereof, and to mitigate effects caused by the extremity of these events.

1.2 Water availability and use in South Africa.

South Africa is a semi-arid country that is water scarce (Dallas & Day, 2004). Water scarcity refers to water supply in terms of volumetric abundance or non-abundance (Mnisi, 2020). The ratio between water consumption and water availability determines whether a region, or country, is water scarce or not. In South Africa, escalating socio-economic water demands and climatic conditions are the principle factors that cause South Africa to be water scarce (Mnisi, 2020; Kock, 2017). Seasonal rainfall and temperatures contribute to the water scarcity in South Africa. Additionally, there are virtually no natural permanent standing water resources to be exploited and so rivers and their impoundments are exploited as freshwater resources (Dallas & Day, 2004).

Rainfall in South Africa amounts, on average, to 500 mm annually, while global annual averages amount to 860mm (DWAF, 1986). Immense pressure is placed on freshwater resources as the annual precipitation is exceeded by the annual evaporation rate (1100 mm – 3000 mm), which results in a net loss of water every year (DWAF, 1986; Dallas & Day, 2004). Human settlements around rivers in South Africa add pressure to the water resource, not only due to an increase in water needed to sustain a growing population but also water that is needed for agriculture and food production. It is evident that water resources must be effectively managed to ensure water security for populations as well as for natural ecosystems (Kock, 2017). The National Water Act (NWA) of 1998 developed by the Department of Water and Sanitation (DWS), previously the Department of Water Affairs and Forestry (DWAF), aims to set criteria for water quality and develop procedures to protect the freshwater ecosystems of South Africa (DWAF, 1998). The main reasons for insufficient freshwater supply are industrial pollution, increased human population, disproportional water distribution and climate change. In addition to this, the uneven

rainfall pattern of South Africa contributes to the lack of access to freshwater for part of the population (Kock, 2017).

1.3 Influence of ENSO on South Africa's rainfall

The Southern Oscillation of El Niño or ENSO effect is a phenomenon driven by changing Sea Surface Temperatures (SST's) in the tropical Pacific Ocean (Neelin *et al*., 1998; Halpert *et al*., 2016). This change in SST is caused by weakening and strengthening of westward-blowing trade winds (Roy & Reason, 2001). Strong trade winds displace more surface water than weak trade winds and essentially this determines how far the equatorial surface water is displaced across the Pacific Ocean (Philander & Rasmusson, 1985).

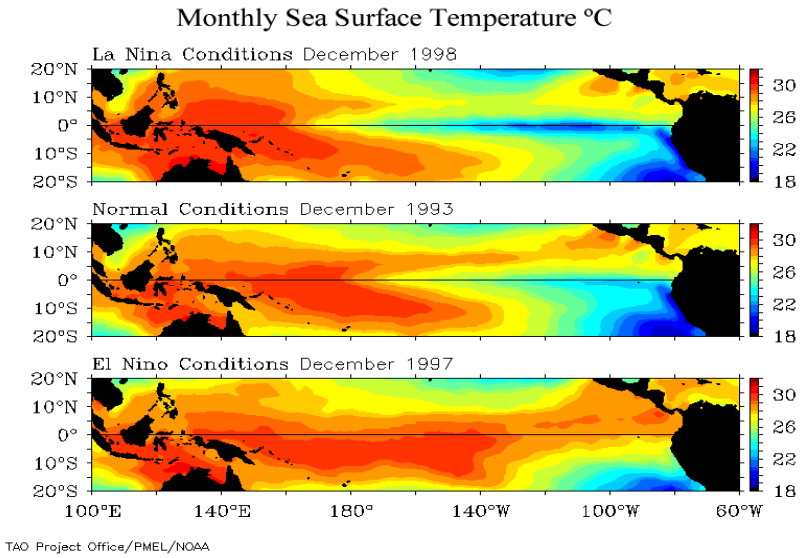

Figure 1: Surface water temperature during the respective phases of ENSO (credit: NOAA climate.gov, 2021).

During normal conditions the westward-blowing trade winds are less intense but not weak and still displace some amount of surface water (Halpert *et al*., 2016). During periods where the respective trade winds weaken, warm equatorial water remains near the eastern equatorial coast of South America and is called an El Niño event or period (Figure 2) (Philander & Rasmusson, 1985). Strengthening of the westward-blowing trade winds causes warm equatorial surface water to move westward across the Pacific Ocean, cooler water is drawn to the surface through upwelling and replaces the warm surface water and the phenomenon is known as a La Niña (Figure 3) (Philander & Rasmusson, 1985; Halpert *et al*., 2016).

The oscillation of these two cycles creates a difference in air pressure, surface winds, SST's and rainfall across the tropical Pacific Ocean. Their cycle can last anywhere between 3 to 7 years on average before a phase shift occurs again (Halpert *et al*., 2016). A neutral phase, between El Niño and La Niña, marks the return of average conditions over the tropical Pacific Ocean.

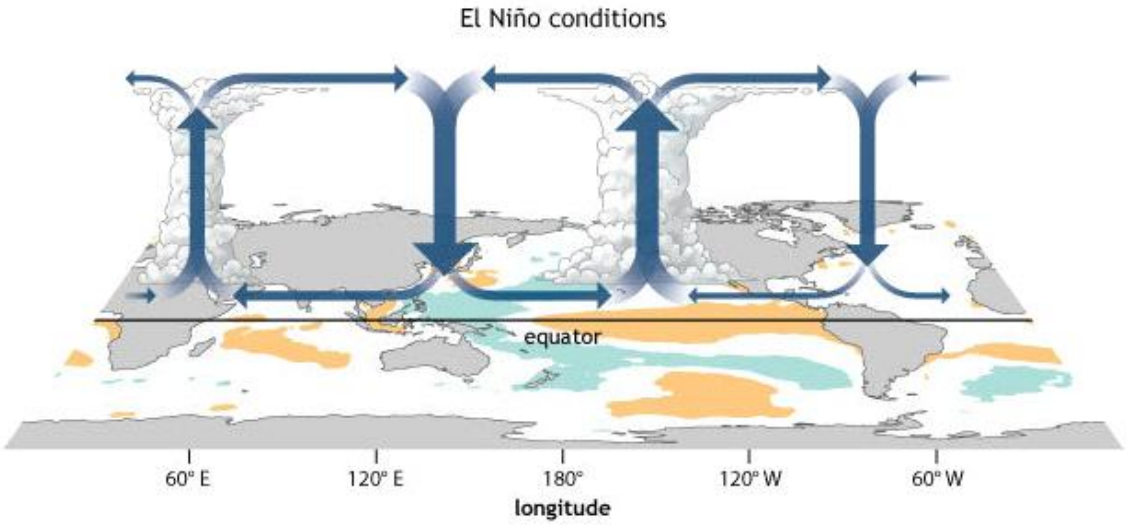

Figure 2: Depiction of global walker circulation as affected by El Niño. Arrows indicate the direction of circulation, while the thickness indicates it strength. A change in SST from cool (blue) to warm (orange) due to weakening of westward blowing trade winds is present over the tropical Pacific Ocean (NOAA climate.gov, 2021).

During El Niño, warm surface water is present in the tropical Pacific Ocean due to weakening of trade winds (Nhesvure, 2020; Philander & Rasmusson, 1985). Warm, humid air rises from the ocean through convection and creates low pressure below (Figure 2). This creates high rainfall and storms (Halpert *et al*., 2016). In areas where cool surface water remains, a sinking air motion, due to Walker circulation, creates high air pressure, leading to decreased rainfall and dryness (Figure 3).

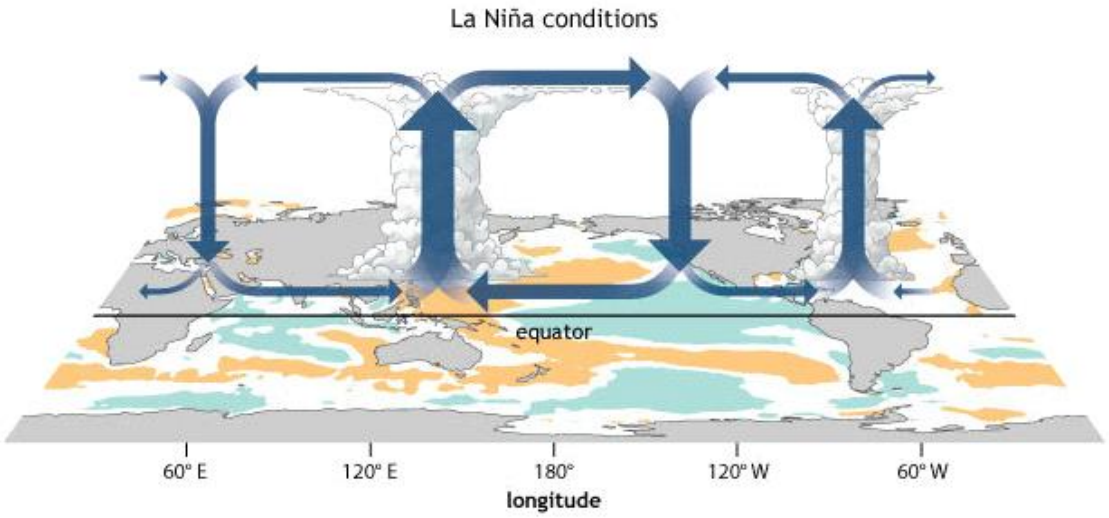

Figure 3: Depiction of global walker circulation as affected by La Nina. A change in SST from warm (orange) to cool (blue) due to strengthening of westward blowing trade winds present over the tropical Pacific Ocean (NOAA climate.gov, 2021).

Although South Africa is not near the Pacific Ocean, the propagation of the ENSO effect has a great impact on the rainfall of South Africa (Nhesvure, 2020). During El Niño, the SST of the east coast of South Africa is warmer than usual, however, during this period high pressure anomalies are also present over southern Africa which decreases the influx of moisture from the Indian Ocean and decreases rainfall (Dieppois *et al*., 2015; Hoell *et al*., 2016). El Niño is therefore commonly associated with drought over much of South Africa (Nicholson & Selato, 2000), and since South Africa is already a water stressed country, this places even more pressure on water security. In contrast, during La Niña the sea surface temperatures are colder, however, low pressure anomalies are present over southern Africa during this time, which increases moisture influx from the Indian Ocean (Hoell *et al*., 2016) and therefore leads to increased rainfall over much of South Africa (Dieppois *et* al., 2015; Nicholson & Selato, 2000).

The impacts of El Niño and La Niña on the west coast are different from their impacts on the rest of South Africa. Here, the upwelling from the Benguela current plays a major role in the rainfall on the western coast of South Africa (Walker, 1990). During El Niño, years the south-easterly winds weaken, creating a less intense upwelling along the west coast (Field & Shillington, 2005) this leads to warmer waters that are generally linked to increased coastal rainfall (Nicholson & Entekhabi, 1986). During La Nina, the strong trade winds enhance the Benguela current in a positive feedback (Field & Shillington, 2005), which create cooler waters and leads to decreased coastal rainfall (Nicholson & Entekhabi, 1986).

Precipitation in South Africa is consequently influenced by the ENSO effect. Therefore, as El Niño and La Niña oscillate, an increase or decrease in seasonal precipitation will occur during the respective times, which will consequently increase or decrease the surface runoff contribution to river discharge.

1.4 Anthropogenic influence of water quantity and quality

The amount of freshwater available in South Africa is in decline in terms of quality and quantity and this is affected by anthropogenic factors (Du Plessis, 2017; Talbot *et al*., 2018). Anthropogenic influences on water quality and quantity include agriculture, afforestation, industry and mining that significantly alter the water holding capacity of soil, and drain and pollute rivers. Although this is true, water is a basic human right and the processes that aim to increase water yield like the building of dams and weirs as well as transfer and abstraction schemes, greatly compromise the quality and ecological integrity of rivers (Dallas & Day, 2004; Kock, 2017; Du Plessis, 2017).

Water resources, such as rivers, dams and lakes have attracted human settlement and development, and have facilitated the demographic growth of humanity (Mithen & Black, 2011). Unfortunately, this has also exacerbated pressure on land-use, fossil fuel resources, natural resources and water resources (Sohoulande & Singh, 2015). Fossil fuels have enabled humanity to usher in a new age of industrialisation and dramatically increased productivity. This enabled society to change from an agrarian society to an industrialised society (Krausmann & Haberl, 2007).

Industrialisation enables societies to increase their manufacturing, which is turn facilitates economic growth (Dowrick & Gemmel, 1991). Manufacturing processes always require large scale usage of energy and often alteration of ecosystems from pristine condition to poor condition (Sohoulande & Singh, 2015). Industrialisation is, therefore, a double-edged sword that on one hand has certainly improved our standards of living, and on the other hand significantly affect the environment and so doing contribute to climate change (Mgbemene *et al*., 2016).

Forestry, has an impact on water quantity, especially in the north-eastern section of South Africa, since plantations take up and transpire large amounts of natural groundwater and hence diminish its contribution to discharge (Dallas & Day, 2004), consequently, removal of trees creates conditions of increased stream flow, due to a loss in evapotranspiration from plantations.

Mining is also a large contributor to pollution in South African rivers, it is a direct source for trace elements of heavy metals and diminishes water quality (Greenfield *et al*., 2012; Addo-Bediako & Rasifudi, 2021). Agriculture is a contributor to pollution as well, although indirectly. Fertilizers applied by farmers are flushed into rivers during heavy precipitation and can quickly increase the trophic status of a river through an increase in primary productivity by algae (Dallas & Day, 2004). Additionally, irrigation return flows greatly contribute to salinisation of many South African rivers (DWAF, 1996a)

The abovementioned impacts on water quantity and quality may have synergistic effects and further exacerbate a dire situation such as a drought or a flood. The water quantity flowing through a river is therefore subject to the effects of land-use impact as describe above. Rivers that are subject to water abstraction for industrial use or irrigation as well as forestry will have a lower than normal quantity of water in the flow regime and will consequently be more susceptible to the impacts of eutrophication, cultural eutrophication and pollution. Eutrophication is defined as the gradual increase in nutrient levels within a water body that results in increased primary production within the system. Cultural eutrophication is regarded as the anthopogenic acceleration of the eutrophication process through further indroduction of fertilisers, detergents, sewage and greater nutrient loads (Britannica, 2022).

1.5 Natural impacts on water quantity and quality

1.5.1 Floods

Flooding results when a stream or river overflows its natural or artificial boundaries, or when periods of excessive rain inundates the surrounding floodplain (Ching *et al*., 2015). Floods can take on a variety of forms of which flash floods, river floods, urban floods and coastal floods are most common. Flooding can occur slowly through prolonged periods of rainfall or can occur very suddenly through extreme rainfall events or failure of impoundments that cause a massive rush of water propagating downstream (Ching *et al*., 2015; Talbot *et al*., 2018). Floods are natural events that regularly occur around the world, however, as with many natural events, anthropogenic influences greatly exacerbate and increase the frequency thereof through processes such as deforestation, urbanisation and agriculture (Anderson & Shepherd, 2013). The magnitude of the flood event will also determine its impact on the water quality of the aquatic system, flooding can have both positive and negative effects on different variables of water quality such as turbidity, Total Dissolved Solids (TDS), dissolved oxygen (DO), nutrient concentrations etc. (Talbot *et al*., 2018). Thus, the magnitude of flood events will determine the

degree to which the event has a positive or negative effect on water quality as well as on aquatic systems.

Smaller floods generally have positive or neutral effects on many ecosystem services that include water quality and primary production (Junk *et al*., 1989). Small flood events contribute nutrients to aquatic systems, and although initially the primary production may be low during high water levels, when water levels decrease, the nutrients are still within the system and available for use by primary producers. Floods can therefore aid in the flux of nutrients in oligotrophic systems that can increase primary production and facilitate food web functions (Alford & Walker, 2013).

Larger floods can excessively increase nutrient concentrations and lead to eutrophication of aquatic systems and consequently altering the dominance of primary producers within the system (Talbot *et al*., 2018). When this happens, cyanobacteria become more dominant than green algae and consequently decrease the water quality due to their toxicity and related aesthetic issues (tastes and odours). Additionally, cyanobacteria are largely inedible to primary and secondary consumers (Ger *et al*., 2016) and thus the food web functioning is severely altered and degraded. Light penetration is an important prerequisite for primary production, when flooding events occur and nutrient concentrations are high as well as the turbidity of the water, then primary production will still be low since light penetration isn't sufficient enough to stimulate high outputs of primary production (Dallas & day, 2004). Thus, the interplay of water quality variables will determine the amount of primary production within a given system. In the case of large flood events, algal growth rates may be exceeded by flushing rates, then the event can decrease algal biomass, even though nutrient concentrations are high (Talbot *et al*., 2018). It is therefore difficult to conclude if flooding increases or decreases primary production because aspects like nutrient concentration, water clarity, flushing rates and grazing of algae are highly dependent on one another.

Surface water pollution is a significant risk associated with flooding due to rivers and drainage systems being overloaded with water (Ching *et al*., 2015). This water, which is mainly rainwater, picks up pollutants and contaminants contained in soils and other waste materials, and carries them into receiving water bodies. Increased precipitation is expected to contribute to deterioration of aquatic systems due to excessive nutrient and pollutant inputs, soil erosion and the presence of pathogens (Coffey *et al*., 2018). However, larger flood events can also aid in the dilution of nutrient loads since there are large amounts of water present during flooding, thereby

decreasing nutrient concentration (Talbot *et al*., 2018). Thus, although the nutrient load might be high, the amount of water is also high and sufficient in diluting these nutrients to mitigate some of these effects caused by them. Dissolved organic matter and sediment concentration also increase during flood events (Williams, 1989; Raymond & Saiers, 2010). Extreme flood events will most likely cause deterioration of water quality, however, the extent to which water quality deteriorates will depend on factors such as mixing and dilution, which is dependent on the relative extremity of the event to the pollution source as well as the vertical connectivity of a river network (Talbot *et al*., 2018).

1.5.2 Drought

Droughts are characterised by low precipitation rates and high temperatures, mainly due to climatic changes which can alter the intensity and frequency of drought conditions (Van Vliet & Zwolsman, 2008). Drought is difficult to define and can be seen as a stalking or creeping effect that generally starts with the abnormal delay of rain (Wilhite & Glantz, 1985). Conditions where rainfall shortages occur over some period of time (weeks, months or years) can be regarded as a meteorological drought (Quiring, 2009). Agricultural drought occurs when the lack of rainfall and high evaporation rates depletes the soil moisture, to a point where crops and terrestrial ecosystems are adversely affected (Mathivha *et al*., 2017). When the continuing drought conditions cause a decrease in groundwater storage and stream flow over one year or consecutive years, it is known as a hydrological drought (Smakhtin, 2001). Tallaksen and Van Lanen (2004) define hydrological drought as the manifestation of low stream-flow and diminished groundwater discharge causing a lack of water in the hydrologic cycle. The study of hydrological drought is crucial for water quality management (Nosrati, 2011).

Much of the attention involving the effects of drought have been given to hydrology (water quantity) and little has been given to surface water quality, however, since the turn of the 21st century more attention has been given to the effects of drought on surface water quality (Van Vliet & Zwolsman, 2008). Methods proposed for the assessment of climatic change on surface water quality, for example empirical relations between water quality and deterministic modelling approaches, assess the effects of climate change on water quality on a regional or continental scale (Van Vliet & Zwolsman, 2008). However, the impacts of climate change on water quality might be obscured by anthropogenic influence that alters the chemical, physical and biological properties of surface water, which includes water re-use factors (increases and decreases in the demand for water), terrestrial factors (soil structure and vegetation changes), hydrological

factors (changes in dilution of point-source emissions) and increases in air temperature (Murdoch *et al*., 2000).

Low-flow conditions, caused by hydrological drought, have adverse effects on water quality and aquatic biota through various chemical, physical and biological processes, and can also contribute to water pollution (Nosrati, 2011). However, little is known about the impact on water quality during low-flow periods. Since periods of prolonged low river flow conditions, in combination with high temperatures, cause water quality to deteriorate, it is essential to gain insight and understanding into the impact drought has on water quality (Nosrati, 2011). The study done by Van Vliet and Zwolsman (2008) illustrated the deterioration of river water quality in the Meuse River, caused by low-flow conditions and high temperatures. This is reflected by eutrophication, high water temperatures, and an increase in major element concentrations. They found that nitrates and heavy metals, with high adsorption affinities for suspended solids, had decreased, which had a positive effect on water quality. Under high water temperatures, caused by drought, less oxygen can dissolve into the water, and in combination with decreased re-aeration caused by low-flow conditions, severe oxygen depletion can occur (Mimikou *et al*., 2000).

Furthermore, Van Vliet and Zwolsman (2008) found that high nutrient concentrations, high water temperatures, low discharge rates and long residence times, caused by drought, favoured the occurrence of algae, which might not be the same for other river systems. Nevertheless, algal blooms cause further deterioration of water quality when they die and decomposition cycles the nutrients, for the next bloom, back into the system (Fallon & Brock, 1979; Wang *et al*., 2015).

The processes that affect water quality during drought periods are the same for different rivers, however, the magnitude of this depends on factors like river flow regime, anthropogenic activities and catchment characteristics (Van Vliet & Zwolsman, 2008). Rivers that have low summer flows and have chemical inputs from point-sources, are the most sensitive to drought conditions because they have high surface temperatures and experience low-flow conditions. However, the inputs from diffuse sources, during low-flow conditions, decreases to such a degree where the water quality becomes stable or even increases during drought conditions (Mosley, 2015). On the other hand, rivers that have high summer discharges will still exert a sufficient dilution of chemicals from point sources (Neal *et al*., 2000).

Although there are positive effects on water quality caused by drought conditions, the negative effects on water quality, especially by eutrophication, greatly outweigh the positive effects. Since

climate change will likely cause an increase in drought frequency and duration, the ecological and recreational potential of a river will likely decrease in accordance (Murdoch *et al*., 2000; Mosley, 2015). This includes a decrease in the amount of available water that is of sufficient quality, for agricultural and domestic use. The quality of drinking water also decreases as temperature increases and the concentration of water quality parameters such as chloride, bromide and fluoride are exceeded (Van Vliet & Zwolsman, 2008). Therefore it is essential to manage pollutant inputs form point-sources during drought conditions.

1.6 Diatoms

1.6.1 What are Diatoms?

Diatoms are a highly ubiquitous group of unicellular algae, they often appear free living but can also be part of a colony (Cox, 1996). These algae have a unique cell wall, called the frustule. This structure is formed by genetically encoded depositions of nano-patterned silica, forming extremely intricate structures that are highly species-specific (Kröger & Poulsen, 2008).

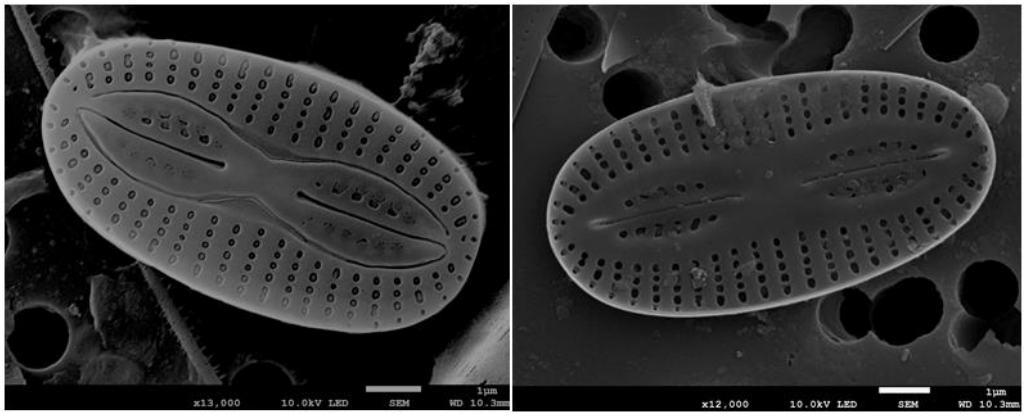

Figure 4: Scanning electron microscope images of the intricate frustule pattern of *Navicula microlyra* (Credit: Willie Landman)

Diatoms colonise marine and freshwater alike and form a principle part of the food web (Round *et al*., 1990; Cox, 1996). Most diatoms are autotrophs and contribute significantly to primary production, especially in marine environments (Sarthou *et al*., 2005). Some diatoms are also heterotrophic, and can compete well under eutrophic conditions (Hellebust & Lewin, 1977). Diatoms produce large amounts of extracellular polymeric substances (mucus) high in dissolved organic carbon that serves as an energy-rich food for microorganisms such as protozoa and macroorganisms such as copepods, crabs and fish. The mucus produced by diatoms also helps stabilise sediments and facilitates carbon transfer to higher trophic levels (Bohórquez *et al*.,

2017). Therefore, diatoms are highly integrated in food webs as a consequence (Cushing, 1989).

In freshwaters, diatoms occur as a golden-brown film on substrata such as rocks and boulders, aquatic macrophytes, mud and sand. Diatoms can also appear on exposed damp substrates outside aquatic environments. Other materials like plastic, paper and metal can also be colonised (Taylor *et al*., 2007b). A colonised substrate is usually identified as slippery or slimy to the touch, due to the mucilage diatoms produce to glide and move in their environment. These gliding movements are made possible by a structure called the raphe. This structure is a longitudinal slit or fissure within the diatom cell wall (Figure 5), where mucilage is secreted onto microfibrils which are controlled by sliding actin and myosin filaments located longitudinally under the raphe (Bertrand, 2021). Mucilage is secreted onto the microfibrils causing a sliding of the actin filament and extension of the microfibril to deposit mucilage, after which the actin filament slides back into place. This causes a wave-like motion of microfibrils that enable diatoms to glide (Bertrand, 2021). However, not all diatoms possess a raphe, these taxa are therefore usually subject to stream flow and form part of the phytoplankton (Round *et al*., 1990).

Diatoms are divided into two groups, in part because of the above-mentioned difference in motility. Pennate diatoms are those that colonise benthic substrates, are elongated and possess lateral symmetry (Round *et al*., 1990) (figure 5 - B). The raphe is the primary axis on which symmetry occurs. Only pennate diatoms possess a raphe, which allows them to be firmly attached to substrates (rocks, mud, sand, etc.) by the secretion on mucus (Round *et al*., 1990). However, not all have or require a raphe to firmly attach to substrates, taxa including *Ulnaria*, *Fragilaria*, *Tabularia, Tabellaria* and *Diatoma* are all araphid (without a raphe) and attach to substrates by means of mucilage stalks (Taylor & Cocquyt, 2016). Centric diatoms are those that occur suspended as part of the phytoplankton in oceans, lakes, dams, and rivers (Roeder, 1977; Harrison *et al*., 1997; Hamm *et al*., 2003). With exceptions, they are generally not able to firmly attach themselves to substrates, and are circular in shape and radially symmetric (Round *et al*., 1990) (figure 5 - A).

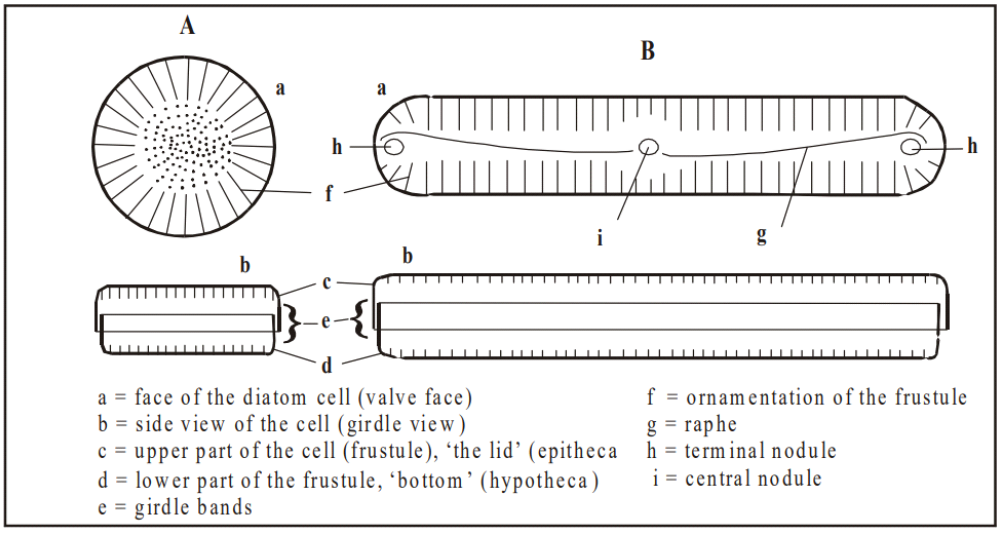

Figure 5: Comparison of the cell wall shape of centric (A) and pennate (B) diatoms (Sorvari, 2001).

1.6.2 Diatoms as indicators of water quality

Water quality assessments of aquatic systems are traditionally done by means of two approaches namely, physico-chemical analysis and biomonitoring. Measurements of water quality can be done by using physico-chemical analysis; however, this fails to provide a holistic view of the water quality because its measurements are instantaneous and fail to integrate physico-chemical variability within the system (De la Rey *et al*., 2004). Biomonitoring, however, can provide an integrated view of water quality by assessing the integrity of biological assemblages to provide a more complete view for the variability of chemical and physical constituents in an aquatic system and incorporates the long-term effects that these constituents have on biota (De la Rey *et al*., 2004). Many organisms are used as bioindicators of which fish and macroinvertebrates are most widely used. Diatoms also serve as important bioindicators (Round *et al*., 1990). Diatoms are important primary producers in aquatic systems (Cox, 1996), they respond directly and rapidly to growth stimulants like nutrients, physical factors like habitat alteration and elevation as well as to other stressors like contaminants (Taylor, 2004; Taylor, 2007b; Dalu & Froneman, 2016).

Diatoms occur in all aquatic environments and are well represented in most, as a result, only relatively small samples need to be taken to conduct an accurate assessment of the community composition of diatoms. Their taxonomy is well established, and many guides are available to aid identification (Reid *et al*., 1995). Diatoms, epitlithic taxa in particular, are very sensitive to water chemistry changes and many species have specific environmental tolerances and optima

(Hall & Smol, 1992; Stevenson & Pan, 2001). Their short cell cycles and the ability to rapidly colonise new habitats allow them to indicate rapid changes in environmental conditions, an aspect that is not represented in physico-chemical analysis (Oemke & Burton, 1986).

The largely cosmopolitan distribution of diatoms may affect the ecological tolerances of species in northern and southern hemispheres, however, it was found that species have similar environmental tolerances regardless of being in the northern or southern hemisphere (Taylor, 2004; Reid *et al*., 1995). When diatoms die, their frustules, which are made of SiO_2, sink to the bottom where they are preserved in the sediments. Since diatom taxonomy is based on characteristics of the frustule, fossilised diatom data can be used to evaluate past conditions of an aquatic system (Reid *et al*., 1995).

Therefore, diatoms can be employed as indicators of water quality with great success and have been long employed to monitor anthropogenic and natural changes in aquatic systems (Dalu & Froneman, 2016). Since the beginning of the 21st century, the use of diatoms to evaluate past and present conditions had increased.

1.6.3 Diatoms for biomonitoring in South Africa

The potential of diatoms as indicators of water quality in South Africa was first realised by Béla Jenö Cholnoky (1899-1972), who was regarded as the father of South African diatomology (Dalu & Froneman, 2016). He stated that he had little faith in the assessment of water quality by only using physico-chemical analyses, and argued that analyses could be done more reliably and cost-effectively by using diatoms (Harding *et al*., 2005). In 1968, Cholnoky adapted the community analysis technique of Thommason (1925) to determine water quality using benthic diatoms (Taylor, 2004). One aspect of water chemistry is chosen, for example, nitrogen, to test the amount of nitrogenous pollution. The genus *Nitzschia* is a good indicator of nitrogenous pollution since it is nitrogen heterotrophic, and the genus *Eunotia* is a good indicator of pH gradients in a river system. However, this required in-depth knowledge of the autecological requirements of diatoms species, although the development of correspondence analysis was able to assign direct tolerance limits to species for different chemical parameters (Taylor, 2004).

This method of Cholnoky was simplified by Schoeman (1976). He achieved this by dividing diatoms into four groups based on their specific ecological requirements and proved that his method could be successfully applied to measure water quality, especially regarding trophic status (Schoeman, 1976). Another classification system that proved to be highly successful and has good relations between water quality and diatom community structures is the saprobian

classification system, which was developed by Lange-Bertalot (1979). This method was tested by Schoeman (1979) and found to be highly successful. The use of diatoms as indicators was only explored again in South Africa in the late 1990's by Bate and Van der Molen. Their work amounted to two publications, Bate et al. (2002) and Bate et al. (2004). The former is a WRC report on the importance of using diatoms as bioindicators of water quality in South Africa. The latter is a proposed water quality index to use with diatoms and is based on water quality class assignments (Bate *et al*., 2004).

After the implementation of diatom monitoring for catchment-wide surveys (e.g., Crocodile-Marico Catchment State of the Rivers Report (RHP, 2005)), diatoms as a biomonitoring tool came to the attention of the then Department of Water Affairs and Forestry (DWAF) and were included in the methods manual for the South African River Health Programme (RHP) as these techniques were considered cost-effective and reliable (Dalu & Froneman, 2016).

South Africa has made considerable progress in the use of diatom-based monitoring in aquatic ecosystems to assess biotic integrity (Dalu & Froneman, 2016). Despite the benefits diatoms provide in a reliable assessment of water quality, such techniques have been difficult to apply to assess anthropogenic influences in Africa, such monitoring is slowly gaining ground albeit at a genus level of identification (Okito *et al.*, 2021). Much work remains to be done on the African continent in terms of identifying and describing diatom species so they can be eventually used in assessments. In South Africa however, the Water Research Commission (WRC) helped lay the foundation for using diatoms in monitoring programs, for both freshwater and estuarine ecosystems (Bate *et al*., 2002; Bate *et al*., 2004; Harding *et al*., 2004).

1.6.4 Diatom indices development

Diatom indices are types of autecological indices that use the relative abundances of taxa in communities or assemblages and their ecological tolerances, specificities or preferences to infer environmental conditions of ecosystems (Stevenson & Pan, 2001). Multiple indices have been developed that use diatoms to monitor water quality. These indices include, amongst others, the Indice de Polluosensibilité Spécifique (IPS), the Generic Diatom Index (GDI), Descy's method (DES), Slàdeček's index (SLA), Trophic Diatom Index (TDI), Biological Diatom Index (BDI) and the Council for European Communities Index (CEC) (Taylor, 2004).

Descy (1979) proposed the first true diatom index using the equation below (Equation 1). The use of Descy's method led to the development of the IPS, based on 189 surveys conducted from 1977 to 1980. After the IPS was developed, the GDI was proposed, this index incorporated

174 taxa including new genera at that time. In 1991 the CEC was developed by Descy to provide general water quality monitoring for rivers across Europe (Taylor, 2004). The wide usage of the IPS and GDI in France led to the development of the BDI to provide an index for monitoring river networks throughout France. The use of the BDI was maximised by combining morphologically similar diatom species and resulted in 209 taxa being kept. Slàdeček' (1986) used the method of Descy (1979) in 1986 to develop the Slàdeček's Index, based on a saprobic system. Saprobity is indicative of the tolerance or sensitivity of diatoms to organic impact/pollution that can be indirectly caused by cultural eutrophication or directly caused by organic-rich pollutants orgininating from industrial and domestic practices (Dallas & Day, 2004). The sensitivity and importance values are attributed to 323 species, based on their affinity for organic material (Slàdeček', 1973, 1986).

In 1982, Watanabe proposed the Diatom Community Index, which is a saprobic index and is not based on the general weighted average formula of Zelinka and Marvan (1961), which is explained below. This index is calculated by using the sum of the pollutant tolerant species added to the relative frequency of ubiquitous taxa (Taylor, 2004). Refinement of the index resulted in the Diatom Assemblage Index of Organic Water Pollution (DAIpo) (Watanabe, 1990).

Internationally, the most commonly used diatom indices are the (TDI), the (IPS), and the (GDI). The GDI and IPS indices were established as indices of organic pollution (Musa & Greenfield, 2018) where the TDI was used to indicate inorganic nutrient contamination to test for sewage effluent (Kelly & Whitton, 1995). The IPS is the most comprehensive of the indices that integrates values for more than 1300 species, where the GDI only incorporates 44 genera. This makes the GDI easier to use because it only incorporates a genus classification (Taylor, 2004). However, the IPS is still a more accurate index to determine the water quality of aquatic systems. It indicates organic water pollution and incorporates many species that improves its efficacy as a determinant for water quality.

The use of diatom indices has increased in popularity within the past decade, to such a degree, that in some cases it has replaced macroinvertebrate indices as the preferred method of assessing water quality, however, in most cases, these are considered as complementary techniques and should be used as such whenever possible (Taylor, 2004). Diatoms possess certain advantages above macroinvertebrates that enable them to be more reliable indicators of water quality. Their frustule is composed of SiO_2 and is well preserved in most samples (Werner, 1977). The use of diatoms is higly accurate and the data is comparable between

countries. Additionaly, the cosmopolitan distribution of diatoms gives them a distinct advantage, especially since their distribution does not affect their response to environmental conditions (Taylor, 2004). However, the use of diatoms is not as cost-effective or rapid compared to macroinvertebrates and, therefore, macroinvertebrates still serve as the preferable bioindicators of water quality change.

There has been an international effort to develop and test diatom indices specific to different countries. In Europe and Great Britain, there is an effort to standardise the routine sampling and processing of diatoms to assess water quality (Kelly *et al*.,1998; Prygiel *et al*., 2002). Most diatom indices are calculated based on a weighted average equation by Zelinka & Marvan (1961) and is redrawn to have the following form:

$$S = \sum_{j}^{n} = a_j \, v_j s_j / \sum_{j}^{n} = a_j v_j$$

Where $\boldsymbol{a}_j$ represents the abundance of species ***j*** in a sample, $\boldsymbol{v}_j$ represents the indicator value for species ***j*** in a sample and $\boldsymbol{s}_j$ represents the pollution sensitivity of species ***j*** in a sample. ***S*** is the calculated index value representing the weighted average sensitivity score of the entire diatom community.

The index gives an overall community sensitivity score (***s***), based on the average sensitivity of the diatom taxa present. However, the abundance of a species is a primary determinant for tolerance toward environmental conditions. Therefore, a simple average of the sensitivity values will not suffice. The abundance therefore serves as an important weight in the calculation of the final score, if Species A is counted 50x and Species B is counted 5x, the sensitivity of the community will be closer to that of Species A due to its greater abundance (Ter Braak & Van Dam, 1989).

The other variable in the index calculation is the indicator value (***v***). This value is indicative of the species' ability to tolerate wide ranges of environmental conditions or not (Ter Braak & van Dam, 1989). In other words, are they specialists or generalist species? Species that specialise can either be indicative of good or bad conditions. These species can occur at both ends of the tolerance spectrum, and so if they are found, their influence has to be great, since they can tolerate only narrow ranges of environmental change (Stevenson & Pan, 2001). Unfortunately, this creates skewed results at the furthest end of the spectrum, since a species that specialises

in polluted conditions will also receive a high indicator value and consequently increases the index score and water quality rating. Therefore, special precaution must be taken when interpreting results if they are unexpected. Fortunately, the low sensitivity score of such a species will prohibit the indicator value from scaling higher and having a greater influence than it already has. This can be observed from the equation, if a species receives a sensitivity value of one, and receives an indicator value of three, the abundance can only be multiplied by three (e.g. **s** = 1 and **v** = 3, then **a** x **v** x **s** = **a** x 3 x 1 or **a** x 3). Conversely a higher sensitivity value will increase the scale by which the abundance is multiplied (e.g. **s** = 1.5 and **v** = 3, then **a** x **v** x **s** = **a** x 3 x 1.5 or **a** x 4.5). Therefore, a low sensitivity value, prohibits the indicator value from having a large impact.

Thus, the index calculates a community sensitivity score by incorporating the abundance of species as well as their indicator value as weights. The performance of these indices depends on the values for ***s*** and ***v*** sourced from literature and expert observations (Taylor, 2004). The values for ***s*** and ***v*** can range from 1-5 and 1-3, respectively.

1.6.5 The Kruger National Park: Diatom studies and recent drought

The Kruger National Park (KNP) is the most prestigious of South Africa's national parks. It hosts a wide variety of plant and animal species, many of which are endemic, and covers an area of 19 485 km^2 (Pienaar, 1982). The park stretches across the Mpumalanga and Limpopo provinces and borders Zimbabwe to the north and Mozambique to the east (Steffens, 1993; Macdonald, 1988).

The park is located in the savannah biome and lies in the middle reaches of five, large, dynamic and diverse trans-boundary river systems (Riddell *et al*., 2019). The park has a record of many decades of applied ecosystem research and is positioned between two trans-boundary river basins, the Incomati and Limpopo basins. A study conducted by (Riddell *et al*., 2019) set out to provide an overview of the challenges facing large protected areas, including the KNP, in terms of upstream pollutants on the viability of aquatic ecosystems. The responsibility to conserve the ecosystems within the KNP remains that of the park and the use of diatoms and other bioindicators of water quality revealed the paramount importance of conserving aquatic ecosystems in terms of exposure to pollutants (Riddell *et al*., 2019).

Studies using diatom indices to assess water quality have been conducted in the KNP over the past decade (Shikwambana *et al*., 2021). Shikwambana et al. (2021) also considered samples collected in 1983 as part of a collaborative CSIR investigation into the park's rivers. Diatom

community structures were used to compare water quality between the years 1983 and 2015 for three perennial rivers in the KNP namely, the Letaba, Olifants, and Sabie rivers. The Letaba River experienced lentification between the late 1960s and 1989, in 1990 the restoration of the perenniality of the Letaba River showed positive results in terms of improving water quality. The Olifants River was influenced by anthropogenic activities during this period. The study indicated an improvement in water quality for the Letaba and Olifants rivers and showed relatively stable water quality for the Sabie River.

A study conducted by Oxley (2021) set out to determine the temporal and spatial changes in water quality for the Sabie-Sand System between years 1983-85 and 2019-20 in the KNP. The study also made use of diatom samples collected previously by staff of the CSIR. Oxley (2021) made use of diatoms as bioindicators in addition to chlorophyll *a* fluorescence (productivity), as an index of environmental change. Results showed an overall decrease in water quality in the Sabie-Sand system over time, from good quality to poor quality, and emphasised the need for water quality monitoring in the park using diatoms.

A study conducted by (García-Rodríguez *et al.,* 2007) focused on analysing the dominant and sub-dominant epipelic diatoms as well as water quality in South African rivers that included the KNP. Results showed that sites within the KNP had high PO_4 and SiO_2 levels, indicating a considerable degree of eutrophication. The diatoms found were indicators of eutrophication, natural and/or cultural, and therefore the rivers within the KNP can be considered to have high levels of primary production.

Gilson and Ekblom (2008) made use of diatoms, among other indicators, to assess the anthropogenic and climatic influences on riverine forests in the Kruger National Park for the past 700 years. The study made use of a multi-proxy approach to enhance the understanding between fire, climate, and vegetation in the past. The diatom assemblages were discussed in terms of lithology zonations, each zone represent a certain time period in the past (Gilson & Ekblom, 2008). The community composition of diatoms was used to determine if water levels were high or low during certain periods. A decrease in the relative density of benthic diatoms indicated the presence of wetter conditions and higher water levels while high diatom densities indicated low water levels.

A recent study conducted by (Malherbe *et al.,* 2020) examined the recent drought periods in the KNP based on the Extreme Climate Index. They set out to evaluate the potential of the ECI to quantify and identify the extent and intensity of the most severe drought periods in the park

since 1980. The most severe droughts in the park, as indicated by the ECI, were regarded as those that occurred in 1982/1983, 1991/1992, 2002/2003, and 2015/2016 (Malherbe *et al.,* 2020), these periods also correlate with El Niño years (MacFadyen *et al*., 2018). The droughts in 1982/1983 and 1991/1992 are regarded as the most spatially extensive extreme droughts in the Kruger National Park, where the 90s drought conditions had a prolonged effect until 1994/1995 that placed more stress on resources and faunal biomass (Malherbe *et al.,* 2020). The 2002/2003 and 2015/2016 droughts were more focused on the central and southern parts of the park, however, lower rainfall was experienced in 2015 and 2016 and thus, the drought of 2015/2016 was considered to be more severe (Malherbe *et al.,* 2020). The number of days experiencing heat waves, as calculated since 1961, was above the 75th percentile in most cases during these drought periods. However, during the 2015/2016 drought, the number of heat waves and heat wave days exceeded the recorded number in previous years by 50 – 100% (Malherbe *et al.,* 2020). The extreme temperatures experienced during this period likely exacerbated the drought effect and are indicative of the necessity to include temperatures in indices that assess the impact of drought conditions (Malherbe *et al.,* 2020). They concluded that given trends in high temperatures, the type of drought experienced during 2015/2016, will likely increase in frequency and intensity during the 21st century.

Data on tourist arrivals and rainfall conditions are available for the Kruger National Park for a considerable number of years. A study conducted recently by (Mathivha *et al.,* 2017), examined the effects of drought conditions on the arrival of tourists in the park. They gathered data from 1963 up to 2015 from the South African Weather Service (rainfall data) as well as from SANParks (tourist data). The rainfall data were analysed using the Standard Precipitation Index (SPI) to determine drought years in the park and Pearson correlation analysis was used to determine the relationship between drought years and tourist arrivals (Mathivha *et al.,* 2017). Their results indicated a negative correlation with tourist arrivals in 19.36% of drought years experienced. Tourist arrivals did show an increasing trend, and in addition, their results showed how fragile the tourism industry is and how it is influenced by environmental conditions.

1.7 Aims and Objectives

1.7.1 Rationale

Within the KNP the main drivers for inter-annual flow regime change is seasonal rainfall, which is generally linked to El Niño and La Niña (MacFayden *et al*., 2018). Therefore, it is presumed to have an effect on water quality, during El Niño water quality will deteriorate and during La Niña water quality will improve. Changes in water quantity in rivers are commonly associated with water quality changes in terms of trophic status, ion composition and organic pollution. The IPS may, therefore, serve as a good indicator for water quality change due to flow alteration, to some degree, although not necessarily intended for such purposes.

1.7.2 Aim

The aim of this study was to assess how an annual increase in seasonal rainfall, from 2018 to 2022, changed the water quality of five perennial rivers in the Kruger National Park.

1.7.3 Objectives

1. Measure and compare the water quality at selected sites, *in situ* and *ex situ* to determine the relationship between ionic compounds and electrical conductivity as well as demonstrate the relationship between IPS scores and electrical conductivity, by using Pearson correlation (r), R^2 analysis and p-values.
2. Determine the diatom community composition of the respective sites and correlate this to measured water quality, by using CCA.
3. To determine the water quality of the respective rivers in terms of trophic status, ionic composition and organic pollution by using diatom autecological preferences (IPS diatom index).
4. Compare IPS scores across time (2018 - 2022) within the studied rivers to illustrate the impact of water quality change in terms of trophic status, ionic composition and organic pollution during variable flow regimes.

Chapter 2: Methods

2.1 Study area

Kruger National Park

The Kruger National Park (KNP) is situated within a semi-arid climatic zone, spanning most of South Africa's north-eastern interior and is further split into two distinct zones (Rutherford & Westfall, 1986). To the north (Limpopo province) is arid bushveld that receives on average 300 – 500 mm of rain annually. The Lowveld bushveld (Mpumalanga province) receives on average 500 – 700 mm of rain annually (MacFadyen *et al*, 2018), 84% of the annual rainfall for the entire park is concentrated in the summer months between November and April (Zambatis, 2003).

The terrain across the KNP is relatively flat with slight undulations, except for three high lying areas (MacFadyen *et al*, 2018). In the south-west section of the park, west of Malelane, sits the Khandizwe hills (Viljoen, 2015). Further north, bordering Mozambique, lays the Lebombo mountain range. It stretches 800 km from the Mkuze River in KwaZulu-Natal into the KNP (Britannica, 2013), the Olifants River cuts through the Lebombo Mountains before it enters Lake Massinger in Mozambique (Viljoen, 2015). Further north-west lays the Shitshova range near Punda Maria, at the Border of South Africa and Zimbabwe (MacFadyen *et al.,* 2018).

The high lying areas create updrafts due to the difference in elevation, which increases rainfall in these areas around Malelane and Punda-Maria. For the remainder of the park, it is generally accepted that rainfall increases from north to south and from east to west, as it approaches the Drakensberg escarpment (MacFadyen *et al*., 2018).

The park has five perennial rivers that may allow for a more integrated analysis of water quality change due to water quantity change across years sampled. Perennial rivers exhibit continuous flow throughout the year and have high habitat connectivity and availability, therefore, any changes in water quality are caused by a large interplay of continuous environmental changes (Soria *et al.,* 2017). River systems in general are well adapted to seasonal flooding, biota within are resilient and can employ various strategies to use their resources and habitats efficiently in accordance with the rise and fall of the water level (Junk *et al.,* 1989) and, therefore, an alteration in the intensity and duration of seasonal flooding will presumably also alter the biotic communities within and consequently also diatom communities.

The data used in Figure 6 is sourced from the SANParks Scientific Services. These data illustrates the total precipitation measured for each month as averaged for the 25 monitoring stations in the park, not the average rainfall for each month.

Figure 6 illustrates two key aspects of the seasonal rainfall over this period. Firstly, it confirms the high precipitation, concentrated around the summer months from October to April. Secondly, it shows an annual increase in the intensity of total monthly rainfall as averaged across the park. During the drought year of 2018 the highest total monthly rainfall occurred in February with 110 mm (Figure 6). However, during 2021 when floods were experienced (Dube, 2022), the highest total monthly rainfall occurred in January with 220 mm, a twofold increase from the highest total monthly rainfall of 2018.

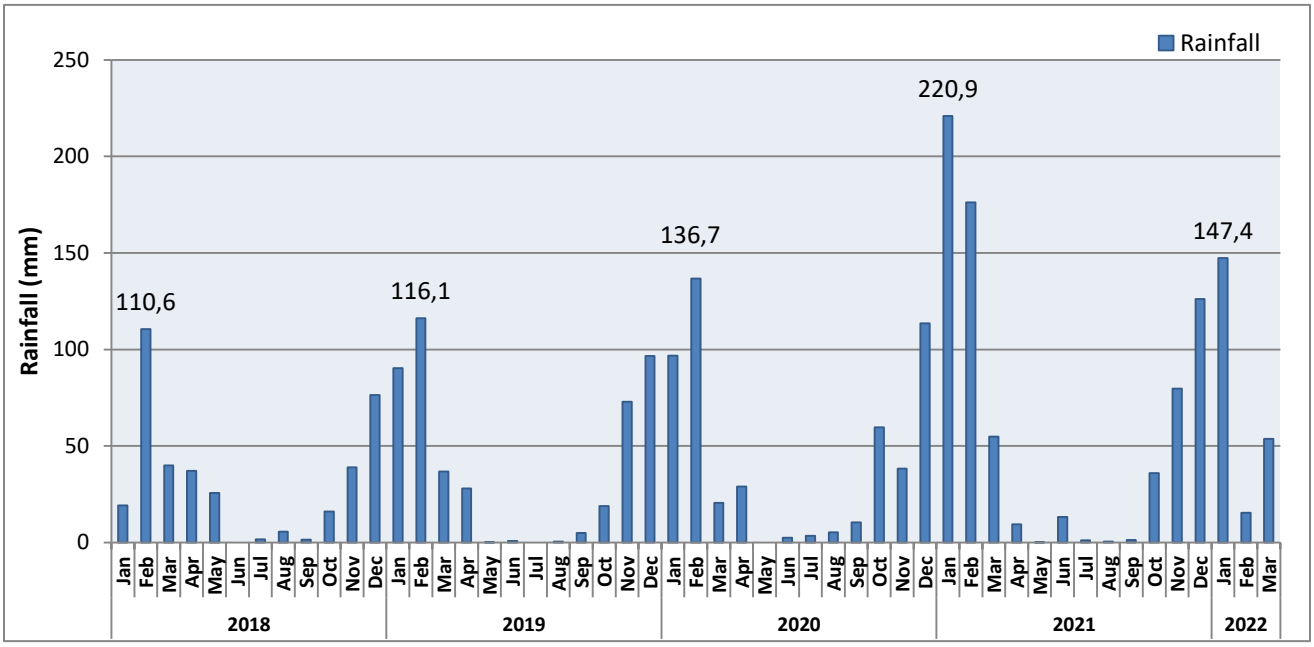

Figure 6: Monthly average rainfall from 25 weather stations in the KNP. Note the annual increase is the amount of season rainfall from January 2018 to March 2022. Values on the graph indicate the highest average measured precipitation, in mm, in each cycle.

2.2 Site selection

The locations of all sites sampled were predetermined by the KNP Scientific Services as part of their internal monitoring program.

Sites were generally selected based on their adherence to certain criteria. Sites must be relatively permanent in terms of flow, allowing future research to be conducted over time. Sites were also spaced along the reach of a river to maximise the usefulness of data gathered pertaining to river health and with enough sites available to allow reliable deductions of a river's ecological status (Alvarez-Vázquez *et al.,* 2012). Additionally, sites must be relatively easily accessible, in order that follow-up sampling is not difficult and time consuming.

2.2.1 Map of sampling sites

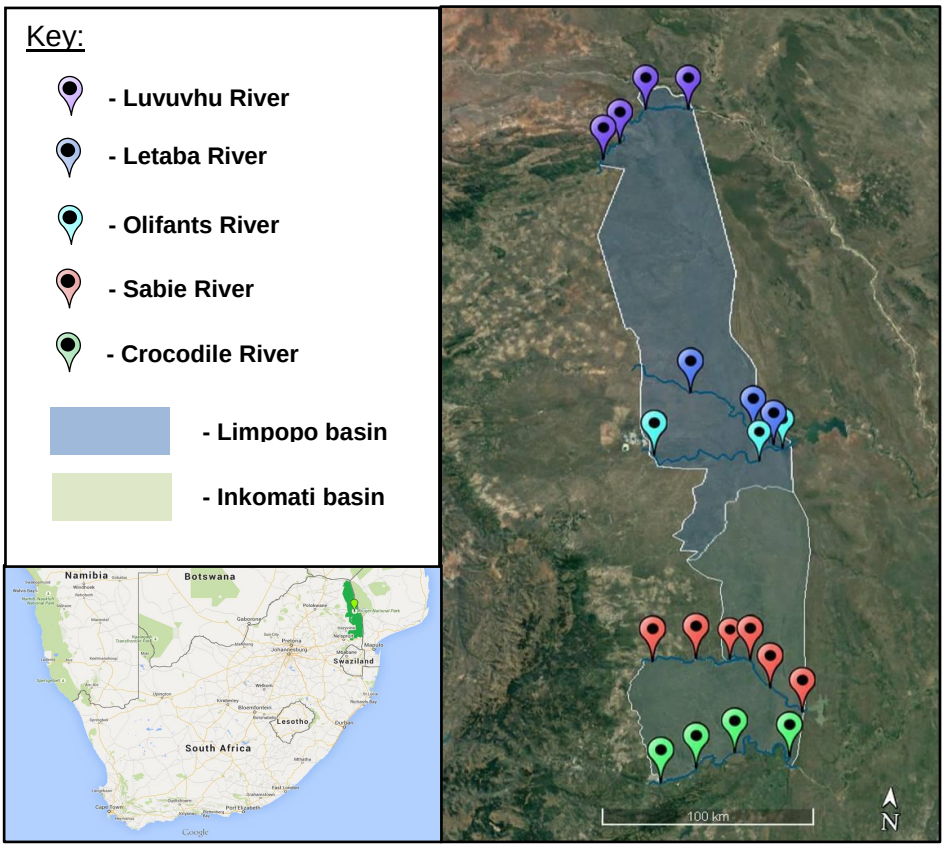

Figure 7: Sampling sites across the entire KNP as determined by the internal monitoring program. Crocodile River (green), Sabie River (red), Olifants and Letaba rivers (light blue and dark blue) Luvuvhu River (purple). Sections highlighted indicate the basin to which the rivers contribute (Incomati basin – green; Limpopo basin - blue).

2.2.2 Crocodile River

Four sites were selected and sampled in the Crocodile River (Figure 8). Only the Marula site was sampled during 2020 and 2021, the Nsikazi site was inaccessible and was not sampled during this time.

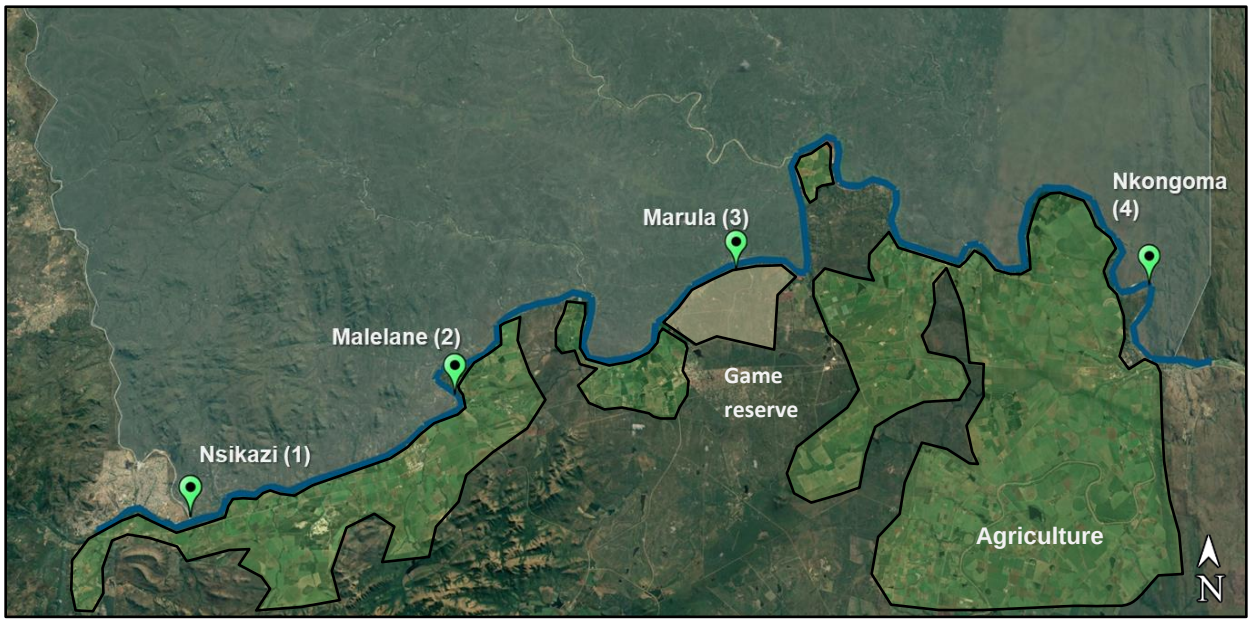

Figure 8: Sampling sites along the Crocodile River, sites also follow the direction of flow from west to east. Agricultural activities and the game reserve are situated on the right banks of the river.

Starting from the west is Nsikazi. This site is located near the town of Nsikazi and is close to the southwest border of the KNP (Figure 8). This site is not in the Crocodile River, but rather in a nearby tributary thereof, the Nsikazi River. From the confluence of the Nsikazi River, the Crocodile River is subject to agricultural practices along its southern banks. Unfortunately, no images are available for this site.

Further downstream, located near the sugarcane farming town of Malalane, is the Malelane site (Figure 8). It is located roughly 19 km downstream from the previous site and is characterised by shallow runs with a substrate consisting of pebbles, sand and rocks (Figure 9 - A). The site is situated under the bridge crossing the Crocodile River to access the Malelane Gate.

From Malelane, the river is bordered by more agricultural lands for roughly 22 km before reaching the Marula site 8 km further (Figure 8). This site is on the opposite bank to the Mjejane private game reserve in Mpumalanga, where most of the surrounding area is still in its natural

state and has not been converted for agriculture. This site is characterised by large boulders with deep pools and scattered riffles (Figure 9 - B).

Following the Mjejane Game Reserve, agricultural practice increases once more along the banks of the Crocodile River until it reaches the border of Mozambique. The last site, Nkongoma (Figure 8) is located near Crocodile Bridge, 50 km from the previous site and 7 km from Mozambique. Similar to the previous site, deep pools and stretches of riffles are present, however, large seams of bedrock are exposed in the immediate vicinity (Figure 9 - C and D).

Figure 9: Sampling sites along the Crocodile River during 2021, site numbering follows flow direction. (A – Malelane; B – Marula; C and D – Nkongoma).

2.2.3 Sabie River

Six sites along the Sabie-Sand river system were sampled (Figure 10). The Sekurukwane and Antholysta sites were the only sites sampled during 2020.

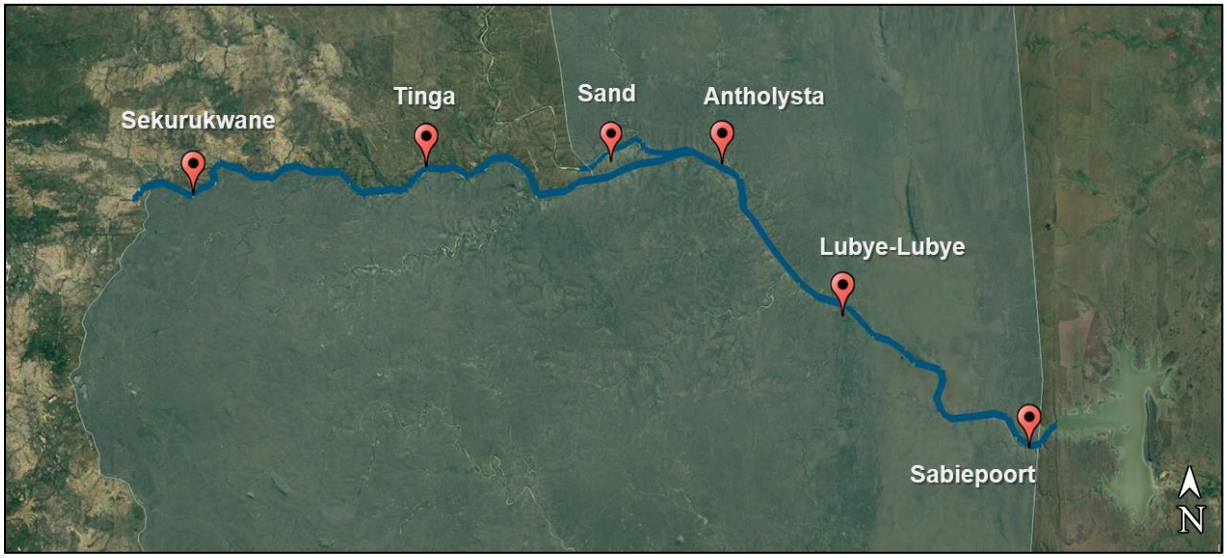

Figure 10: Sampling sites along the Sabie River with flow direction from west (Sekurukwane) to east (Sabiepoort).

From the West, the first site is Sekurukwane (Figure 10). This site is located near a large area of rural settlements. This site is characterised by sandy banks and abundant riparian vegetation (Figure 11 - A).

The next site, Tinga, is located 3 km downstream of the Paul Kruger Gate and roughly 25 km from the previous site (Figure 10). There is little anthropogenic activity in the vicinity of this site, an abundance of wildlife is usually present. The site is characterised by meandering runs flowing through scattered vegetation patches (Figure 11 – B).

A single site in the Sand River was also sampled, the river flows into the Sabie River roughly 4 km downstream from the sampling site (Figure 10). The Sand River, as the name suggests, is characterised by its large quantities of sandy sediment. Few boulders and rocks were present at the site (Figure 11 - C).

The Antholysta site is located 3 km downstream, from the confluence of the Sand and Sabie rivers and is within a stretch covered by a dense canopy, 18 km downstream of Antholysta is Lubye-Lubye (Figure 10). This site is located near the Lubye-Lubye Bridge (Figure 11 - D), many biotopes were present as well as an abundance of riparian vegetation. The stream flow

was incredibly strong at this site, and deep pools were present at various locations in the river channel.

The Sabiepoort site (Figure 10) lies 18 km further downstream from Lubye-Lubye, it is located 1 km upstream of where the Sabie River flows into Sabiepoort Dam (Figure 11- F), which is in Mozambique. This site is characterised by turbid waters and high sediment loads after floods. Many small boulders were present as well as scattered vegetation patches (Figure 11 - E).

Figure 11: Sampling sites along the Sabie River. Photos were taken during 2021. (A – Sekurukwane; B – Tinga; C – Sand; D – Lubye-Lubye; E – Sabiepoort; F – Sabiepoort Dam).

2.2.4 Olifants and Letaba rivers

2.2.4.1 Olifants River

Three sites were sampled along the Olifants River (Figure 12). No samples were taken during 2020 due to lockdown restrictions, however, all sites were sampled during 2021.

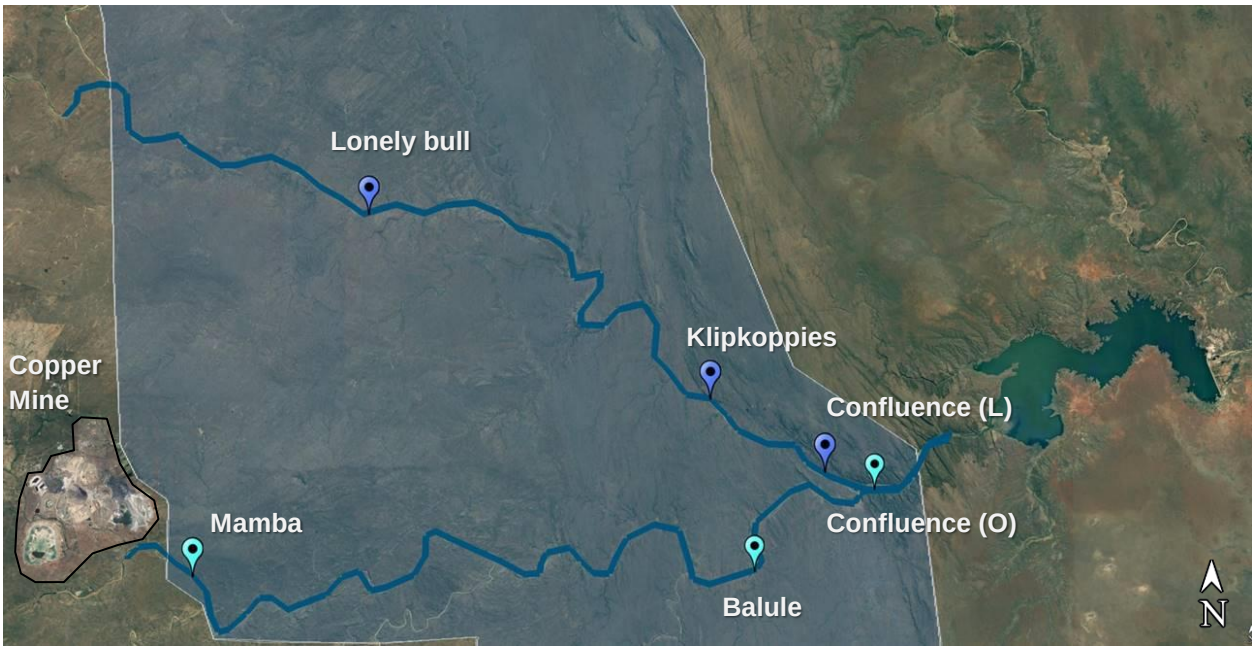

Figure 12: Olifants River (bottom) and Letaba River (top) as well as their confluences. The Palabora copper mine is indicated in red.

The first site in the Olifants River (Mamba) was located in the far west of the park, close to its border, and is one of the most remote sites sampled (Figure 12). This site is possibly subject to the nearby mining activities of the Palabora Mining Company.

This site was characterised by dense algal biofilm on instream boulders, an abundance of such boulders were present. Unfortunately no photos of the biofilm were taken. Riparian vegetation were scarce with scattered small trees along the banks (Figure 13 - A).

Roughly 70 km downstream of the Mamba site is the Balule site (Figure 12). This site was deep within the park and located relatively close to the confluence of the Olifants and the Letaba rivers. This site was located downstream of the Balule bridge, small boulders were present on the sandy outcrops of the river's channel (Figure 13 - B).

The confluence site was the last in the Olifants River, located 7 km downstream from the Balule site (Figure 12). This site is not to be confused with the Letaba confluence site. The Olifants

confluence site was located immedietly upstream of the true confluence point, whereas the Letaba confluence site was located 1 km upstream from the true confluence point (Figure 12).

The site was rather remote and located at the bottom of a steep gorge. The site was situated in the middle of three high lying areas, with a similar abundance of boulders present to others sites in the Olifants River (Figure 13 – C).

Figure 13: Sampling sites along the Olifants River (Mamba – A; Balule – B; Confluence - C) and one site in the Letaba River (Lonely Bull - D).

2.2.4.2 Letaba River

A total of three sites were sampled along the Letaba River. Only one site (Lonely Bull) was sampled during 2020. All sites were sampled during 2018, 2019 and 2021.

The lonely Bull site was the first site sampled in the Letaba River (Figure 12); it was located more or less in the middle of the river's course through the park. The stream channel was deeper than in the Olifants River, with larger boulders occurring less frequently. Algae was also present in high abundance (Figure 13 - D).

The Klipkoppies river site was located approximately 50 km downstream of the Lonely Bull site (Figure 12). This site was located near the confluence of the Olifants River and was quite remote. No image of this site is available. This site was located near a limited access bridge where the steam channel was relatively narrow. However, the riparian zone was wide and characterised by scattered reed patches and large boulders.

The Letaba Confluence site was located approximately 7 km downstream of the Klipkoppies site (Figure 12). Access to the site was difficult and no photos were taken of the site. The site was different from the others in the Letaba River, the river channel was shaped in such a way that many small and medium sized boulders had accumulated on the edges of the channel, ideal for diatom colonisation.

2.2.5 Luvuvhu River

Four sites were sampled in the Luvuvhu River (Figure 14), however, one of the sites (Bobomane) was not sampled during 2020 and 2021 due to flood alteration of the site morphology.

Figure 14: Sites along the Luvuvhu River, the last site (Bobomane) was located 10 km before the confluence with the Limpopo River.

The first site sampled, Dongadzhiva, was located near a rural settlement (Figure 14). The access to this site was difficult as the landscape surrounding this site was particularly hilly. Biotopes at this site were abundant and diverse, with patches of riparian vegetation, with boulders and large immovable bedrock exposed (Figure 15 – A & B).

From this site, the river flows through a high escarpment, weaving through the mountain scape until it reaches the Xindzivhani site (Figure 14). The Xindzivhani site was characterised by stretches of riffles, interrupted by occasional deep pools, creating runs (Figure 15 – C). It meanders along a deep escarpment for 3.5 km before flowing on relatively flat landscape, after which it reaches the Mutale confluence point (Figure 14).

The Mutale River joins the Luvuvhu River roughly 35 km downstream from the Xindizivhani site. The site was located near a weir in the Mutale River (Figure 16 - F), 1.7 km from its confluence

with the Luvuvhu River. Long stretches of slow moving water flow through a wide channel with large trees along the banks (Figure 16 - E). Riffles were present as stream flow increased below the weir as well as further down at the sampling point.

The Bobomane site, the furthest downstream, was characterised by a sandy bed and was morphologically altered by the floods of 2020 and 2021.

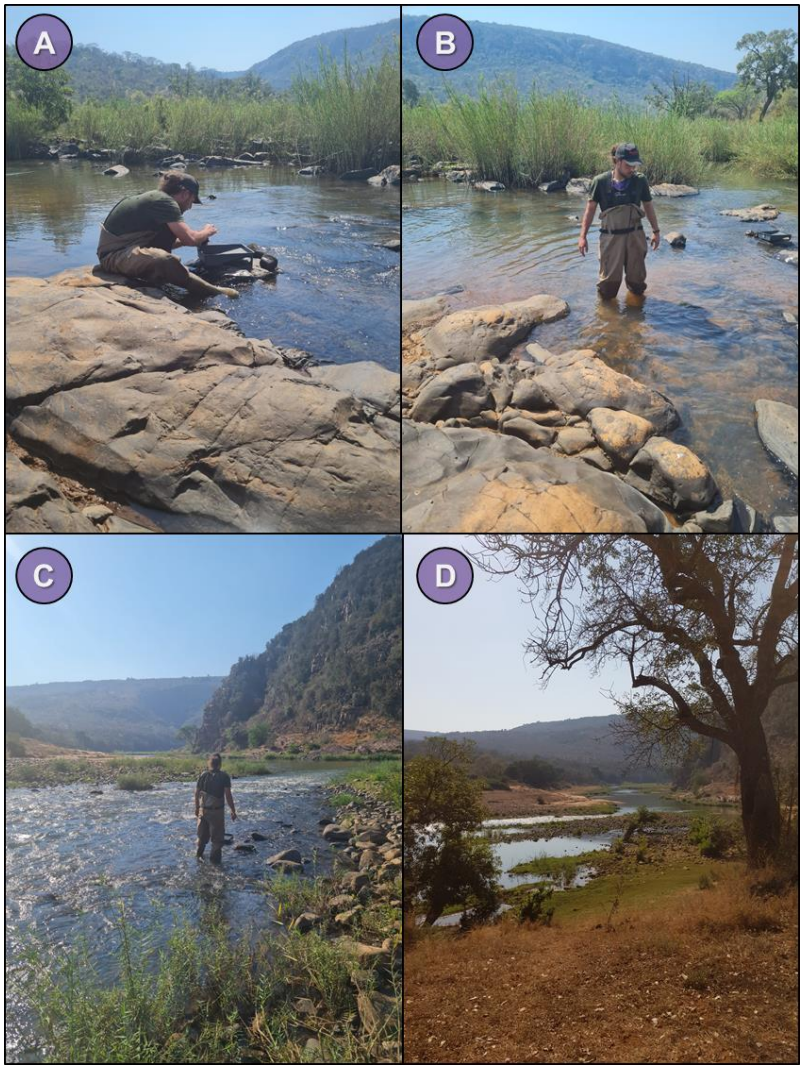

Figure 15: Two sampling sites along the Luvuvhu River. (A and B – Dongadzhiva; C and D - Xindzivhani).

Figure 16: Sampling site in the Mutale tributary, 1.7 km from confluence with Luvuvhu River (Mutale site).

2.3 Sampling

During the course of this project, samples were collected from various sites, as determined by the KNP's internal monitoring programme. Samples collected during 2018, 2019 and 2020 were taken by the KNP staff involved in the monitoring programme. Samples taken during 2021 were collected personally, together with staff of the KNP. Samples were collected during September of each respective year. Diatom sampling was done as described in Taylor et al. (2007a) and will be described in more detail below.

2.3.1 Diatoms

Diatom material from solid substrata (epilithon) was collected at each site. Diatoms were collected from 5 - 10 instream rocks and/or boulders from various locations within the sampling site (Figure 17). Afterward, the exposed side of each rock or boulder was scrubbed rigorously with a well-cleaned toothbrush to remove the diatoms. The substrate was then rinsed with some river water in a sample collection tray (Figure 18). The concentrated sample from the 5 - 10 rocks or boulders was then poured into a labelled (date and location), clean sample vial and preserved with 70% ethanol for later analysis (Figure 19).

Figure 17: Collecting rocks and boulders in-stream.

Figure 18: Scraping diatom material from rocks and boulders to obtain a concentrated sample.

Figure 19: Diatom samples, labelled and preserved, prior to processing.

Samples collected at each site were considered representative of the environmental conditions of that site. If time allowed, sub-samples were collected from different biotopes that were available, such as pools and rapids, for comparison as well as to determine if some biotopes serve as habitats for species not found in flowing waters, these types of subsamples were mostly collected in 2020.

2.3.2 Water quality

In conjunction with diatom samples, chemical water quality data were also collected, *in situ*, at sites for later comparison with diatom community composition (Figure 20). pH, electrical conductivity (EC), nitrate (NO_3^-) and sodium (Na^+) were measured using a Horiba LAQUA-twin test kit (Figure 21, left). Temperature (°C) and dissolved oxygen (DO) were measured by using a Hanna multi-oxygen meter (Figure 21, right). EC measurments are divided into low electrolyte content (50 - 100 µS/cm), moderate electrolyte content (100 - 500 µS/cm) and high electrolyte content (500 - 1000 µS/cm) (Coste in CEMAGREF, 1982). Water samples (1 L) (Figure 20 – bottom left) were also collected at the sites for laboratory analysis (*ex situ*) to determine the amount of inorganic compounds present. These compounds included chloride (Cl^-), phosphate as orthophosphate (PO_4^{3-}), sulphate (SO_4^2) and ammonia (NH_3).

Figure 20: Collecting *in situ* water quality by using a Hanna DO-meter (top left) and a Horiba LAQUA-twin multi-meter test kit (bottom left and right).

Figure 21: Test kits used for *in* situ water quality measurement; Horiba LAQUA-twin Test kit (Left) and Hanna DO-meter (Right).

Laboratory analysis of water samples was done by means of spectrophotometry, which entails the measurement of absorbance caused by dissolved solutes within a sample (Morris, 2015). A HACH DR3900 spectrophotometer was used and each test was completed on all samples on the same day, to ensure more reliable results. For the respective tests (PO_4^{3-}, SO_4^{2-}, Cl^- and NH_3) guidelines were followed according to (HACH, 2021).

2.4 Diatom sample processing and slide preparation

2.4 1 Processing

Sample processing was done as set out in Taylor *et al*. (2007a) according to the hot $KMnO_4$/HCl method. Figures 23 and 25 present the work-flow by which these samples were processed and how permanent slides were prepared.

Before samples were processed, the samples were settled for at least 12 h prior to processing (Figure 22 - A). The supernatant of each sample was decanted and discarded to obtain a concentrated sample for processing (Figure 22 - B). A small amount of concentrated sample (2-3 ml) was poured into a labelled heat-resistant test tube, the remainder of the sample was poured into a separate 10 ml vial for archiving and labelled accordingly.

The first step in processing the sample entailed the oxidation of biological material by using saturated potassium permanganate ($KMnO_4$), this helps to break down cell membranes and organelles. (Hasle & Fryxell, 1970) prior to acid digestion (Figure 22 – C) and ensures the exothermic reaction of HCl and organic material in the next step to be less volatile. Approximately 5 ml of $KMnO_4$ was added to each test tube and left overnight to complete oxidation (Figure 22 - D).

Concentrated HCl (30%) was then added to the oxidised sample and placed inside a 90°C water bath for 15 minutes, this step is the first part of the acid digestion process (Figure 22 - E). Acid digestion removes all the organic material in the sample; the sample will turn clear yellow when all or most organic material has been digested (Taylor *et al* 2007a). A few drops of 65% concentrated hydrogen peroxide (H_2O_2) were then added to each sample to ensure all organic material had been dissolved, no or weak bubbling will occur when all organic material has been removed (Figure 22 - F).

The final step of the process entails removal of the added chemicals from the sample before archiving and preservation can be done. The samples were washed with distilled water by means of centrifugation at 2500 rpm. Three to four cycles were run for 10 minutes at a time,

depending on the amount of digestive chemicals used. The cleaned sample was then poured into a labelled clean glass sample vial for storage and slide preparation (Figure 22 - G).

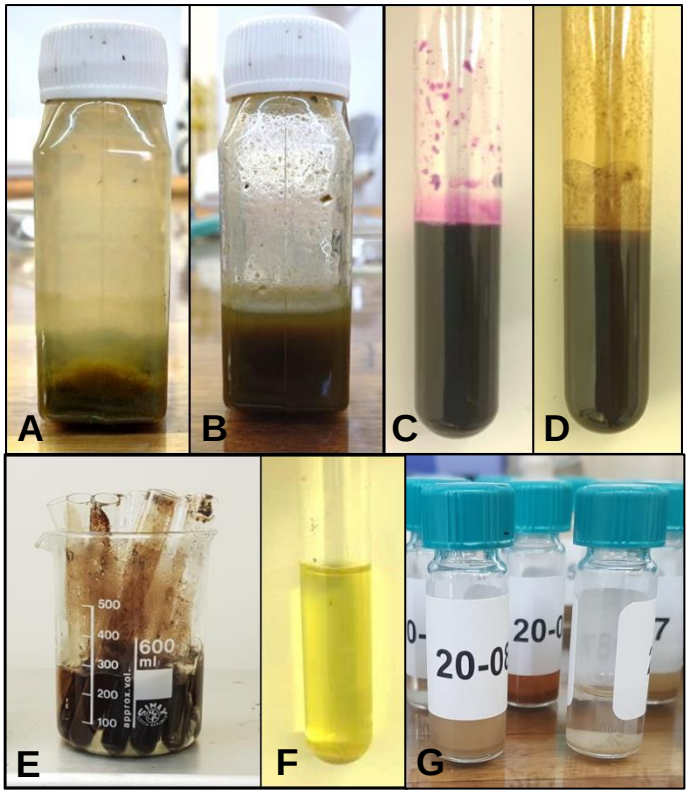

Figure 22: Diatom samples collected and processed by acid digestion. (A – Preserved sample; B – Decanted sample; C – Sample with $KMnO_4$; D – Oxidised sample; E – Acid digestion of sample with HCl; F – Sample after acid digestion; G – Clean sample in a labelled sample vial).

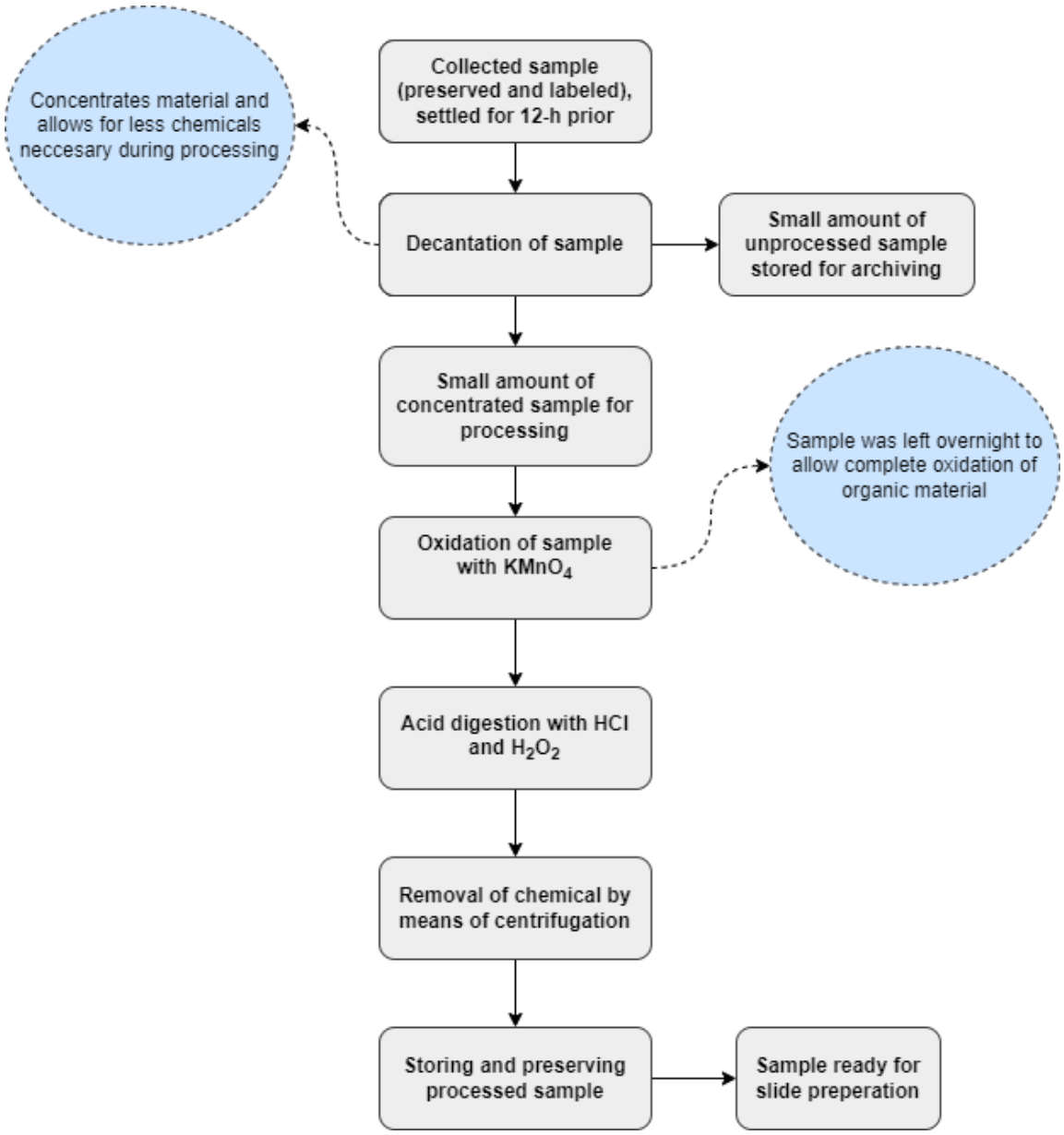

Figure 23: Diagrammatic overview of the acid digestion (hot KMnO4/HCl method) processing steps.

2.4.2 Microscope slide preparation

The samples were prepared before permanently mounting on microscope slides by mixing distilled water, ammonium chloride (NH_4Cl) and small amounts of processed samples in test tubes. The NH_4Cl neutralises the surface charge on the diatom cells and sediment particles and allows diatoms valves to be evenly spaced and not clustered together (Taylor *et al*., 2007a). This step allows permanent slides to be more easily inspected and identifications to be made with greater confidence, ultimately improving the reliability of results.

To prepare permanent diatom slides, a small amount of the diluted sample (400 µl) was added to a round coverslip until a bubble of water was formed, which pushes the frustule-rich water to the edges. This was then allowed to air-dry overnight (Figure 24 - A). The use of a round coverslip also allows for an even distribution of diatom valves as the coverslip dries, natural desiccation also allows a slow and even settlement of diatom valves on the coverslip.

Once dry, the coverslips were placed on a hotplate at 255°C and left for a few seconds until the NH_4Cl had sublimated (Figure 24 - B), when this does not occur in completion, NH_4Cl crystals form within and on diatom valves, obscuring diagnostic features and further complicates identification.

A small drop of Pleurax mounting medium (Von Stosch, 1974) was placed on the face of the coverslip (Figure 24 - C) after which a labelled microscope slide was lowered on top and immediately turned over when joined (Figure 24 - D). The slide was left on the hotplate for a few minutes to harden and set the Pleurax. If the Pleurax fails to set, diatom valves can migrate on the slide (Von Stosch, 1974). Pleurax has a refractive index of 1.73 and skews the path of the light slightly as it passes through the mount, this increases the visibility of the diagnostic features of diatom cells.

2.4.3 Permanent slide inspection

Slides were inspected with a Nikon Eclipse 80i light microscope (LM) (Figure 24 - E) with Differential Interference Contrast (DIC) under 100x magnification (Figure 24 - F). DIC aids in illuminating the diagnostic features of taxa more clearly (Round *et al*., 1990), which is important for diatom identification to species level.

In each field observed under LM, the diatoms present were identified and enumerated before moving to the next field. A total of 400 valves were counted and identified on each slide to represent the community structure at each site. Diatoms were identified to genus and species level using the reference works listed below, photographs were taken for confirmation of identification and archiving.

References used for diatom identification include: Gasse, 1986; Krammer, 2002; Krammer, 2003; Krammer & Lange-Bertalot, 1986; Krammer & Lange-Bertalot, 2004a; Krammer & Lange-Bertalot, 2004b; Krammer & Lange-Bertalot, 2007a; Krammer & Lange-Bertalot, 2007b; Lange-Bertalot, 2001; Lange-Bertalot & Metzeltin, 1996; Lange-Bertalot *et al*., 2011; Lange-Bertalot *et*

al., 2017; Levkov, 2009; Simonsen, 1987a; Simonsen, 1987b; Simonsen, 1987c; Taylor *et al*., 2007b; Taylor & Cocquyt, 2016.

Figure 24: Slide preparation and inspection. (A - Dried sample on coverslip; B – Coverslip after NH_4Cl has sublimated; C – Coverslip with drop of Pleurax; D – Coverslip mounted to a microscope slide; E – Nikon 80i eclipse microscope; F - Diatoms viewed under DIC).

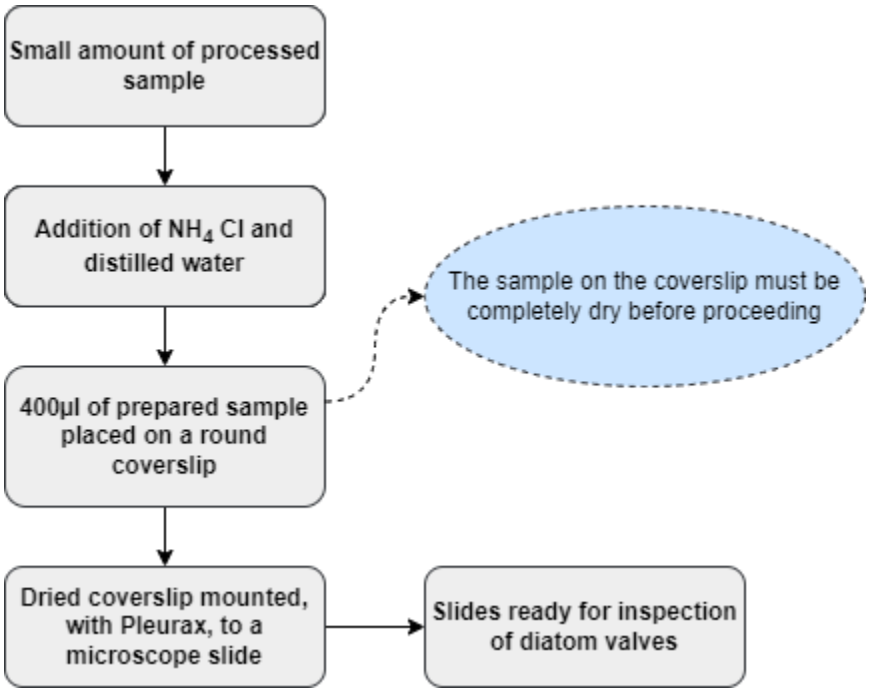

Figure 25: Overview of the microscope slide preparation steps.

2.5 Data analysis

2.5.1 Correlation analysis

Pearson correlation (r analysis) and R^2 analysis were used to determine the strength of relationship between *in situ* measured ionic compounds and electrical conductivity, to determine which ions had the greatest contribution to the overall electrical conductivity. Correlation was carried out between all sites sampled in all rivers and not between sites within each river sampled. Some rivers were sampled at only three sites, which is not enough to conduct separate correlation analysis. Additionally, correlation analysis was conducted on the IPS scores and measured EC to illustrate the influence of electrolyte content on the index scores obtained. Prior to analysis, all water quality data were standardised by log transformation. STATISTICA v10 was used to calculate Pearson correlation coefficients (r) as well as R^2 and p-values.

STATISTICA v10 was also used to plot the relationship between IPS scores, as averaged for each river during each year, with the total average rainfall across the entire park from 2018 to 2021. This is explained further in section 2.5.3.

Pearson correlation is a measure of how strong a relationship is between two variables. The absolute value can only range from 0-1 where 0 indicates zero correlation and 1 indicates absolute correlation, consequently a value of 0.5 indicates a moderate correlation (Schober *et al.*, 2018). The r value can, however, be negative or positive while ranging from 0 - 1. Therefore it follows that r can range from -1 to 0 and from 0 - 1; the latter being a positive correlation and the former a negative or inverse correlation. Two variables can only correlate to an extent of 0% or 100%, therefore the r value will always be between 0 and 1, whether that be on a positive or negative scale.

An R^2 value, on the other hand, indicates the amount of variation in one variable that is responsible for the variation in another (Miles, 2005). This means that two variables can have a strong correlation (r) but the change in the values for those variables is not necessarily due to one or the other's influence (R^2).

The R^2 value is highly useful in indicating how much of the variance in the dependant variable (response variable or Y) can be explained by the variance in the independent variable (predictor variable or X) (Miles, 2005). This means that if two variables have an R^2 value of 0.31, only 31%

of the variance in the dependant variable can explain the variance in the independent variable, and therefore the correlation is considered weak.

p-values allow for further additional information pertaining to the significance of the correlation. A p-value will indicate how significant the correlation is between two variables, two variables can have a strong correlation but with little or much significance.

p-values range from 0 to 1, however, are interpreted differently than r values. Lower p-values indicate greater significance than higher p-values. The p-value indicates on the influence of randomness accounting for the correlation between variables. When $p < 0.05$, it implies that the chance that random events cause the correlation between variables is only 0.5% (Vildirim, 2020). The threshold for significance is set at $p < 0.05$ and was also used in the present study.

2.5.2 Multivariate analysis

Canonical Correspondence Analysis (CCA) was used to determine and illustrate the relationship between diatom community structures and their autecological preferences with environmental variables at the respective sites sampled.

CCA is a direct ordination technique that assumes unimodal distributions of species along environmental gradients (Ter Braak, 1995a). The software program commonly used for these purposes is CANOCO, also used in the present study. CCA is also constrained, which eliminates the arch effect caused by the unimodal species distribution curves exerted by diatoms (Ter Braak, 1995a).

Ordination illustrates results in a graphically interpretable way, it ordinates (plots) the correlation between variables in a dimensional space to show the relationships between them (Ter Braak, 1995b). Indirect ordination (PCA and DCA) plots the response variable (species) and then adds the predictor variable (environmental) as a way of explaining the variance in the first. Direct ordination (CCA) on the other hand, considers the response variable to be function of the predictor variable and thereby considers the variance in both variables at the same time (Ter Braak & Prentice, 1988).

Only CCA was used to illustrate the relationships between diatom autecology and environmental variables. The reasons for this are twofold. Firstly, only DCA and CCA were considered appropriate given the available data since they assume unimodal species distributions under environmental gradients, which diatoms adhere to, as mentioned. Secondly, CCA incorporates three components at once (species, sites, and variables) while DCA only

incorporates two components (species and sites). Therefore, a CCA plots best illustrate the autecological relationships of diatom taxa toward environmental variables.

A DCA plot was, however, created for sites sampled during 2020, since no water quality data were collected. This provides a good opportunity to illustrate that, if no water quality is available, the autecology of diatoms can be used to extrapolate water quality in an indirect ordination plot, given the technique used assumes unimodal species distributions under environmental gradients.

2.5.3 Diatom Index calculation

The IPS, which was the preferred index for this study, allocates a score to each of the genera, or species, occurring in a specific biotope subjected to environmental pressures to determine the degree of nutrient, ionic and organic pollution present.

The magnitude of the environmental disturbance and autecology of taxa determine the diatom community composition (Tornés *et al*., 2015). The index is very reliable and has been used recently in the KNP previously by Shikwambana et al. (2021) and Oxley (2021). The index score is scaled from 0 – 20 and given a corresponding ecological class (A - E) as well as a trophic state (Table 1). Diatom index scores were calculated using Omnidia version 5.3 (Lecointe *et al*., 1993). The water quality data obtained by using diatoms were compared between years sampled to determine which rivers had lower water quality and which had higher water quality in terms of trophic status, ionic concentrations and organic material.

An increase in trophic state is associated with increased nutrient loads, these nutrients are dissolved when in water and contribute to the overall ionic charge, in addition to the other ionic compounds present, such as sodium, chloride, calcium, magnesium, etc. that also contribute to the ionic load in water. A change in nutrient concentration and ionic composition of water will, therefore, alter the electrical conductivity. Thus, a change in nutrients (trophic state) and ionic load will alter the inferred water quality (IPS score), since diatoms are sensitive to such change. The relationship between IPS scores and measured electrical conductivity will also be illustrated. Additionally, the IPS scores were averaged across sites in each river for each year and compared to the average total rainfall for the respective year, to illustrate the change in IPS in response to the increased average total rainfall from 2018 to 2021. As the total average rainfall increased, a dilution or flushing effect was expected, thereby reducing pollutant, nutrient and ionic load in rivers. A positive relationship between IPS scores and average total rainfall is therefore expected.

Table 1: Ecological classes for IPS scores. Redrawn from (Shikwambana *et al.*, 2021).

Ecological Class	Water Quality	Trophic level	IPS Score
A	High	Oligotrophic	> 17
B	Good	Oligo-mesotrophic	15 – 17
C	Moderate	Mesotrophic	12 – 15
D	Poor	Meso-eutrophic	9 – 12
E	Bad	Eutrophic	< 9

Chapter 3: Results and discussion

3.1 Water quality

This section is divided into two parts, the first section deals with water quality measured during 2018 and 2019 (Table 2), and the second part deals with water quality measured during 2021 (Table 3). The reasons for this were twofold. Firstly, no water quality was measured during 2020 due to lockdown restrictions. Secondly, different water quality parameters were measured during 2018, 2019 and 2021. During 2018 and 2019 only pH, salinity, EC and turbidity were measured. During 2021 Na^+, EC, pH, NO_3^-, DO and temperature were measured *in situ*, and Cl^-, NH_3, SO_4^{2-} and PO_4^{3-} were measured *ex situ*. Therefore, only spatial changes in water quality are illustrated for each respective year in which water quality was available. Temporal changes in water quality were illustrated by using diatoms since samples were taken in each year from 2018 to 2021.

3.1.1 2018 and 2019

The water quality for 2018 and 2019 was only measured in situ. pH, EC, turbidity and salinity were measured; however, salinity was not included in the results because it is essentially calculated from EC. Also, turbidity measurements were not taken for all sites, the sites with missing information are marked with N/A. Site numbers (CCA nr and EC graph nr) only pertain to specific years (Table 2). Corresponding site numbers for years should be used in corresponding graphs and figures pertaining to the results of the same year. The CCA nr refers to the number given to a specific site in the CCA plot (Figure 40); the same site has two numbers, one for 2018 and one for 2019. The two numbers for the same site are also coloured the same to aid in the visual interpretation of the graph. The EC graph number refers to the number given to a specific site in the EC graph (Figure 26 and 27), here the specific sites for both years have the same number.

Table 2: Water quality measured, *in situ*, during 2018 and 2019.

Year	River	Site name	CCA Nr	EC graph nr	pH	EC (µS/cm)	Turbidity (NTU)
2018	Crocodile	Nsikazi	1	6	8.57	501	83
		Malelane	2	7	8.68	413	76
		Marula	3	8	8.41	440	81
		Nkongoma	4	9	8.79	593	86
	Sabie	Sekurukwane	5	1	9.04	126.8	84
		Tinga	6	2	8.86	132.3	79
		Antholysta	7	3	8	133.8	71
		Lubye-Lubye	8	4	8.39	144.6	15
		Sabiepoort	9	5	7.71	156	48
	Olifants	Mamba	10	10	8.8	577	24
		Balule	11	11	8.89	613	21
		Confluence	12	12	8.79	645	76
	Letaba	Lonely Bull	13	13	8.78	598	62
		Confluence	14	14	9.93	537	97
	Luvuvhu	Dongadziva	15	15	7.96	146.8	N/A
		Xindzivhani	16	16	8.3	158.3	N/A
		Mutale (Outpost)	17	17	8.61	152.8	N/A
		Bobomane	18	18	8.69	160.9	N/A
2019	Crocodile	Nsikazi	19	6	8.71	518	88
		Malelane	20	7	8.95	485	86
		Marula	21	8	8.43	582	80
		Nkongoma	22	9	9.08	817	97
	Sabie	Sekurukwane	23	1	8.6	121.5	89
		Tinga	24	2	8.45	128.1	75
		Antholysta	25	3	8.41	143.6	62
		Lubye-Lubye	26	4	8.3	153.4	18
		Sabiepoort	27	5	7.6	154.8	57
	Olifants	Mamba	28	10	9.21	773	65
		Balule	29	11	8.95	762	58
		Confluence	30	12	8.89	705	59
	Letaba	Lonely Bull	31	13	8.2	598	62
		Confluence	32	14	9.58	537	97
	Luvuvhu	Dongadziva	33	15	8.26	164.4	N/A
		Xindzivhani	34	16	8.33	166.3	N/A
		Mutale (Outpost)	35	17	8.4	267	N/A
		Bobomane	36	18	8.84	216	N/A

3.1.1.1 Measured water quality

The water quality parameters measured during 2018 and 2019 include salinity, pH, EC and turbidity. Salinity and EC are essentially measurements of the same environmental parameter, ionic salts (DWAF, 1996b).

pH does not vary much between sites in the various rivers. Similarly, across years, pH change is not highly evident (Table 2). Rivers in South Africa are generally well-buffered with pH ranges between 6 and 8 (DWAF, 1996b). The pH for all sites sampled are, however, above 8 except for three sites (2018 – Antholysta, Dongadzhiva; 2019 - Sabiepoort). In the Sabie River, pH seems to decrease with flow direction, the same profile is followed during 2019. The average pH for 2019 (8.27) was lower than in 2018 (8.4), however, only slightly. pH also fluctuates diurnally through alteration of the carbonate/bicarbonate equilibrium (DWAF, 1996b) and hence changes often within rivers.

A clear distinction can be made between the studied rivers in terms of EC. Sites in the Sabie and Luvuvhu rivers had an EC of less than 300 µS/cm during both 2018 and 2019 (Figure 26 & 27), this indicates moderate to low electrolyte content (Cox, 1996). The EC range is similar between sites across years, little variation occurs in the EC value from 2018 to 2019, and little variation occurs with flow direction (Figures 26 and 27).

The EC measured in the Crocodile River during 2018 had moderate EC, however, some sites approached 500 µS/cm, bordering on high electrolyte content (Cox, 1996). The Nkongoma site has an EC value close to 600 µS/cm (Figure 26) which is within the range for high electrolyte content (500 – 1000 µS/cm) (Cox, 1996). A general increase in the EC is observed from 2018 to 2019 in the Crocodile River; the EC range is within moderate to high levels (Figures 26 and 27). The EC measured for the Nkongoma site increased with more than 200 µS/cm from 2018 to 2019 and was close to the upper threshold for high electrolyte content (1000 µS/cm) at 817 µS/cm.

A similar high EC is evident for the Olifants and Letaba rivers during 2018 and 2019, however, little change occurred from 2018 to 2019 in the Letaba River, while in the Olifants River, a general increase in EC was evident (Figures 26 and 27). The electrolyte content for these rivers was also considered moderate to high according to Cox (1996) classification scheme.

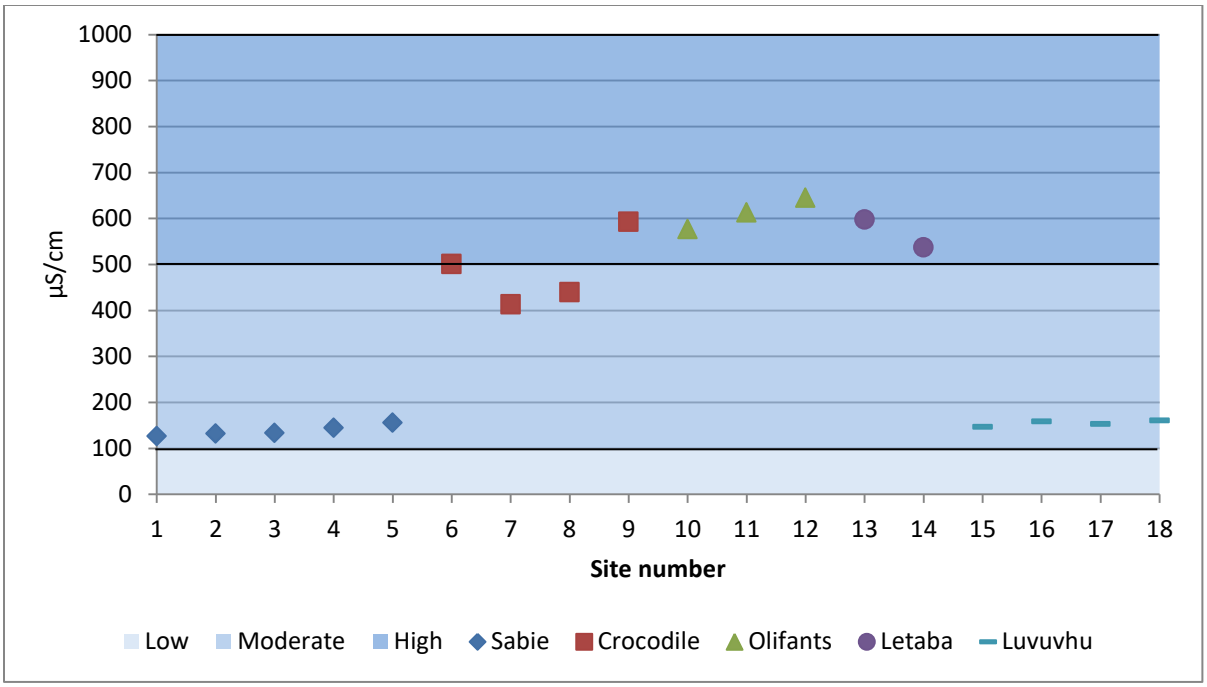

Figure 26: EC measured for all sites sampled during 2018. (Refer to Table 2 for site names).

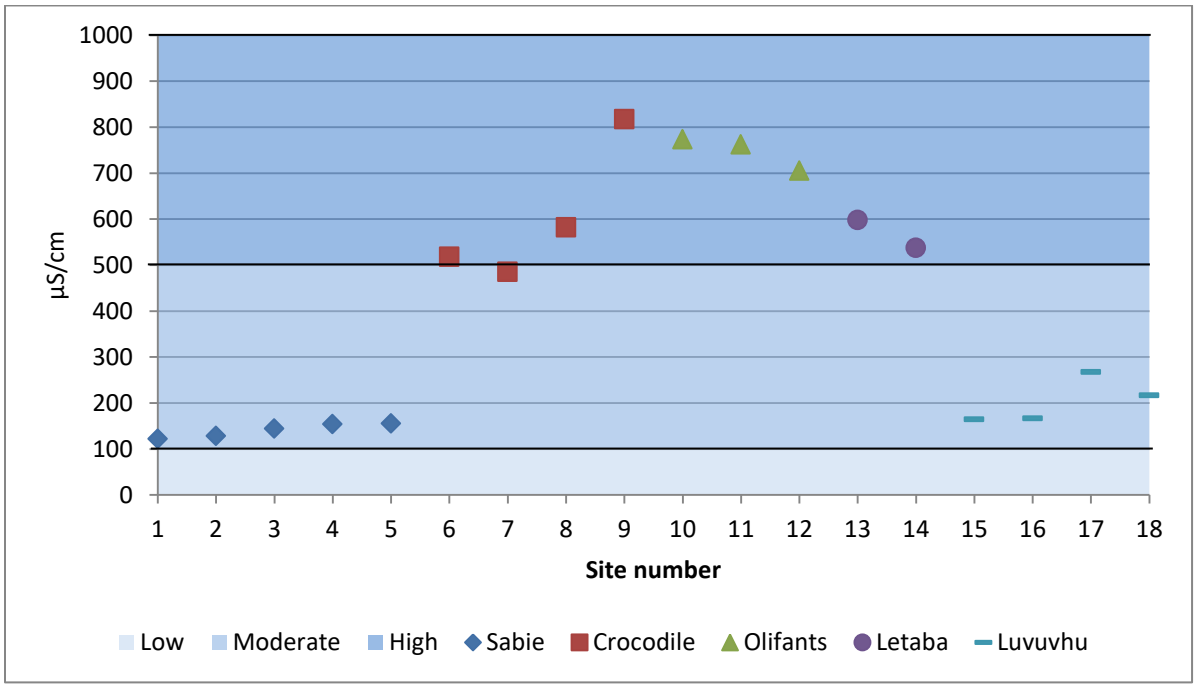

Figure 27: EC measured for all sites sampled during 2019. (Refer to Table 2 for site names).

With regard to turbidity, the highest values were observed in the Crocodile River, not fluctuating much between years, however, the values during 2018 were slightly lower (Table 2). Turbidity for the Letaba River did not change from year-to-year but increased with distance downstream, however, only data for two sites were available during 2018 and 2019. Turbidity is also best used when compared to the reference turbidity for respective rivers to examine changes from natural conditions (DWAF, 1996b), data on the reference turbidity was not available for rivers sampled.

The turbidity in the Olifants River was higher during 2019 than 2018, it was also similar across sites during that year (Table 2). During 2018 at the Mamba and Balule sites, turbidity was very low and gradually increased toward the confluence site (Table 2). The Sabie River seem to have higher turbidity than most rivers sampled at three of its sites. The Sekurukwane, Tinga and Antholysta sites had higher turbidity in both 2018 and 2019. The Lubye-Lubye site on the other hand had a very low turbidity across years sampled (Table 2). The Sabiepoort site had an average turbidity compared to other sites within the Sabie River.

3.1.2 2021

This section deals with the water quality parameters measured during 2021, parameters were measured *in situ* and *ex situ* (Table 3). The ionic compounds measured include Na^{+}, NO_3^{-}, Cl^{-}, NH_3, SO_4^{2-} and PO_4^{3-}. EC was also measured, *in situ*, as a collective representation of the ionic compounds present at each site in addition to pH, DO and temperature. The correlations between the ionic compounds measured and EC were done using Pearson correlation and R^2 analysis. This aims to explain which ionic compounds measured contribute most to the variation in EC.

Table 3: Water quality parameter values measured and calculated during 2021.

				in situ						*ex situ*			
				mg/L	µS/cm		mg/L	mg/L	°C	mg/L	mg/L	mg/L	mg/L
Year	**River**	**Site**	**Nr**	**Na^+**	**EC**	**pH**	**NO_3^-**	**DO**	**Temp**	**Cl^-**	**NH_3**	**SO_4^{2-}**	**PO_4^{3-}**
2021	**Sabie**	Sekurukwane	1	7	148	7.35	16	4.7	21.6	0.2	0.24	69.5	0.08
		Tinga	2	9	165	7.55	13	5.12	24.8	1	0.32	83.6	0.13
		Sand	3	30	234	8.24	14	5.29	27.9	10.8	0.06	69.8	0.03
		Lubye-Lubye	4	12	176	8.21	7	6.56	20.8	2.8	0.18	69.6	0.17
		Antholysta	5	16	178	8.37	12	5.98	28.1	6	0.16	92.4	0.07
		Sabiepoort	6	13	209	7.37	8	5.37	23	2.8	0.06	72.9	0.1
	Crocodile	Malelane	7	40	518	7.28	17	6.34	18.7	35.9	0.31	198	0.53
		Marula	8	48	570	8.11	11	6.75	19	11.5	0.04	90	0.07
		Nkongoma	9	69	742	8.23	17	7.13	21	39.4	0.18	94.1	0.05
	Olifants	Mamba	10	72	852	7.72	17	8.39	24	24.9	0.19	166	0.28
		Balule	11	49	738	8.42	21	5.73	27.6	25.2	0.18	129	0.06
		Confluence	12	60	620	8.44	20	7.19	24.2	35.4	0.32	537	0.12
	Letaba	Lonely Bull	13	54	335	6.31	14	6.62	20.3	17.4	0.17	69.1	0.07
		Klipkoppies	14	49	476	8.75	15	7.4	27.6	26.2	0.16	70.9	0.13
		Confluence	15	70	502	7.76	23	5.3	24.4	57	0.38	89.8	0.38
	Luvuvhu	Dongadzhiva	16	11	145	7.73	15	5.21	24.7	1.7	0.15	67.6	0.03
		Xindizivhani	17	11	142	8.04	10	5.77	25.5	1.8	0.15	68.4	0.02
		Mutale/Outpost	18	48	145	6.33	14	6.16	21.9	11.7	0.21	68.4	0.04

3.1.2.1 Measured water quality

A clear distinction can be seen in terms of electrical conductivity (EC) in the various rivers. The Crocodile and Olifants rivers had moderate (100 – 500 µS/cm) to high (500 – 1000 µS/cm) EC values compared to the Letaba, Sabie and Luvuvhu rivers (Figure 28). The EC values for the Letaba River were, however, closer to those measured in the Crocodile and Olifants rivers and are considered moderate (100 – 500 µS/cm) (Cox, 1996). The EC values for the Luvuvhu and Sabie rivers were considered to be moderate as well, however, no values exceeded 300 µS/cm. None of the sites sampled had low electrical conductivity (0 -100 µS/cm) (Cox, 1996).

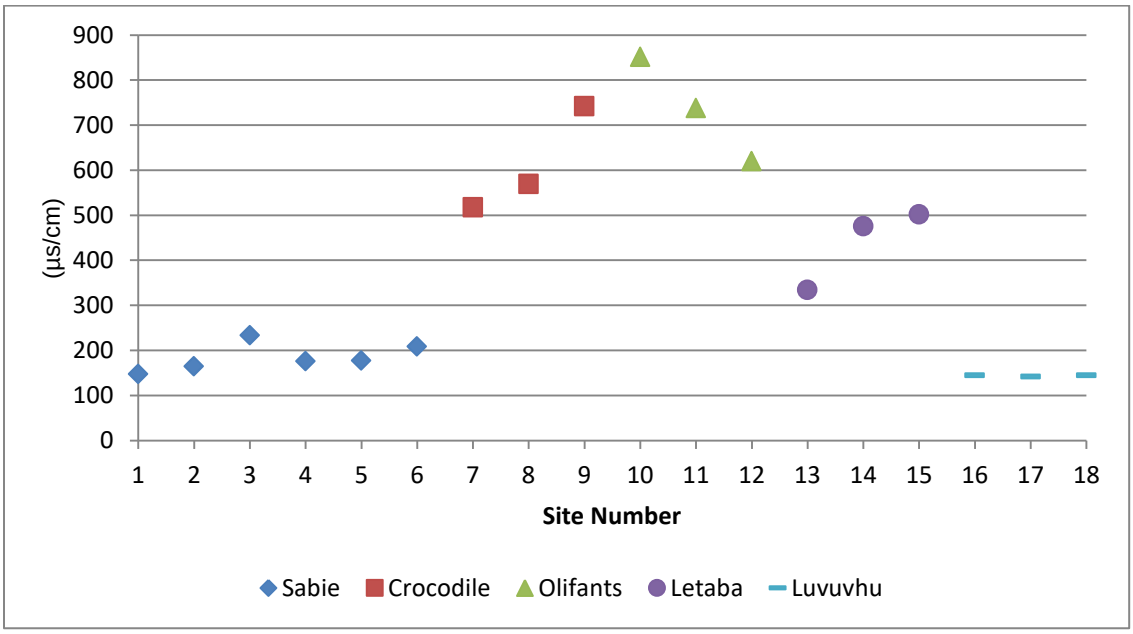

Figure 28: EC measured for all sites sampled in 2021 (Refer to Table 3 for site names).

The Letaba, Olifants and Crocodile rivers had sodium concentrations ranging between 40 and 70 mg/L, in addition to one site in the Mutale River (48 mg/L) (Figure 29). The remaining sites in the Luvuvhu River and all the sites in the Sabie River had sodium levels less than 16 mg/L, except for the Sand River (30 mg/L) (Table 3). Sodium occurrence is generally ubiquitous and depends on the surrounding geology, it often occurs as sodium chloride (NaCl) and also sodium nitrate ($NaNO_3$) (DWAF, 1996c). The occurrence of sodium is generally linked to rainfall, rivers in areas that experience low mean annual rainfall generally have higher levels of sodium. In contrast, rivers in areas that receive high mean annual rainfall, have lower levels of sodium (DWAF, 1996c).

Rainfall in the KNP is generally higher in the southern part of the park than in the north. However, near Punda-Maria (Luvuvhu River), the rainfall increases due to the updraft created by the Shitshova hills, as explained in section 2.1. Similarly rainfall is higher near the southwest border of the park, near the Khandizwe hills, due to updrafts created as well as the general increase in rainfall from east to west (MacFadyen *et al*., 2018).

Taking this link between sodium and rainfall, as described above, a higher sodium level is expected for the Olifants and Letaba rivers due to their position in the middle of the park that receive less rain. Similarly, the sodium levels in the Sabie, Crocodile and Luvuvhu rivers are expected to be lower due to the higher rainfall in these areas compared to the aforementioned rivers. In most cases the correlation between rainfall and measured sodium can be observed, however, according to the results of this study, sites in the Crocodile River have much greater sodium levels compared to other rivers that receive similarly high rainfall, such as the Sabie and Luvuvhu rivers. The Letaba and Olifants rivers had similar sodium levels to the Crocodile River, however, the rainfall in the middle of the park was generally lower and can constitute lower dilution of sodium (refer to the description on page 22 together with Figure 7). This suggests a possible increase in sodium levels within the Crocodile River due to runoff from the surrounding agricultural practices, as these activities are typically associated with increases in sodium levels through surface runoff from irrigated soil as well as with the general increase of sodium concentration associated with water re-use (DWAF, 1996c).

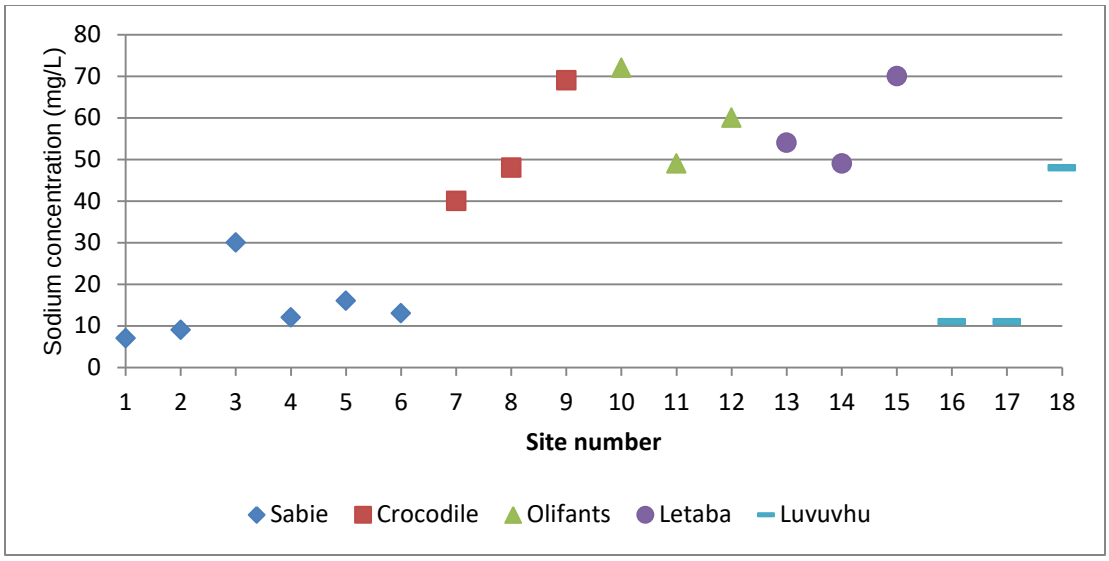

Figure 29: Sodium (Na^+) concentration measured for all sites sampled in 2021 (refer to Table 3 for site names).

Similar to sodium, chloride is ubiquitous in nature and usually leech from salt deposits in the lower rock strata and therefore the concentration thereof, in rivers, depends on the geology of the surrounding area (DWAF, 1996a; DWAF, 1996d). Levels can range from 0 mg/L to a few hundred mg/L in freshwater and chloride contributes greatly to electrolyte content and total suspended solids (TSS) (DWAF, 1996d).

Chloride levels were lower in the Sabie and Luvuvhu rivers than in the Crocodile, Letaba and Olifants rivers. Most sites in the Sabie River had chloride concentrations between 0 - 3 mg/L (Figure 30 and Table 3), the Antholysta site, however, had chloride concentrations of 6 mg/L, and the Sand River had a higher chloride concentration of 10.8 mg/L. Chloride levels in the Luvuvhu River ranged between 0 - 2 mg/L (Figure 30 and Table 3), except for the site sampled in the Mutale River, which had a chloride concentration of 11.7 mg/L.

For the Crocodile, Letaba and Olifants rivers, chloride concentration were seldom below 20 mg/L, only two sites (Marula and Lonely Bull) had lower chloride levels of 11.5 mg/L and 17.4 mg/L, respectively (Figure 30 & Table 3). The remaining sites in the Crocodile River had chloride levels between 35 and 40 mg/L while the remaining sites in the Letaba River had more variable concentrations with 26.2 mg/L at the second site sampled (Klipkoppies) and 57 mg/L at the last site sampled (Confluence). All sites in the Olifants River had chloride levels between 25 and 36 mg/L (Figure 30 and Table 3).

As with sodium, chloride concentration and rainfall intensity are often linked. However, chloride levels were high in the Crocodile River and were similar to that of the Letaba and Olifants rivers and not to those of the Sabie and Luvuvhu rivers (as was the case for sodium). Increases in chloride levels are often due to irrigation return flows and sewage effluent discharges, re-use of water increases the chloride concentration with each cycle (DWAF, 1996a). The higher chloride concentration in the Crocodile River may be due to similar reasons as discussed for sodium, however, these values are relatively low and do not show high levels of salinisation (DWAF, 1996a; DWAF, 1996d).

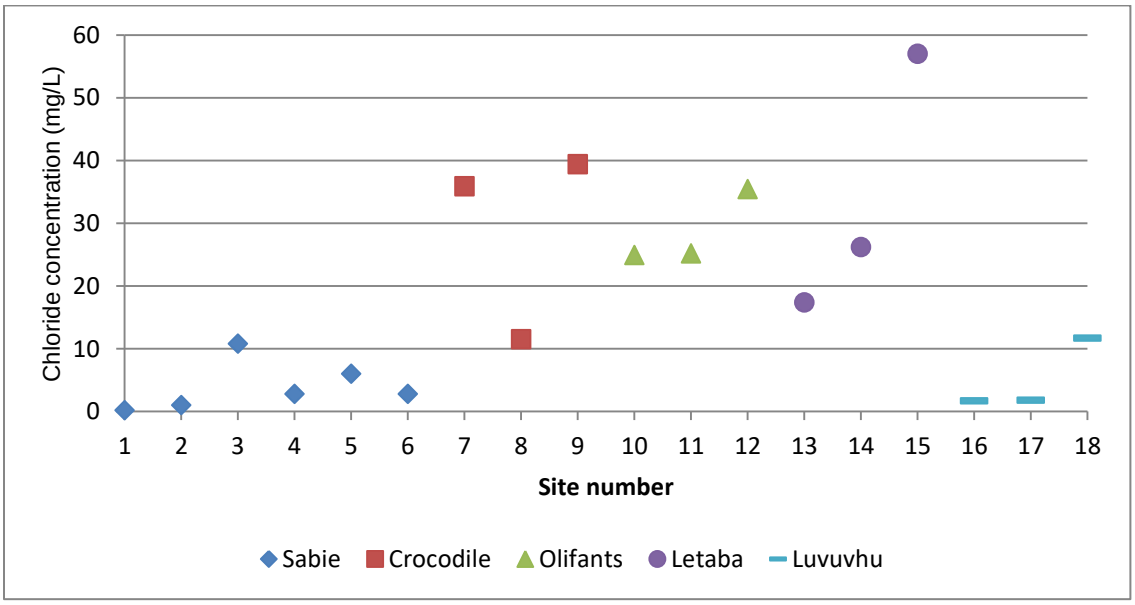

Figure 30: Chloride (Cl^-) concentration measured for all sites sampled in 2021 (refer to Table 3 for site names).

There were no discernable trends in pH in the rivers sampled, most pH levels were between 7 and 9 (Figure 31), with two sites having a pH lower than 7 (Letaba – Lonely Bull; Luvuvhu - Mutale), Table 3.

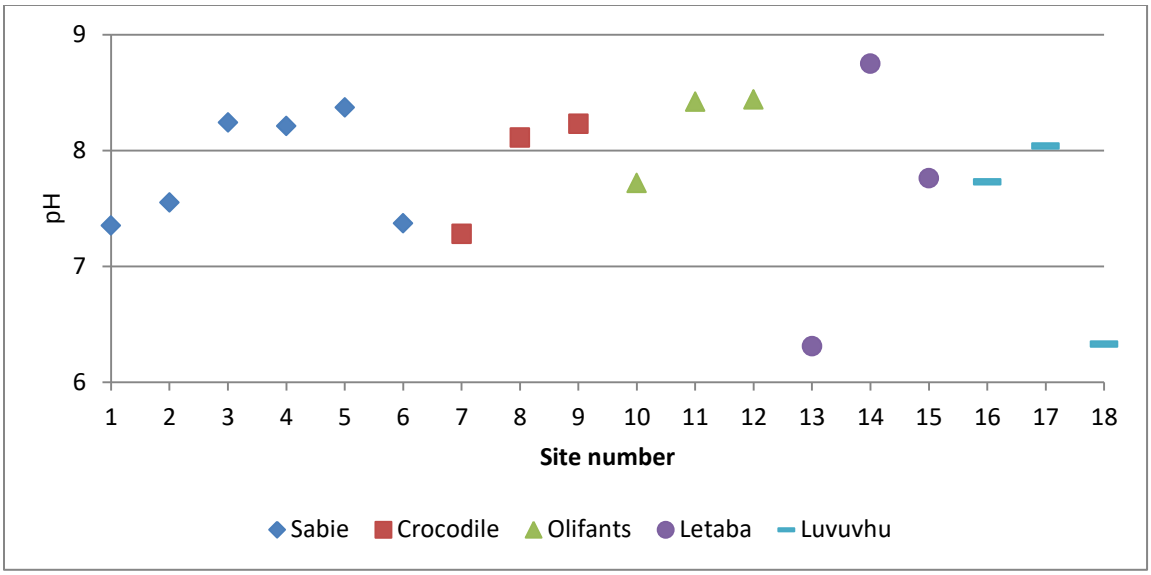

Figure 31: pH measured for all sites sampled in 2021 (refer to Table 3 for site names).

Nitrate concentration for all rivers were lower than 22 mg/L (Figure 32), except for the Letaba confluence site (23 mg/L), which was considered normal (DWAF, 1996d), measured nitrate levels also did not vary much between sites sampled or across rivers. Increased concentrations of nitrate were associated with decomposition of organic matter, sewage effluent and agricultural runoff (DWAF, 1996d).

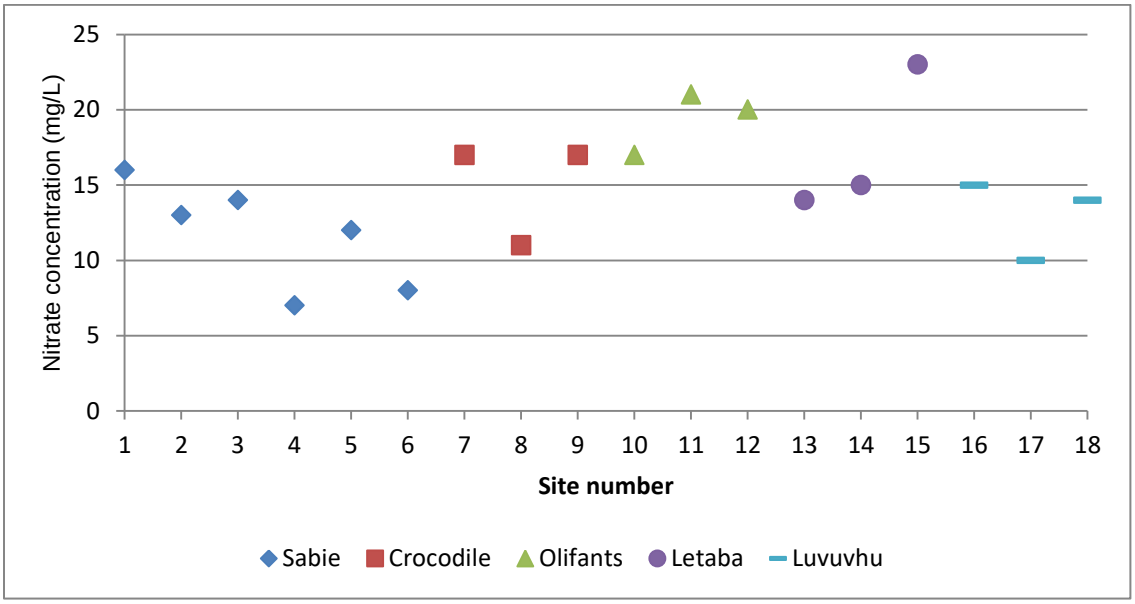

Figure 32: Nitrate (NO_3^-) measured for all sites sampled in 2021 (refer to Table 3 for site names).

Dissolved oxygen concentrations were between 5 mg/L and 9 mg/L for all sites sampled, except one site in the Sabie River (1 – 4.7 mg/L) (Figure 33). DO levels are usually close to saturation in unpolluted freshwater, at sea level DO is generally 10.08 mg/L at 15°C and 9.09 mg/L at 20°C and decreases with an increased surface temperature (DWAF, 1996b).

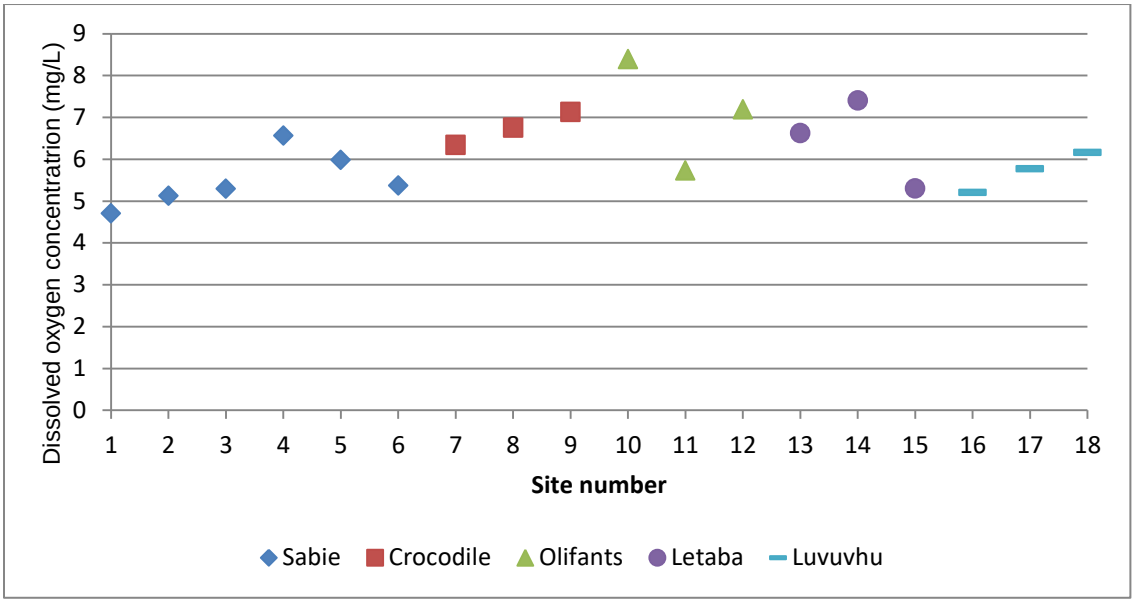

Figure 33: Dissolved oxygen (DO) measured for all sites sampled in 2021 (refer to Table 3 for site names).

Temperatures for all sites sampled ranged between 18°C and 28°C (Figure 34). For South African inland waters, the temperature generally ranges from 5 - 30°C and is dependent on many factors such as, season, altitude, river discharge, channel form, air temperature and cloud cover (DWAF, 1996b). Considering these various factors it is unsurprising that temperature values measured showed no clearly defined trend across sites sampled. The Sand River had the second highest measured temperature of all sites measured (27.9°C), the stream depth at this site was extremely shallow compared to other sites sampled. The highest temperature (28.1°C) was measured at the Antholysta site. This site was situated in a stretch of dense canopy cover and therefore the surface water temperature was expected to be low, in contrast to the measured temperature.

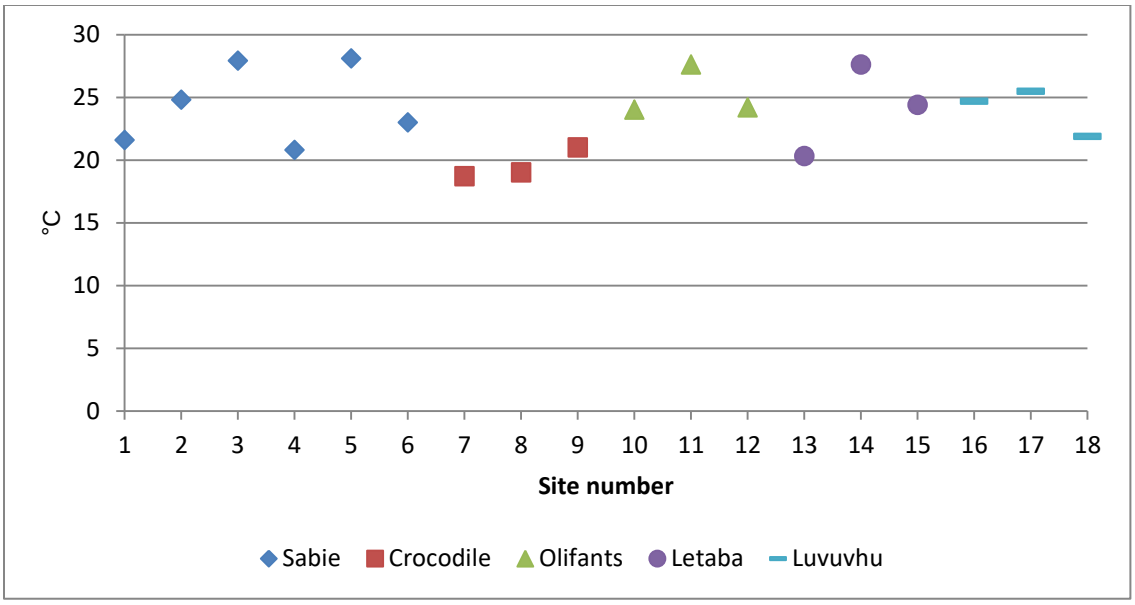

Figure 34: Temperature (°C) measured for all sites sampled in 2021 (refer to Table 3 for site names).

The ammonia concentrations measured were below 0.4 mg/L for all sites sampled in all rivers (Figure 35). Ammonia is considered toxic to many aquatic organisms (DWAF, 1996b), however, the concentrations measured were low, some ammonia is expected to be found in unpolluted surface water due to normal biological degradation (DWAF, 1996d). High concentrations of ammonia are associated with untreated sewage, agricultural practices and certain industries such as gas and coal (DWAF, 1996d).

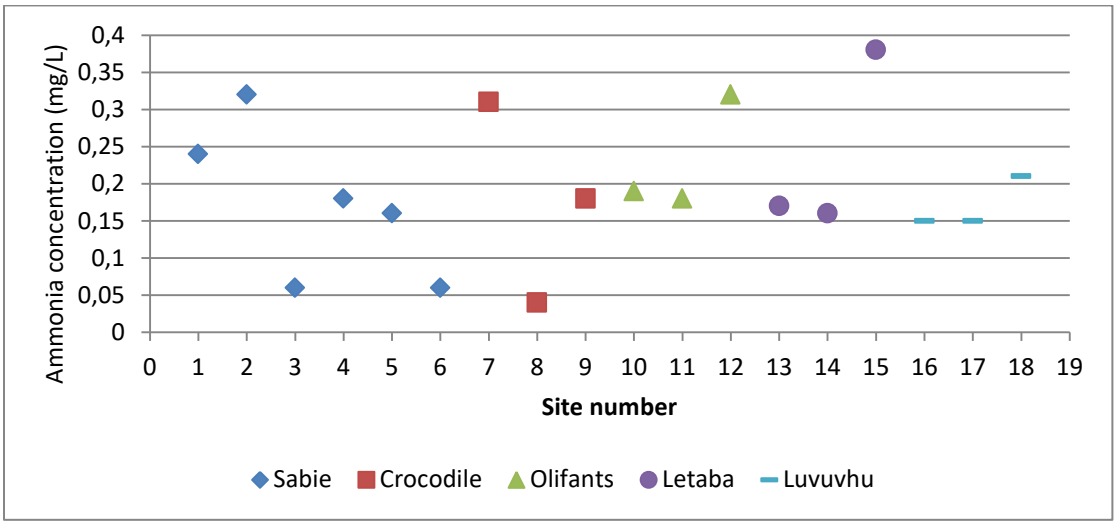

Figure 35: Ammonia (NH_3) concentration measured for all sites sampled in 2021 (refer to Table 3 for site names).

Sulphate concentrations generally ranged between 69 mg/L and 92 mg/L, across all sites, except for one site in the Crocodile River (Malelane – 198 mg/L) and all sites in the Olifants River (Confluence – 537 mg/L) (Figure 36). The Olifants Confluence site had an extremely high sulphate level while other sites in the river had lower sulphate levels (Mamba – 166 mg/L; Balule – 129 mg/L). Sulphate is not uncommon in freshwater and usually occurs in low concentrations (5 mg/L), however, when high amounts of sulphate mineral dissolution occur, the value can increase to several hundred mg/L. High levels of sulphate are also linked to anthropogenic impact such as acid mine drainage (AMD) and effluent discharge from industries that use sulphuric acid in their processes (DWAF, 1996c).

The Palabora copper mine, located just outside the park, discharges effluent into the Ga-Selati River, which then flows into the Olifants River, this effluent commonly contains toxic sulphate compounds (De Villiers and Mkwelo, 2009). If there was a major influence from the mining company on the sulphate concentration in the Olifants River, the first site sampled (Mamba) would reflect high levels of sulphate, however, measured sulphate was not as high (166 mg/L) as at downstream sites. This suggests the high concentration of sulphate at the confluence site (537 mg/L) was due to a different impact than mining activities and may be natural.

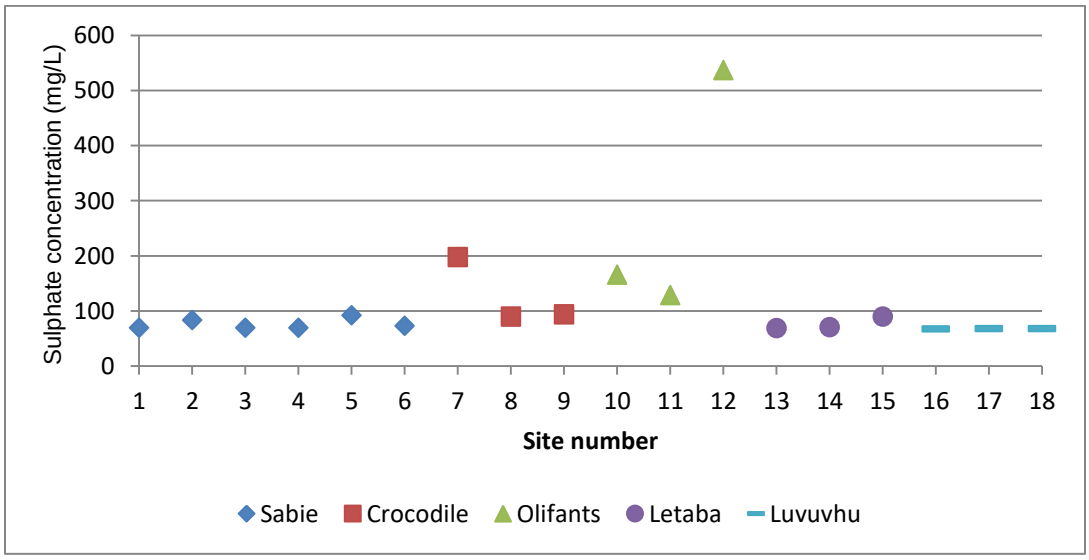

Figure 36: Sulphate (SO_4^{2-}) concentration measured for all sites sampled in 2021 (refer to Table 3 for site names).

Phosphate (orthophosphate) levels were below 0.05 mg/L in the Luvuvhu River and the Sand River while in the Sabie River phosphate levels ranged between 0.07 – 0.17 mg/L. One site in the Crocodile River had very high phosphate levels (Malelane - 0.53 mg/L) while the remaining sites had phosphate concentrations below 0.07 mg/L (Table 3). Most sites in the Olifants and Letaba rivers had phosphate levels similar to the Sabie River, except for two sites, one in the Olifants River (Mamba – 0.28 mg/L) and one in the Letaba River (Confluence – 0.38 mg/L). According to Qi et al. (2022) limits for orthophosphate, or SRP (soluble reactive phosphate), should be below 0.04 mg/L to reduce and control phytoplankton biomass in natural alkaline lakes (i.e., to prevent the symptoms of eutrophication) (Qi *et al*., 2022). However, the thresholds used in South Africa were more applicable to the current study. According to DWAF (1996b) the thresholds for orthophosphate are as follows; oligotrophic (< 0.05 mg/L), mesotrophic (0.05 - 0.25 mg/L), eutrophic (0.25 - 2.5 mg/L) and hypereutrophic (> 2.5 mg/L). According to the results of the current study the sites in the Luvuvhu River were oligotrophic, together with one site in the Sabie-Sand river system (Sand) and one site in the Crocodile River (Nkongoma). Three of the sites were considered eutrophic with orthophosphate concentrations greater than 0.25 mg/L (7 – Malelane, 10 – Mamba and 15 - Confluence). All the remaining sites were mesotrophic; most sites fall within this category.

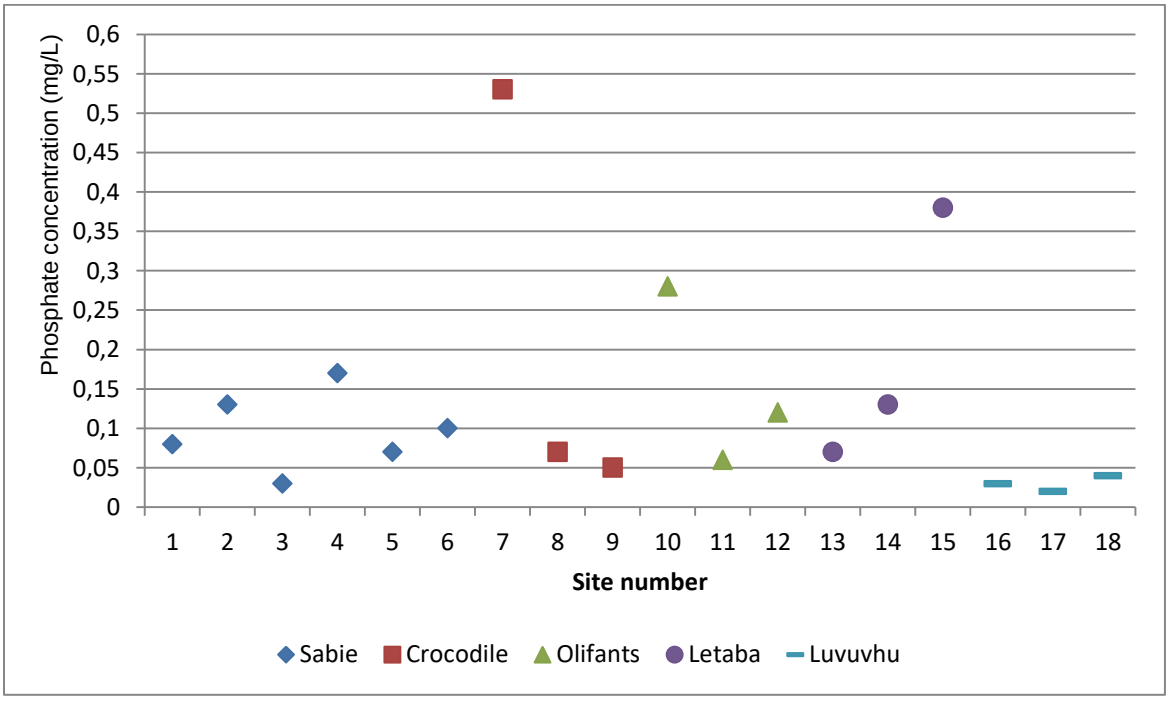

Figure 37: Orthophosphate (PO_4^{3-}) concentration measured for all sites sampled in 2021 (refer to Table 3 for site names).

3.1.2.2 Correlation of measured ionic compounds with electrical conductivity

The sensitivity of diatom taxa in the IPS is based on their ecological preference for the concentration of dissolved salts (ionic composition), nutrient concentration and organic pollution (Coste in CEMAGREF, 1982). Nutrients and inorganic matter can be dissolved when in water, resulting in an increased ionic load and consequently higher electrolyte content. Naturally occurring minerals, leaching from the surrounding geology, also contribute to the ionic load and increase the electrolyte content (DWAF, 1996a). However, it might not be clear which ions contribute most to the electrolyte concentrations. In an attempt to explain which ionic compounds contribute most to the electrical conductivity across all sites sampled, Pearson correlation and R^2 analysis were conducted.

3.1.2.2.1 Pearson correlation

From Table 4 It is evident that sodium, chloride, and nitrate have strong positive correlations with EC. This suggests that these ions have a greater influence in determining the EC for the rivers sampled. Of the ions that contribute to higher EC, chloride and sodium have the greatest correlation with electrical conductivity with r = 0.74 and r = 0.84 respectively (Table 4). Sulphate, phosphate and ammonia do not have very strong correlations with EC having r values lower than 0.5, additionally, p values are > 0.05, indicating no significance (Table 4). Phosphate usually occurs in very low concentrations (compared to the major anions and cations) and would not necessarily contribute much to the change in EC values, the low correlation of ammonia with EC indicates that it did not contribute much to changes in EC levels and also has no significant correlation, with p values > 0.05. Sulphate has an r value similar to phosphate, indicating both variables have a moderate correlation with EC (Table 4).

Table 4: Calculated Pearson correlation (r) and R^2 values for all ionic compounds measured vs electrical conductivity, significant correlations ($p < 0.05$) are indicated in bold.

EC	Chloride (Cl^-)	Ammonia (NH_3)	Sulphate (SO_4^{2-})	Phosphate (PO_4^{3-})	Nitrate (NO_3^-)	Sodium (Na+)
Pearson (r)	**0,7375**	0,1464	0,4374	0,3496	**0,6097**	**0.8360**
R^2	**0,544**	0,021	0,191	0,122	**0,372**	**0.699**
p	**0,00048**	0,56214	0,0695	0,15495	**0,00723**	**0.00002**

3.1.2.2.2 R^2 correlation

An R^2 value provides information on how much variation in one variable (response variable) is due to variation in another variable (predictor variable). Electrical conductivity provides a collective measurement of the ionic compounds in water and therefore incorporates the abundance of sodium, chloride, nitrate, phosphate and all other ions present as a collective measure. However, it may not be clear which of these ions contribute most to changes in the EC values measured.

R^2 values calculated for the correlations between electrical conductivity and the respective ions are illustrated in Figure 38. It is evident a strong relationship is present between EC and chloride as well as between EC and sodium. The R^2 value between EC and sodium is 0.7, which means that 70% of the variation in EC can be explained by the variation of measured sodium. The same is true for EC and chloride, however, this value is slightly lower at 0.54 but also still represents a relatively strong correlation, this may be explained by the generally lower chloride concentrations measured compared to measured sodium (Table 3).

Sodium has the strongest correlation with EC with r = 0.83. The p value for this relationship is extremely low at p = 0.0002 (Table 4), which indicates a high significance. The relationship between sodium and EC is therefore strong and significant.

Chloride has an r value of 0.74 and a R^2 value of 0.54 (Table 4 and Figure 38). This indicates on a relatively strong correlation between chloride and EC, the R^2 is still high and does explain much of the variance in EC together with sodium. The p value indicates a significant relationship between EC and chloride with p = 0.00048 (Table 4). The variation in measured chloride levels, *ex situ*, can therefore explain 54% of the variation in EC values measured *in situ* and also has high significance. For comparison, the variation in calculated nitrate values can only explain 37% of the variation in EC. This value is weak; however, the r value still indicates a strong correlation, and the p value indicates the correlation is significant at p = 0.0073 (Table 4). The correlations of other measured variables (sulphate, phosphate and ammonia) are weak, and no significance exists between them. Therefore, the greatest contribution to the electrical content and ionic load at sites sampled is due to chloride, sodium and nitrate in descending order of influence.

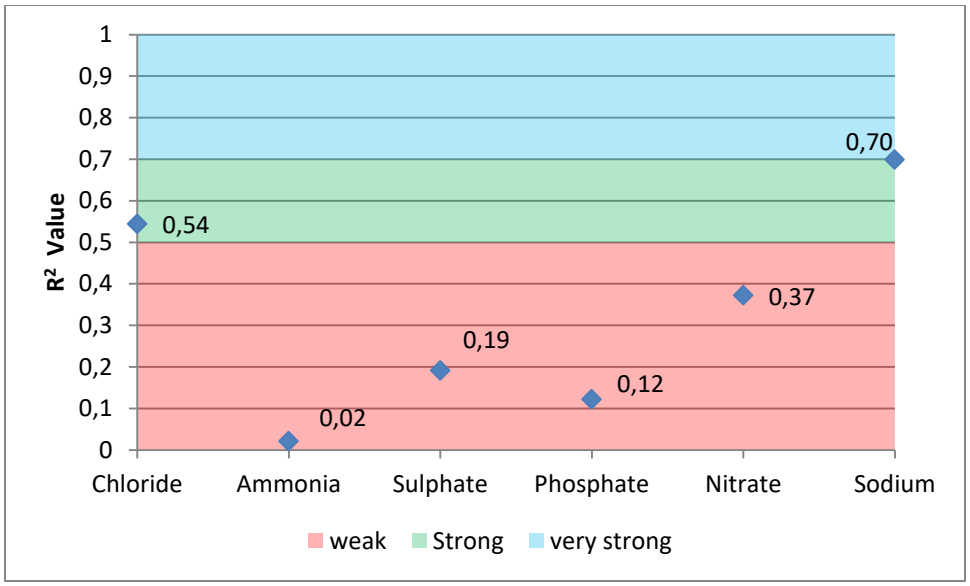

Figure 38: R^2 values for ions measured, *in situ* and *ex situ,* correlated with EC values.

3.1.2.3 Summary

The ionic compounds measured have a clear correlation with EC. The variables that were strongly correlated with EC measurements in descending order of influence, sodium, chloride and nitrate. The ionic compounds that are weakly correlated with EC are in descending order of influence, sulphate, phosphate and ammonia. The variation in EC measured can therefore be mostly explained by the variation in sodium, chloride and nitrate levels and to a lesser degree by the variation in sulphate, phosphate and ammonia.

3.2 Diatom communities in relation to measured water quality

During 2020, no *in situ* water quality data were collected and so a decision was made to conduct CCA on the results of 2018 and 2019 in a separate analysis as well as using CCA to illustrate the results obtained in 2021 in separate analyses. The split between CCA graphs is due to the nature of water quality variables measured. The water quality variables measured during 2018 and 2019 were not the same as for 2021. During 2018 and 2019, EC, turbidity, salinity and pH were measured. While during 2021, EC, pH, NO_3^-, DO, temperature, Cl^-, NH_3, SO_4^{2-} and PO_4^{3-} were measured. Therefore, relationships between diatom taxa and measured variables are best illustrated separately.

3.2.1 2018 / 2019

3.2.1.1 Diatom community composition 2018

Overall, 112 diatom taxa were documented of which 18 were dominant across all sites and had an abundance of greater than 4%. The remaining 94 taxa had abundances lower than 4% across all sites and therefore did not contribute significantly to the IPS calculation as the final score is weighted by species abundance.

Table 5: The most abundant diatom taxa across all sites in 2018, comprising more than 4% of the community composition. A full species list may be found in Appendix A.

Abbreviation	Name of taxa	Trophic preference or range
ACHD	*Achnanthidium* sp.	Oligo- to eutrophic
ADUL	*Anorthoneis dulcis* Hein	Oligotrophic
CPED	*Cocconeis pediculus* Ehrenberg	Meso- to eutrophic
CPLA	*Cocconeis placentula* Ehrenberg	Meso- to eutrophic
CTGL	*Cymbella turgidula* Grunow	Oligo- to mesotrophic
ENLS	*Encyonopsis leei* var. *sinensis* Metzeltin & Krammer	Oligo- to mesotrophic
ESOR	*Epithemia sorex* Kützing	Meso- to eutrophic
FRAG	*Fragilaria* spp.	Oligo- to eutrophic
FUMP	*Fallacia umpatica* (Cholnoky) D.G. Mann	Meso- to hyper eutrophic
GVNU	*Gomphonema venusta* Passy, Kociolek & Lowe	Oligo- to mesotrophic
HIPO	*Hippodonta* Lange-Bertalot, Metzeltin & Witkowski	Oligo- to eutrophic
NAVI	*Navicula* spp.	Oligo- to eutrophic
NIFR	*Nitzschia frustulum* (Kützing)	Eutrophic
NITZ	*Nitszchia* Hassall	Oligo- to eutrophic
NMCY	*Navicula microlyra* Cholnoky	Oligo- to mesotrophic
NVDA	*Navicula vandamii* Schoeman & Archibald	Eutrophic
PRST	*Planothidium rostratum* Lange-Bertalot	Oligo- to mesotrophic
TFAS	*Tabularia fasciculata* (Agardh) Williams & Round	Meso- to eutrophic

3.2.1.2 Diatom community composition 2019

Overall, 104 taxa were found of which 13 were dominant across all sites and had an abundance greater than 4%. The remaining 91 taxa had abundance lower than 4% across all sites.

Table 6: The most abundant diatom taxa across all sites in 2019, representing more than 4% of the community composition.

Abbreviation	Name of taxa	Trophic preference or range
ACHD	*Achnanthidium* Kützing	Oligo- to eutrophic
CKOL	*Cymbella kolbei* Hustedt	Oligotrophic
CPLA	*Cocconeis placentula* Ehrenberg	Meso- to eutrophic
CTGL	*Cymbella turgidula* Grunow	Oligo- to mesotrophic
CTUM	*Cymbella tumida* (Brébisson) Van Heurck	Oligo- to mesotrophic
ENLS	*Encyonopsis leei* var. *sinensis* Metzeltin & Krammer	Oligo- to mesotrophic
ESOR	*Epithemia sorex* Kützing	Meso- to eutrophic
NAVI	*Navicula* spp.	Oligo- to eutrophic
NCTE	*Navicula cryptotenella* Lange-Bertalot	Oligo- to eutrophic
NIFR	*Nitzschia frustulum* (Kützing)	Eutrophic
NITZ	*Nitszchia* spp.	Oligo- to eutrophic
PRST	*Planothidium rostratum* Lange-Bertalot	Oligo- to mesotrophic
RABB	*Rhoicosphenia abbreviata* Lange-Bertalot	Eutrophic

3.2.1.3 CCA

The CCA triplot shows a clear separation of sites along the vertical axes. The sites on the right hand site of the vertical axis show general positive correlations with increases in the respective water quality parameters, while the sites on the left hand side show a general negative correlation with the water quality parameters.

Sites on the left of the horizontal axis (Sabie and Luvuvhu rivers) all have a strong negative correlation with increase electrical conductivity, pH and turbidity (Figure 39). The negative correlation between sites in the Luvuvhu River and turbidity exists because no values for turbidity were available for these sites (Table 2). This can possibly skew the results in the graph, however, there is little alteration to the other vectors as well as to the position of sites and species since there are many other variables that determine positions for entities on the graph.

Taxa occurring on the left side of the vertical axis including*, Encyonopsis leei* var. *sinensis* (ENLS)*, Planothidium rostratum* (PRST) and *Gomphonema venusta* (GVNU) all have trophic preference for low to moderate nutrient levels (Table 5) as well as low to moderate electrolyte content (Taylor *et al.,* 2007b). *Cymbella turgidula* (CTGL) also occurs in water with lower electrolyte content (Foged, 1948, 1954a, 1954b; Hustedt, 1957; Weber, 1970) and prefers oligo-mesotrophic states (Taylor *et al*., 2007b) which correlates with water quality measured.

Cymbella kolbei (CKOL) is sensitive to EC change, it can compete well and thrive under oligotrophic conditions (Taylor *et al.,* 2007b; Cholnoky, 1962a) but decreases in abundance as trophic level increases. This taxon prefers more alkaline conditions (Cholnoky, 1962a) which corresponds with the measured water quality, since all pH measurements for the Sabie River were above 8 for 2018 and 2019, except the Sabiepoort site during 2018 (Table 2). *Tabularia fasciculata* (TFAS) is situated in the middle of the CCA graph, it has a non-specific preference for water quality variables and a more general ecological range, however, this species can tolerate high levels of pollution and can be indicative of critically polluted wastewater and higher levels of EC often occurring in brackish and coastal waters (Taylor *et al.,* 2007b).

Achnanthidium spp. (ACHD), *Fragilaria* spp. (FRAG) and *Navicula* spp. (NAVI) also appear on the left side of the CCA. *Achnanthidium* spp. is generally associated with oligotrophic fast flowing water (Taylor & Cocquyt, 2016) which corresponds with its strong negative correlation with EC. *Fragilaria* has a wider ecological range but more species within in the genus occur in greater abundance in oligo-mesotrophic conditions. *Navicula* has a very wide ecological range,

species in this genus can occur in high abundance in both oligo and eutrophic conditions such, as *Navicula cryptotenella*. This species can also occur in low to high electrolyte content (Taylor *et al*., 2007b). This genus holds many generalist species that occurs in all trophic states.

The diatom communities in the Sabie and Luvuvhu rivers were therefore comprised of those preferring, and better able to compete under, low to moderate nutrient levels and moderate to low levels of EC.

The sites on the right-hand side of the vertical axis are those in the Crocodile, Olifants and Letaba rivers, these sites have positive correlations with measured water quality variables (Figure 39). Taxa on the right-hand side of the vertical axis are correlated with increases in the variables measured. *Nitzschia frustulum* (NIFR)*, Cocconeis pediculus* (CPED) and *Epithemia sorex* (ESOR) can all tolerate wide ranges of electrolyte content. *Nitzschia frustulum* (NIFR) occurs over a wide range of electrolyte content (Simonsen, 1962), its growth is thought to be stimulated by increases in salt concentration (Hustedt, 1957; Foged, 1964) and is common brackish conditions (Cholnoky, 1962c; Cholnoky, 1966; Cholnoky, 1968), and therefore correlates with high salinities. This taxon is also associated with eutrophic conditions (Cholnoky, 1968; Taylor *et al*., 2007b). *Cocconeis pediculus* and *E. sorex* are common in waters with elevated electrolyte content, and can extend into brackish conditions (Hustedt, 1930; Scheele, 1952; Simonsen, 1962; Cholnoky, 1968). *Epithemia sorex* is common in eutrophic conditions (Cholnoky, 1968) while *C. pediculus* is not found in such conditions.

Taxa such as *Rhoicosphenia abbreviata* (RABB), *Nitzschia* spp. (NITZ) occur in conditions with elevated electrolyte content and can tolerate increased levels of pollution (Taylor *et al*., 2007b). *Cocconeis placentula* (CPLA) is found in meso- to eutrophic conditions (Taylor *et al*., 2007b), however, it cannot tolerate high salt concentrations (Jørgensen, 1952; Hustedt, 1957; Marilainen, 1967). The position of these taxa in the graph in relation to measured water quality confirm their autecological affiliations toward these variables. The CCA graph therefore succeeded in illustrating how the autecology of diatom taxa is correlated with environmental variables and sites sampled during 2018 and 2019.

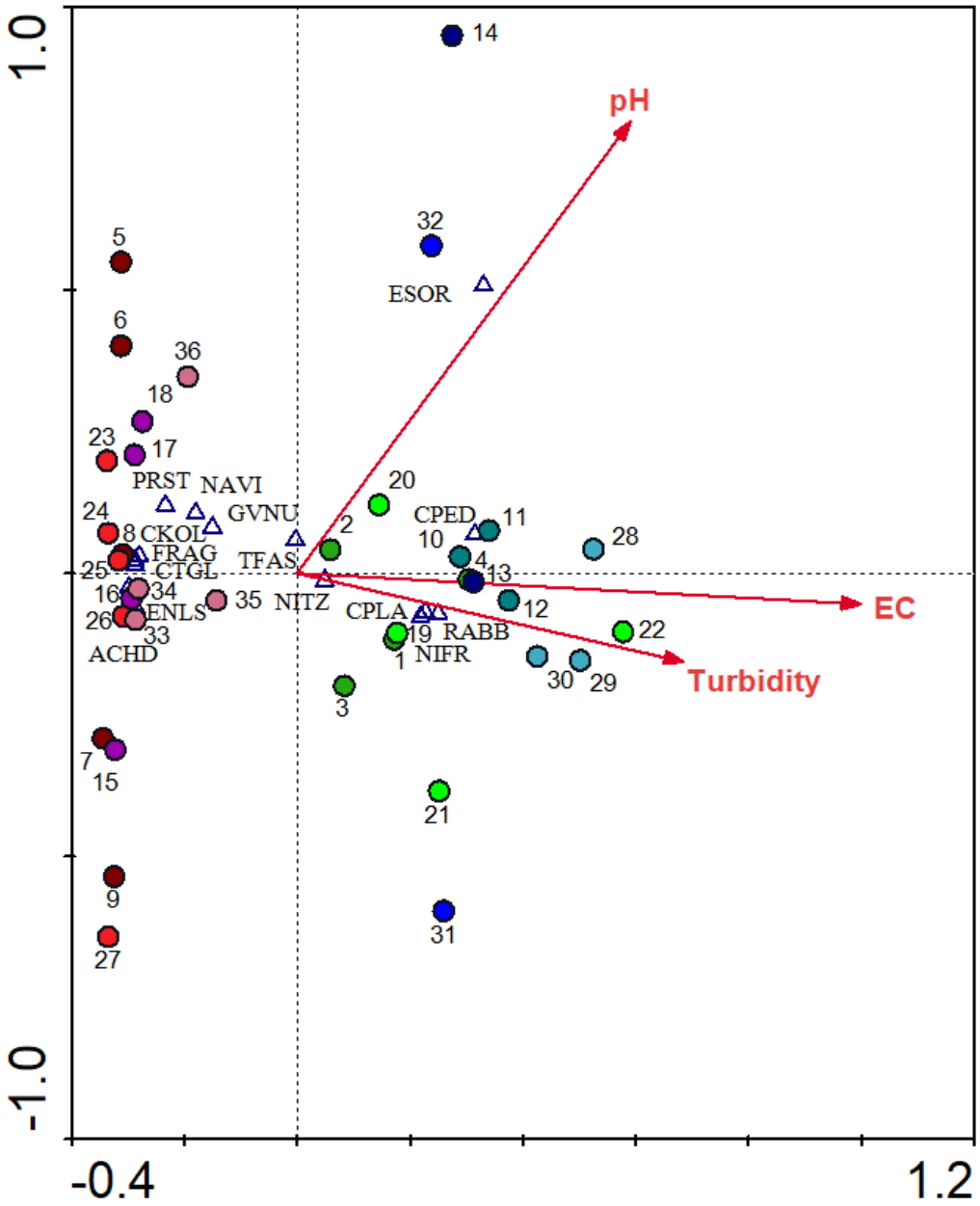

Figure 39: CCA triplot illustrating the relationship between diatom species, water quality variables and sites for 2018 and 2019 (refer to Table 2 for site numbers).

3.2.2 2020

3.2.2.1 Diatom community composition

Overall, 115 taxa were counted and identified to genus level, some of which were also identified to species level. Seventeen of the taxa present represent 4% or more of the diatom valves counted and will therefore have the greatest influence on the calculation of diatom indices.

Table 7: The most abundant diatom taxa across all sites in 2020, representing 4% or more of the community composition.

Abbreviation	Name of taxa	Trophic preference or range
ACHD	*Achnanthidium* spp.	Oligo- to eutrophic
ADMI	*Achnanthidium minutissimum* Kützing	Oligotrophic
ADUL	*Anorthoneis dulcis* Hein	Oligotrophic
CPED	*Cocconeis pediculus* Ehrenberg	Meso- to eutrophic
CPLA	*Cocconeis placentula* Ehrenberg	Meso- to eutrophic
CTGL	*Cymbella turgidula* Grunow	Oligo- to mesotrophic
ENLS	*Encyonopsis leei* var. *sinensis* Metzeltin & Krammer	Oligo- to mesotrophic
ENMI	*Encyonema minutum* D.G. Mann	Oligo- to mesotrophic
FUNG	*Fragilaria ungeriana* Grunow	Oligo- to mesotrophic
GNUN	*Gomphonitzschia ungeri* Grunow	Oligo- to mesotrophic
GPAR	*Gomphonema parvulum* Kützing	Eutrophic
GVNU	*Gomphonema venusta* Passy, Kociolek & Lowe	Oligo- to mesotrophic
MVAR	*Melosira varians* Agardh	Meso- to eutrophic
NAVI	*Navicula* spp.	Oligo- to eutrophic
NITZ	*Nitzschia* Hassal	Oligo- to eutrophic
RGIB	*Rhopalodia gibba* Ehrenberg	Meso- to eutrophic
TFAS	*Tabularia fasciculata* (Agardh) Williams & Round	Meso- to eutrophic

3.2.2.2 DCA

Three groups can be seen from Figure 40. Group A consists of taxa closely related or associated with site 1 (Crocodile River) and sites 2 – 4 (Letaba River). As mentioned, *Cocconeis placentula* (CPLA) increases in abundance in higher trophic levels, however, it cannot tolerate high salt concentration. *Gomphonema parvulum* (GPAR), similarly cannot tolerate high salt concentration according to Cholnoky (1962a) and requires fluctuating nitrogen concentrations to grow optimally, however, it can occur over a wide range of electrolyte concentrations (Taylor *et al*., 2007b). *Rhopalodia gibba* (RGIB), on the other hand, increases in abundance under moderate to high electrolyte content (Taylor *et al*., 2007b).

The taxon occurring in the highest abundance at sites 1 - 4 was *C. placentula*, it comprises more than 50% of the community in three of the four sites. In site 1 *C. placentula* comprises more than 90% of the community composition (Table 14). Due to high abundance of *C. placentula* at the Crocodile River Marula site, the IPS score increased to 15.2 indicating meso-oligotrophic conditions, on the lower threshold of mesotrophic (IPS - 15), this might seem high, however, as discussed above *C. placentula* can only tolerate small amounts of salt (Jørgensen, 1952; Hustedt, 1957; Marilainen, 1967) and hence a low electrolyte content which is a significant contributor to the IPS score. Sites 2 - 4 were different biotopes sampled within one site (Lonely Bull) and did not share similar abundances of one particular taxon, *C. placentula* comprised more than 50% of the community structure within the rapids (54%) and pool (51%) biotopes. The remaining biotope, run, had a lower abundance of *C. placentula* (32%) and a higher abundance of other taxa such as *Tabularia fasciculata* (TFAS), *Nitzschia* spp. (NITZ) and *Rhopalodia gibba* (RGIB) that favour moderate to high electrolyte content (Taylor *et al*., 2007b). Consequently, the IPS score for the Letaba River in 2020 is meso- eutrophic at 11.2 (Table 1), indicating poor water quality. Although it is considered poor, there was an increase in water quality, since the IPS scores for 2018 and 2019 were lower than 11. *Anorthoneis dulcis* was also present in group A, little is known of the ecology for this species, however, it has been reported in alkaline oligotrophic waters (Taylor & Cocquyt, 2016).

Group B is a cluster of taxa closely associated with two of the samples, 12 and 13. They were also not different sites, but rather samples from different biotopes within one site. This site, Sekurukwane, was situated in close proximity to rural settlements (Figure 10) and has the second lowest water quality rating (IPS score) of all sites in the Sabie River (Table 9). Taxa associated with this site, including *Navicula* spp. (NAVI) and *Nitzschia* spp. (NITZ), occur across

wide ranges of environmental conditions (Taylor *et al*., 2007b). *Melosira varians* (MVAR) and *Encyonema minutum* (ENMI) were present in moderate abundances, the former can tolerate elevated electrolyte content and become particularly abundant in brackish conditions (Cholnoky, 1968; Taylor *et al*., 2007b), the latter species, cannot tolerate such conditions and prefers oligo- to mesotrophic states with moderate electrolyte content (Taylor *et al*., 2007b). *Cymbella turgidula* (CTGL) was also present in this group, however, it only represented 6-7% of the community at this site. This species cannot tolerate high salt concentrations (Hustedt, 1957; Weber, 1970) and prefers lower trophic states (Taylor *et al*., 2007b).

Group C includes sites in the Luvuvhu River as well as the Antholysta site in the Sabie River. Taxa in this group such as *Encyonopsis leei* var. *sinensis* (ENLS) and *G. venusta* (GVNU) occur in greater abundance under moderate to low electrolyte content (Taylor *et al*., 2007b). *Achnanthidium minutissimum* (ADMI) has a similar preference for low electrolyte content and cannot tolerate high osmotic pressure (Cholnoky, 1962a). Additionally, the species is associated with fast flowing water with high oxygen content (Cholnoky, 1962a; Taylor *et al*., 2007b). *Gomphonitzschia ungeri* (GNUN) was also present in this group, comprising 6% of the community in the Mutale site (Table 10). This was the only tropical species of its genus (Taylor & Cocquyt, 2016) and has not been previously recorded in the KNP before or since 2020.

Although no *in situ* water quality was collected during 2020, a distinction can be made in terms of the water quality by using the autecology of taxa. As discussed, sites in the Crocodile and Letaba rivers were associated with species indicating increased electrolyte content as well as some pollutant tolerant taxa. Sites in the Luvuvhu River had taxa that cannot tolerate high electrolyte content or high trophic states. Taxa occurring in the Sabie River indicated both high and low water quality. The water quality obtained from diatoms during 2020 (IPS) compares well with such scores generated with measured water quality during 2018, 2019 and 2021.

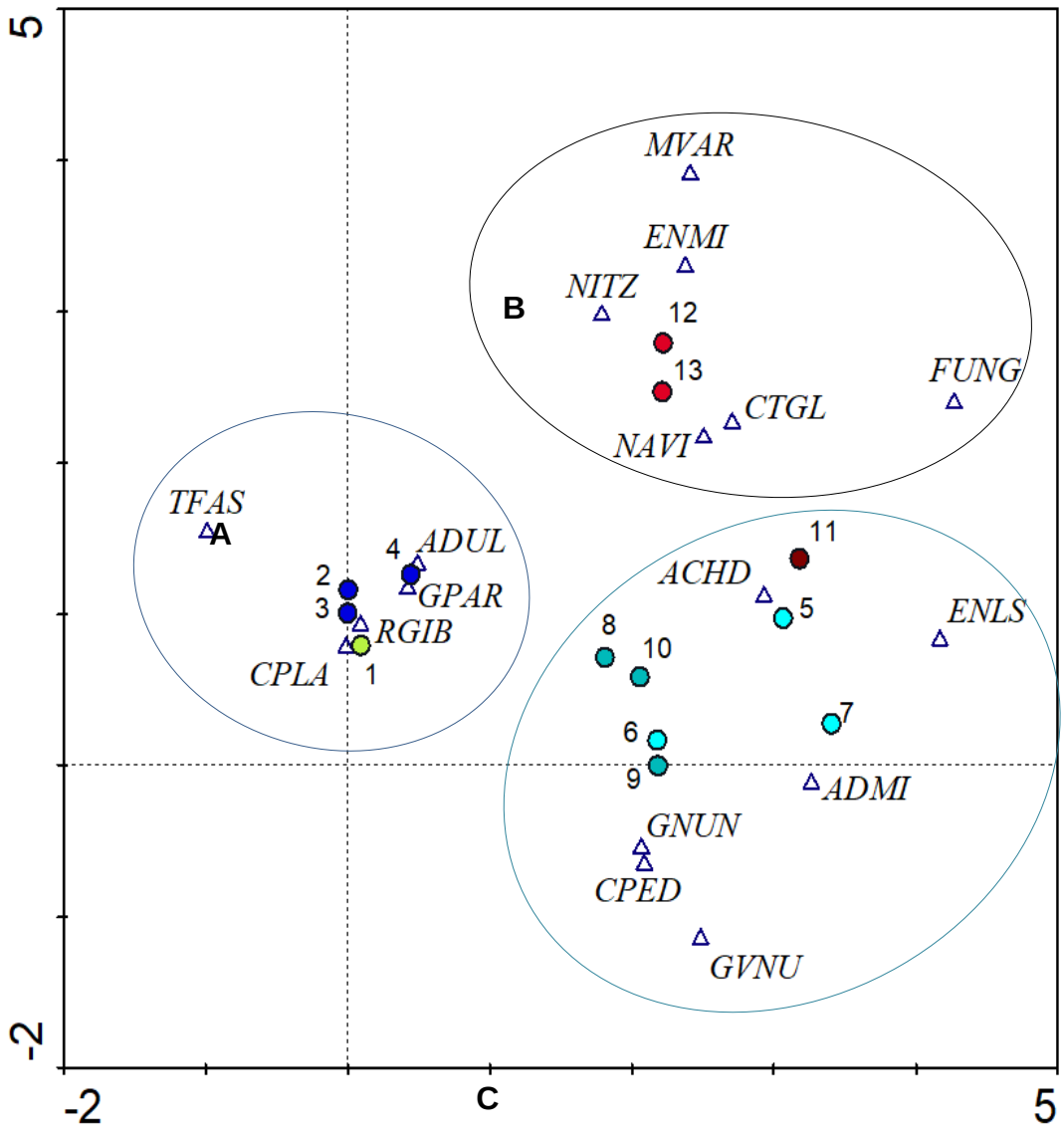

Figure 40: DCA illustrating the correlation of diatom taxa with sites sampled (dark blue – Letaba; green – Crocodile; red – Sabie; turquoise - Luvuvhu).

3.2.3 2021

3.2.3.1 Diatom community composition

Overall, a total of 99 species were identified and counted during 2021. Fourteen of these taxa had an abundance greater than 4% across all sites and contributed the most to the calculation of the diatom index scores. Twenty-three species had an abundance greater than 2% and are included in the discussion below.

Table 8: The most abundant diatom taxa across all sites in 2021, comprising 2% or more of the community composition.

Abbreviation	Name of taxa	Trophic preference or range
ACHD	*Achnanthidium* spp.	Oligo- to eutrophic
ADCR	*Achnanthidium crassum*	Oligo- to mesotrophic
ADMI	*Achnanthidium minutissimum* Kützing	Oligotrophic
ADUL	*Anorthoneis dulcis* Hein	Oligotrophic
CPED	*Cocconeis pediculus* Ehrenberg	Meso- to eutrophic
CPLA	*Cocconeis placentula* Ehrenberg	Meso- to eutrophic
CTGL	*Cymbella turgidula* Grunow	Oligo- to mesotrophic
CTUM	*Cymbella tumida* (Brébisson) Van Heurck	Oligo- to mesotrophic
CYMB	*Cymbella* spp.	Oligo- to mesotrophic
ENLS	*Encyonopsis leei* var. *sinensis* Metzeltin & Krammer	Oligo- to mesotrophic
FUMP	*Fallacia umpatica* Cholnoky	Meso- to eutrophic
GOMP	*Gomphonema* spp.	Oligo- to eutrophic
GPAR	*Gomphonema parvulum* Kützing	Eutrophic
GPRI	*Gomphonema pumulim* var. *rigidum* Reichardt & Lange-Bertalot	Meso- to eutrophic
GVNU	*Gomphonema venusta* Passy, Kociolek & Lowe	Oligo- to mesotrophic
KPLO	*Kolbesia ploenensis* (Hustedt) Kingston	Oligo- to mesotrophic
NAMP	*Nitzschia amphibia* Grunow	Eutrophic
NAVI	*Navicula* spp.	Oligo- to eutrophic
NDIS	*Nitzschia dissipata* (Kützing) Grunow	Oligo- to mesotrophic
NITZ	*Nitszchia* spp.	Oligo- to eutrophic
NROS	*Navicula rostellata* Kützing	Eutrophic
NVDA	*Navicula vandamii* Schoeman & Archibald	Eutrophic
SSEM	*Sellaphora seminulum* (Grunow) D.G. Mann	Eutrophic

3.2.3.2 CCA

From Figure 41 it is evident that all the sites on the right-hand side of the vertical axis are positively correlated with the water quality variables (EC, DO, nitrate, sulphate and phosphate), sites 13, 14 and 15 (Letaba River) were negatively correlated with pH.

The sites on the right side of the graph are again those sampled in the Crocodile River (light green), the Letaba River (dark blue) and the Olifants River (dark turquoise). The variables having the greatest influence on the position of the sites on the graph are those with the longest vectors and are, in descending order, EC, nitrate, DO, phosphate, sulphate and pH. All sites on the left hand side of the origin are those sampled in the Sabie River (red) and the Luvuvhu River (light blue). These sites are negatively correlated with the measured water quality parameters, except sites 2 and 6 (Sabie River) that are positively correlated with pH.

A strong correlation is especially true for EC since most sites on the left-hand side of the axis have a very small perpendicular distance to the inverse of the vector, only two sites (6 and 18) are outside this cluster. The Crocodile and Olifants rivers had the highest correlation with EC, the Letaba River on the other hand was neutral to positively correlated with EC. This river had a stronger positive correlation with nitrate; EC and nitrate had a correlation coefficient of 0.61 which is biologically significant (Table 4).

Taxa positively correlated with sites in the Crocodile and Olifants rivers were *Nitzschia* spp. (NITZ) and *Cocconeis pediculus* (CPED) as well as *Gomphonema* spp. (GOMP) and *Cocconeis placentula* (CPLA). *Nitzschia* spp. and *Gomphonema* spp. have wide ecological ranges and can occur under low to high electrolyte content (Taylor *et al*., 2007b). *Cocconeis pediculus* is common in brackish conditions and can tolerate high salt content (Scheele, 1952; Simonsen, 1962) while *C. placentula* cannot tolerate high salt concentrations but is common under meso- to eutrophic states (Jørgensen, 1952; Hustedt, 1957; Marilainen, 1967; Taylor *et al*., 2007b).

Taxa occurring on the CCA graph (Figure 42) not found in high abundance during 2018, 2019 or 2020 are *Achnanthidium crassum* (ADCR)*, Navicula vandamii* (NVDA) and *Navicula rostellata* (NROS). *A. crassum* is found in slow-flowing water with higher pH levels (Taylor *et al*., 2007b). The position of the species in relation to the DO vector supports the ecological preference for slow-moving water since there is less aeration and consequently lowers DO saturation in slow-flowing waters. However, the species does show a slight negative correlation with pH, which is slightly in contrast to its documented ecology. *Navicula vandamii* and *N. rostellata* are species

that occur in eutrophic conditions with elevated electrolyte content (Taylor *et al*., 2007b), however, this does not correspond with their relative positions on the CCA graph (Figure 41), which shows a negative relationship with electrolyte content for *N. vandamii* and a neutral-positive relationship for *N. rostellata*. The CCA graph also illustrates a negative correlation of these two species with phosphate and nitrate, which is also unexpected as in the literature the taxa are documented as occurring under eutrophic conditions (Taylor *et al*., 2007b). However, both taxa are very commonly occurring with broad ecological tolerances and not only found in the conditions as described above.

The autecology of other taxa including *Achnanthidium* spp. (ACHD), *A. minutissimum* (ADMI), *Encyonopsis leei* var. *sinensis* (ENLS), *Cymbella turgidula* (CTGL) and *Cocconeis pediculus* (CPED) as described in sections 3.2.1.3 and 3.2.2.2 correlate with their positions in relation to water quality variables. Other taxa such as *Sellaphora seminulum* (SSEM) and *Anorthoneis dulcis* (ADUL) are also illustrated on the CCA plot. The former species was found in high abundance at site 6 (Sabiepoort), it prefers oligo- to eutrophic conditions and can tolerate extreme levels of pollution (Jørgensen, 1952; Taylor *et al*., 2007b), this species can also tolerate high salt concentrations (Foged, 1948; Patrick & Reimer, 1966). The latter (ADUL) is the only species of its genus occurring in tropical African oligotrophic freshwaters (Taylor & Cocquyt, 2016), based on the CCA it has a significant relationship with slightly elevated electrical conductivity.

The CCA plot (Figure 41), as for the previous years (2018 and 2019), illustrates the relationships between diatom species and water quality parameters. The known ecology of the species as described in the literature again correlates with their ordination on the plot with the measured water quality parameters. The index values calculated from these ecological preferences such as the IPS are illustrated in Table 9. The sites on the left of the vertical axis have high IPS scores and consequently, those on the right have lower scores. This also illustrates the inverse relationship between IPS scores and water quality parameters, such as EC. Therefore, the ecology of species correlates well with water quality measured.

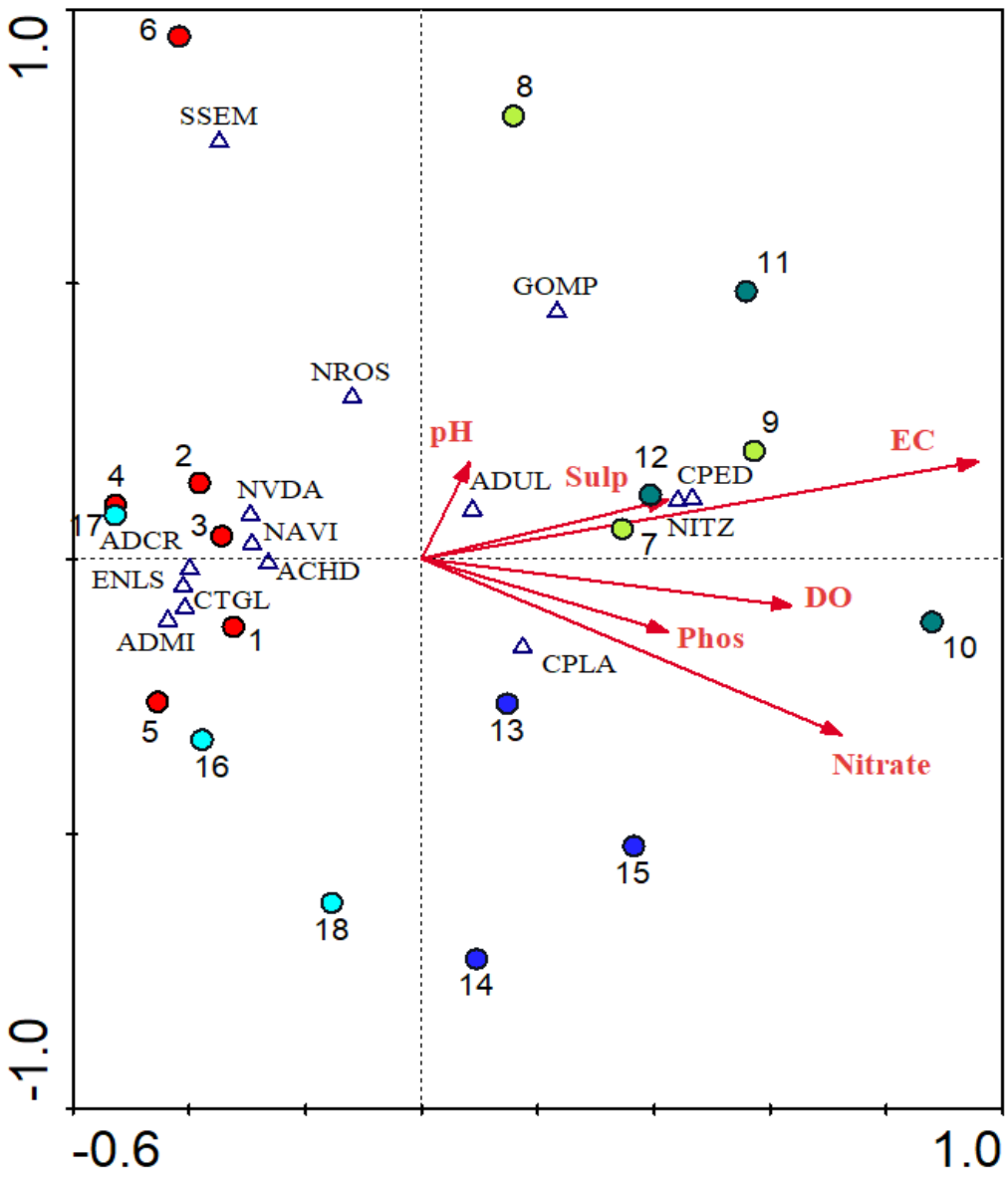

Figure 41: CCA between sites, species and water quality variables sampled during 2021 (refer to Table 3 for site names).

3.3 Evaluation of diatom index application

3.3.1 IPS correlation with EC

The IPS index is based on the sensitivity of diatom taxa to nutrient concentrations, organic material, and ionic compounds. Nutrients are generally dissolved when in rivers and therefore contribute to ionic load - in addition to other ionic compounds present. The EC increases when ionic compounds become more abundant, therefore, a correlation analysis between the IPS scores and measured EC was illustrated (Figure 42).

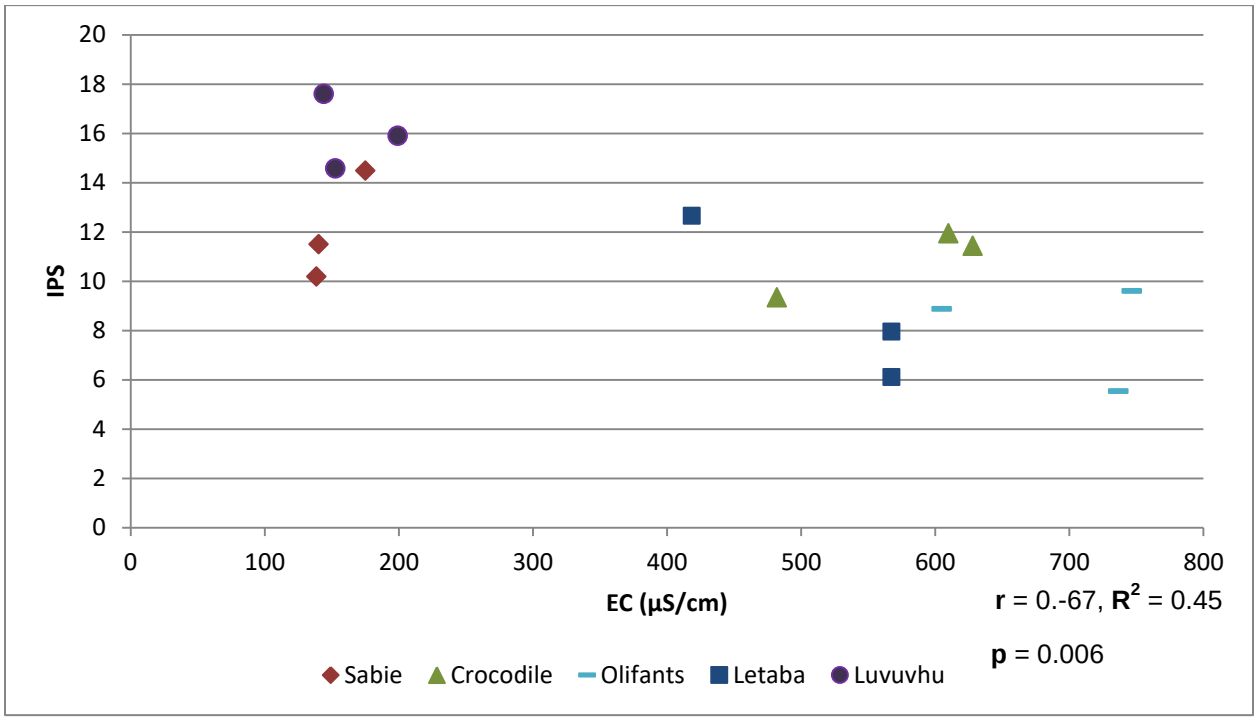

Figure 42: The inverted correlation between calculated IPS scores and EC measurements.

Each river is represented by three data points on Figure 42. Each of the three points for the respective rivers represent the average IPS per year (2018, 2019 and 2021) plotted against the average EC for that respective year, data points are in no particular order. From Figure 42 it can be seen that the IPS scores and the EC measurements, taken *in situ,* have a strong relationship with each other. A negative correlation is immediately visible, as the EC increases, the IPS score decreases. A Pearson correlation coefficient of 0.67 between IPS and EC indicates a strong correlation. A R^2 value of 0.45 was also obtained, which means 45% of the variation in the IPS index values can be accounted for by the variation in measured EC. Additionally, a p value of 0.006 was calculated for IPS and EC, which is highly significant. This means that the

calculation of the IPS (based on diatom community characteristics), has a strong and very significant correlation with the EC measurements taken *in situ*.

3.3.2 IPS correlation with average total rainfall

In the above section, it is illustrated how the IPS scores decrease with increasing electrical conductivity. This correlation is strong, however, does not account for all of the variation in the IPS scores. These scores, again, are determined by the autecological preferences of diatom taxa to nutrients, ionic load and organic composition, and therefore other external influences, such as rainfall, may account for the remaining variation in these values (IPS scores).

The calculated IPS scores (averaged across sites) for the rivers sampled show a clear correlation with the average total rainfall, however, not all of the rivers follow the same profile (Figure 43). Three of the rivers (Luvuvhu, Sabie and Letaba) show distinct positive correlation, as the average rainfall increases for each year, the average calculated IPS scores increases. The Crocodile River does also show a general increase in average IPS with increased rainfall; however, the trend is less obvious and slightly weaker than the latter rivers. The nature of the trend is due to the higher average IPS for 2020 compared to the other IPS scores for this river. The reason for this is explained further in section (5.2.1) and is due to the complete dominance of one diatom taxon, *Cocconeis placentula*. Interestingly, the profile followed by the Olifants River does not show an increase in average IPS with increased total average rainfall as expected, this suggests the higher average rainfall has increased the nutrient, ionic and/or organic load of the river. High rainfall is correlated with increased surface water pollution derived from diffuse sources; however, this river is subject to possible effluent flow from the Palabora mining company which discharges into the Ga-Selati River, and is therefore a source of point pollution and not diffuse. Additionally, the rivers generally known to be healthy and have little anthropogenic impact such as the Sabie, Luvuvhu, and to a lesser extent the Letaba River, all show clear increases in water quality with higher rainfall and the rivers known to be heavily subject to anthropogenic activities such as the Olifants River show a decrease in water quality with increased average seasonal rainfall.

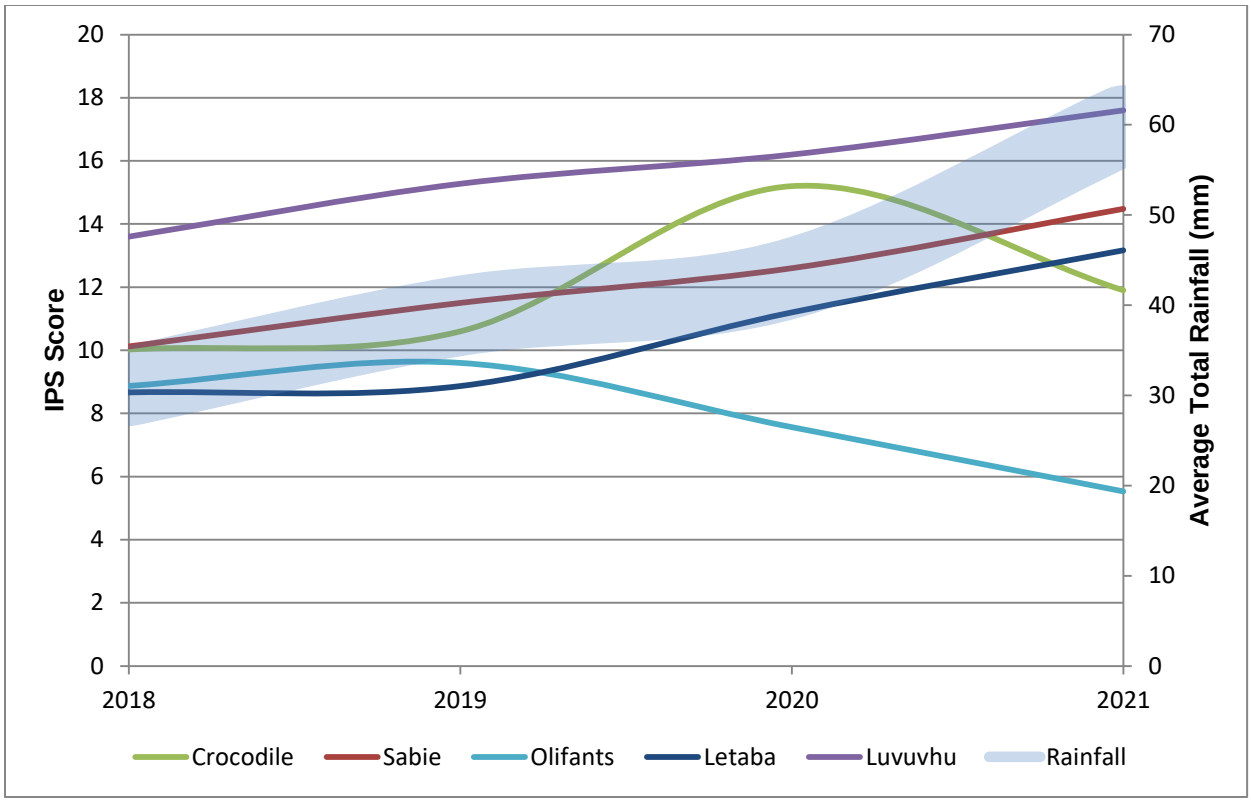

Figure 43: The correlation between inferred water quality (IPS) and average total rainfall in each year for all rivers.

3.3.3 Spatial and temporal changes in IPS scores

3.3.3.1 Crocodile River

Nsikazi

During 2018, the diatom community composition at the Nsikazi site was comprised of *Cocconeis placentula* (66%), *Nitzschia* spp. (10.8%) and *Gomphonema minutum* (10%) (Table 14). *Nitzschia* spp. are known to be pollution tolerant and can occur over a range of trophic states and electrolyte content (Taylor & Cocquyt, 2016). *Cocconeis placentula* cannot tolerate high salt concentrations and occurs in meso- to eutrophic conditions as described in section 4.1.3, 4.2.2 and 4.3.2. *Gomphonema minutum* is associated with similar trophic conditions and salt concentrations, however, it cannot tolerate more than moderate levels of pollution (Taylor *et al*., 2007b).

During 2019, *Nitzschia* spp. increased in abundance (29%) while *C. placentula* decreased in abundance (24%). Other taxa such as *Rhoicosphenia abbreviata* (usually associated with elevated nutrient) became rather abundant compared to other taxa (21%) (Table 14). The

greater abundance of *Nitzschia* spp. and *R. abbreviata* and the lower abundance of *C. placentula* in 2019 compared to 2018 suggests an increase in nutrient concentrations and electrical conductivity, and explains the low IPS score for 2019 (8.1) compared to 2018 (12.1) (Table 9 and Figure 44). This site was only sampled during drought years where no flushing and limited dilution occurred, constituents, such as organic pollutants, nutrients and ionic compounds are more concentrated in such conditions thereby increasing the electrical conductivity and trophic state (Dallas & Day, 2004). These conditions give rise to poor water quality which is consequently reflected by the diatom communities present.

The town of Nsikazi is nearby and may contribute to the increase in organic pollutants through surface runoff, thereby lowering the water quality. Organic substances in rivers can either be dissolved or particulate, the degree of organic pollution relates to quantity, size and texture of substances (Dallas & Day, 2004). Particulate Organic Matter (POM) is usually larger than Dissolved Organic Matter (DOM) and occurs naturally from sources such as leaf litter and branches. Natural DOM includes humic and fulvic substances that absorb and reflect light. Anthropogenic DOM and POM tends to be soluble and occurs as small biologically labile compounds within rivers that commonly originates from domestic sewage, animal feedlots and abattoirs (Dallas & Day, 2004). Organic pollution is defined as those substances that originate from or is produced by living organisms. While the increase in organic substances might not be directly toxic to biota, the biological oxygen demand (BOD) of aquatic biota increases thereby decreasing the DO concentration, which can have severe negative effects (Dallas & Day, 2004).

Malelane

The diatom community at this site was comprised mostly of *Cocconeis placentula* and *Nitzschia* spp. across all years sampled, however, other taxa including *Eolimna subminuscula* were also present.

Cocconeis placentula represents slightly more than half of the community structure during 2018 (51%), while *Nitzschia* spp. (11%), *E. subminuscula* (9%) and *Gomphonema venusta* (7%) were present in lower abundances (Table 14). *Cocconeis placentula* occurs in waters with moderate to low electrolyte content and meso- to eutrophic conditions while *Nitzschia* spp. and *E. subminuscula* can occur in greater abundance under higher electrolyte content and higher trophic levels (Taylor & Cocquyt, 2016; Taylor *et al*., 2007b). *Eolimna subminiscula* can also tolerate extreme levels of pollution (Taylor *et al*., 2007b). *Gomphonema venusta* is associated

with low to moderate electrolyte content and oligo- to mesotrophic conditions (Taylor *et al*., 2007b).

In 2019, however, *C. placentula* dominated the community with 82% relative abundance. *Nitzschia* spp. decreased (4%) while other species like *Encyonopsis leei* var. *sinensis* (2%), *Navicula veneta* (2%) and *Navicula microlyra* (1%) replaced those previously present (Table 14) which were *E. subminiscula* (9%)*, G. venusta* (7%) & *Eolimna minima* (4%). *Encyonopsis leei* var. *sinensis* occurs in higher abundance under oligo- to mesotrophic conditions with moderate to low electrolyte content. *Navicula veneta*, however, is extremely pollutant tolerant and occurs in higher electrolyte content and trophic levels (Taylor *et al*., 2007b). The high abundance of *C. placentula* and the presence of *E. leei* var. *sinensis* is the reason the IPS increases from 10.4 to 13.5 (Table 9 & Figure 44).

As in 2018 and 2019, *C. placentula* occured in high abundance during 2021, however, with abundances lower than in 2019 (62%). *Nitzschia* spp. once again increased in abundance (21%) together with *E. subminiscula* (7%). Other pollution tolerant taxa such as *Nitzschia amphibia* were also present at 5% relative abundance. *Nitzschia amphibia* is found in waters with elevated electrolyte content (Taylor *et al*., 2007b) and contributes to the low IPS score of 8.9 (Table 9).

The diatom communities at this site, across all years sampled, suggest elevated electrolyte content, elevated nutrient content and a meso- to eutrophic state. During 2018 and 2019, water quality was expected to be low due to the drought conditions experienced, and then expected to increase as the average annual rainfall increases. However, during 2021, the community was still comprised of taxa associated with elevated electrolyte content and meso- to eutrophic states, additionally, *E. subminuscula* was present during 2021, which can tolerate extreme levels of pollution and suggests an increase in organic substances. The average rainfall around the Malelane site is generally high due to the updrafts created by the Khandizwe hills, and so the water quality at this site was expected to be higher, however, it seemed that the seasonal flushing did not imporve the water quality.

Marula

This site had a similar high dominance of *Nitzschia* spp. and *Cocconeis placentula* in 2018, compared to Malelane. The former taxa does, however, occur in greater abundance (44%) than the latter (28%). *Gomphonema pumilum* var. *rigidum* was also present at this site in relatively low abundances (6%) (Table 14). This taxon occurs in meso- to eutrophic conditions with

moderate electrolyte content and cannot tolerate more than moderate amounts of pollution (Taylor *et al*., 2007b). *Navicula viridula* and *Navicula schroeteri* were among the dominant diatoms with 3% and 2% relative abundances respectively. Both of these taxa are tolerant of strongly polluted conditions and occur in elevated electrolyte content (Taylor *et al*., 2007b), however, *N. viridula* is considered a rare species in South Africa by Cholnoky (1962a). The presence of these pollution-tolerant taxa during 2018 explains the low IPS score of 5.5 (Table 9).

Cocconeis placentula and *Nitzschia* spp. were again the most abundant taxa during 2019. The former represents 51% of the community composition, while latter represents 13% and decreased from 2018. Other taxa including *N. viridula, Navicula schroeteri* and *G. pumilum* var. *rigidum* were no longer found amongst the abundant taxa present in the community. *Gomphonema venusta* (10%), *Navicula cryptotenelloides* (5%) and *Nitzschia amphibia* (4%) occurred in greater abundance. *G. venusta* occurs in low electrolyte content and oligo- to mesotrophic levels (Taylor *et al*., 2007b). The other taxa present, *N. cryptotenelloides* and *N. amphibia* can however tolerate increased trophic states and elevated electrolyte content (Taylor *et al*., 2007b). The greater abundance of *C. placentula* and *G. venusta*, and the lower abundance of *Nitzschia* spp. in relation to other taxa present explains the increase in IPS from 5.5 to 10 (Table 9 and Figure 44).

An entirely different community is present during 2020. *C. placentula* is abundant and accounts for 91% of the community composition. Taxa previously present were no longer found and other less pollutant tolerant taxa appeared in slightly higher abundances. *Gomphonema minutum*, *Achnanthidium minutissimum*, *G. pumilum* var. *rigidum* and *Kolbesia ploenensis* were present at abundances of between 1 and 2% of the community structure (Table 16). *G. minutum* can tolerate higher trophic levels with elevated electrolyte content, it can, however, not tolerate more than moderate amounts of pollution. *Achnanthidium minutissimum* on the other hand occurs in greater abundance in water with low electrolyte content (Taylor *et al*., 2007b) as well as in oxygen-rich nutrient-poor (oligotrophic) waters (Cholnoky, 1962a). *Cocconeis placentula* cannot tolerate more than moderate levels of pollution and with its high abundance, the IPS score is on the threshold of mesotrophic with 15.2 (Table 1), however, still within a meso-oligotrophic range.

Gomphonema spp. and *Nitzschia* spp. increased in abundance from 2020 to 2021 with 37% and 6% abundance, respectively. *Cocconeis placentula* and *Achnanthidium* spp. were still present, however, in lower abundances with 54% and 1%, respectively. *Gomphonema* spp. greatly

increased in abundance and formed 37% of the community composition during 2021 (Table 14). This increase in more pollution tolerant taxa reflects the shift from meso-oligotrophic conditions (IPS – 15.2) to meso-trophic conditions (IPS – 13) (Table 9).

Similar to the Nsikazi and Malelane sites in 2018 and 2019, this site was dominated by taxa occurring in elevated electrolyte content, meso- to eutrophic conditions and higher degrees of organic pollution. During the drought years the abovementioned conditions were not uncommon and saw a general deterioration in water quality due to the lack of dilution or flushing of the system (Van Vliet & Zwolsman, 2008; Nosrati, 2011). However, during 2020 the diatom community was comprised of taxa associated with moderate to low electrolyte content, taxa occurring under high electrolyte content decreased in abundance. *Achnanthidium minutissimum* was also encountered during 2020, this taxon is common under higher stream velocities. This suggests the higher rainfall for 2020 had increased the stream discharge at this site. A similar increase in water quality was expected during 2021, however, taxa associated with high electrolyte content and higher nutrient concentrations became more abundant, which is in contrast to the expected dilution and flushing effect of the increased average rainfall. The rainfall period was, however, more intense during 2021 compared to 2020, intense rainfall typically accumulated greater amounts of pollutants and nutrients from surrounding areas and can contribute to a decrease in water quality (Ching *et al*., 2015).

Nkongoma

This site also had a high abundance of *Cocconeis placentula* across all years sampled, however, the abundance decreased with time. During 2018, this taxon represented almost 61% of the community composition while other taxa such as *Anorthoneis dulcis* (4%), *Gomphonema pumilum* var. *rigidum* (4%), *Nitzschia* spp. (4%) and *Navicula vandamii* (3%) were present in lower abundances (Table 14). The latter three taxa can tolerate elevated electrolyte content and elevated pollution levels (Taylor *et al*., 2007b; Taylor & Cocquyt, 2016). The ecology of *A. dulcis* is not well known although it is thought to prefer alkaline oligotrophic conditions (Taylor & Cocquyt, 2016). The high abundance of *C. placentula* which cannot tolerate high levels of pollution, together with the other taxa, indicates water in a meso-eutrophic trophic state with an IPS score of 12.1 (Table 9).

During 2019, *C. placentula* slightly decreases in abundance while other pollution tolerant taxa that prefer elevated electrolyte content increased in abundance. *Gomphonema minutum* and *G. parvulum* can tolerate increased levels of pollution and high electrolyte content, similar to

Nitzschia spp. which also increased in abundance. This change in community structure explains the drop in IPS score from 12.1 to 10.8 from 2018 to 2019 (Table 9 and Figure 44).

A similar abundance of *C. placentula* was present during 2021, however slightly lower than in 2019 with 49% of the community composition. *Anorthoneis dulcis* increased in abundance (21%) and *Gomphonema* spp. together with *Nitzschia* spp. decreased in abundance with 5% relative abundance each. *Cocconeis pediculus* was also present with 6% abundance (Table 14). This taxon occurs in elevated electrolyte content (Scheele, 1952; Simonsen, 1962), but cannot tolerate high levels of pollution (Taylor *et al*., 2007b). Consequently the community structure during 2021 showed an increase in water quality from meso- eutrophic conditions to mesotrophic with IPS = 13.9 (Table 9 & Figure 44).

A high abundance of *C. placentula* characterised this site across all years sampled. As mentioned, this taxon occurs in meso- to eutrophic conditions, and low to moderate electrolyte content. During 2018, other taxa that are associated with elevated electrolyte and organic content were also abundant, which correlates with water quality changes associated with drought. A further decrease in water quality occurred during 2019 as reflected by the greater abundance of *G. minutum* and *Gomphonema parvulum*. Water quality was expected to increase from 2018 to 2019, however, this was not the case. From 2019 to 2021, an increase in water quality was observed. This is due to the greater presence of *Anorthoneis dulcis* and *C. pediculus* and low presence of *Nitzschia* spp. and *Gomphonema* spp. The diatom communities present at this site indicate a moderate to high electrolyte content with little organic pollution and consequently indicate a general improvement in water quality in terms of lower electrolyte content and lower nutrient concentrations. It therefore seems that the increased average rainfall has aided in the dilution of constituents at this site across years sampled.

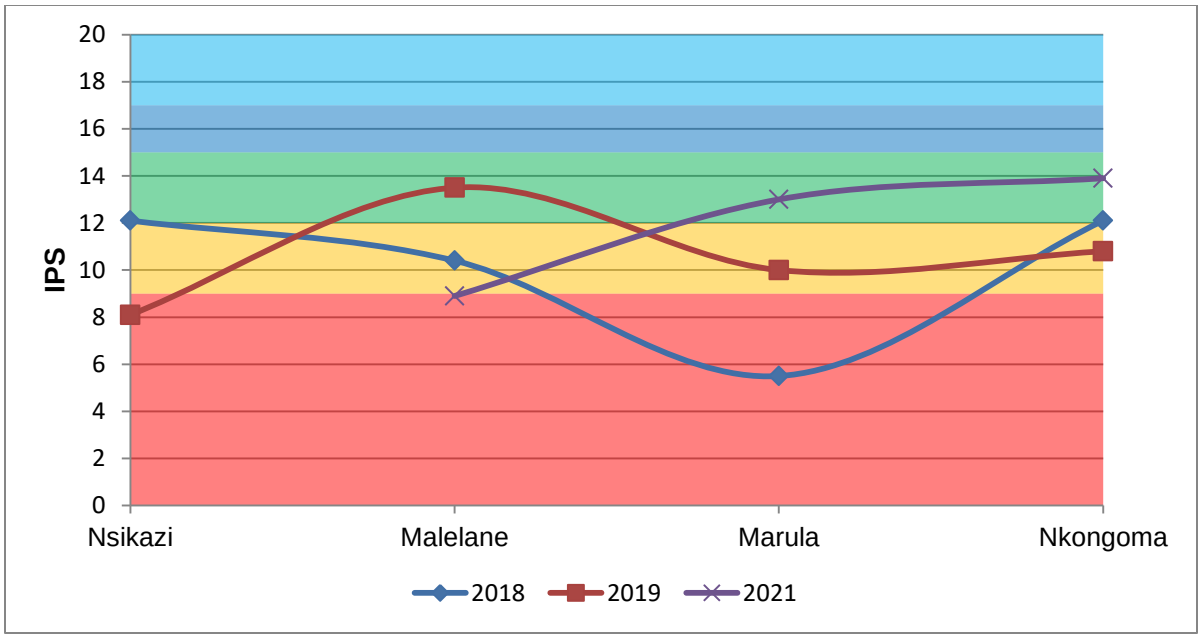

Figure 44: IPS scores for sites in the Crocodile River from 2018 to 2021.

Summary

The taxon associated most with the Crocodile River was *Cocconeis placentula*. This species occured in the greatest abundance across most sites sampled, *Nitzschia* spp. were the second most common taxon and occured in greater abundance that *C. placentula* at two sites sampled (Nsikazi – 2019; Marula- 2018). *Cocconeis placentula* is associated with moderate to low electrolyte content and meso- to eutrophic conditions, this species can also not tolerate elevated organic pollution. Consequently the general inferred water quality for the Crocodile River is moderate, and differs from site to site based on the relative abundance of other taxa present as described for the individual sites.

A general increase in water quality was evident from 2018 to 2021. The Malelane site had the best water quality during 2019, however, during 2021, the water quality was very poor, on the border of eutrophic and meso-eutrophic. The profile followed by the Marula site indicates an improvement in water quality over the study period, it slightly decreases in 2021, however, still remained within the mesotrophic classification. The profile for the Nkongoma site indicates a clear improvement in water quality from 2018 to 2021.

Figures 44 and 45 illustrate how the water quality in the Crocodile River has generally improved or recovered with distance downstream in terms of ionic composition, nutrient concentrations and organic pollution. The water quality change from 2018 to 2021 also indicated an

improvement across years sampled. The Nkongoma site during 2021 showed an increase in water quality with an IPS score of 13.9, the second highest score of all sites across all years in the Crocodile River. The Marula site during 2020 had an IPS greater than 15, indicating the river at this site to be of good water quality and in a meso-oligotrophic state.

The water quality changes for the Crocodile River from 2018 to 2021 correlated with a decrease in electrolyte content, a decrease in nutrient concentrations (lower trophic state) and a generally low amount of organic pollution, as reflected by the diatom communities. These respective changes in electrolyte content, nutrient concentration and organic pollution can be attributed to an increased dilution and flushing rate caused by the increased average seasonal rainfall, because, as the general amount of rainfall increased, the water quality inferred by diatom communities also improved (Figure 46).

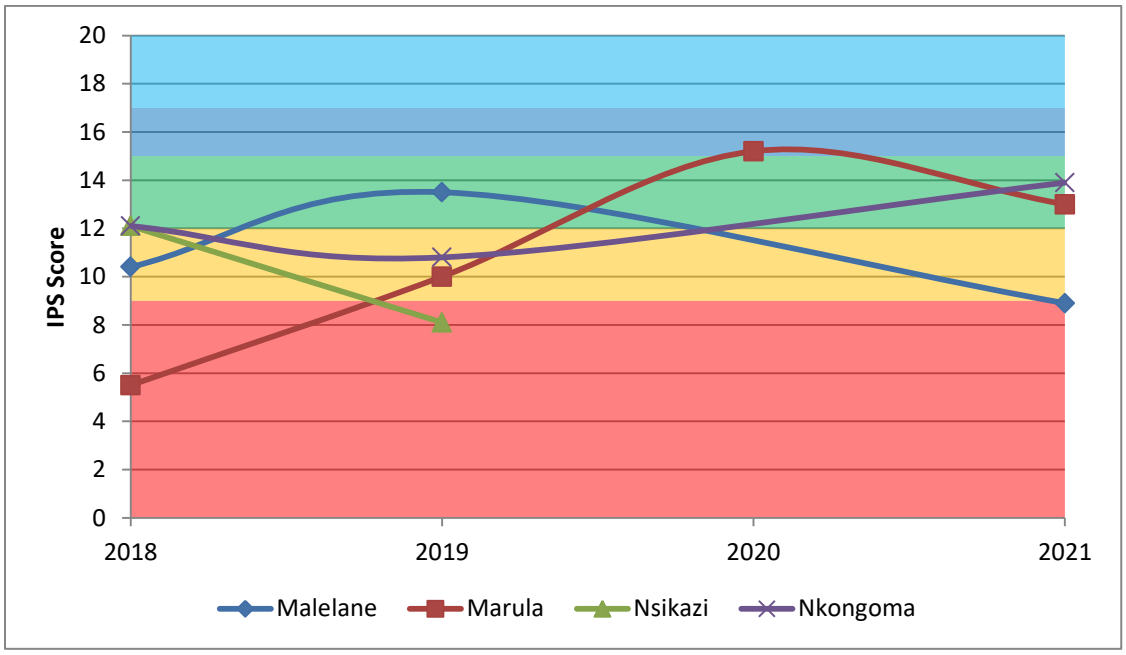

Figure 45: The annual fluctuation IPS scores in the Crocodile River from 2018 to 2021.

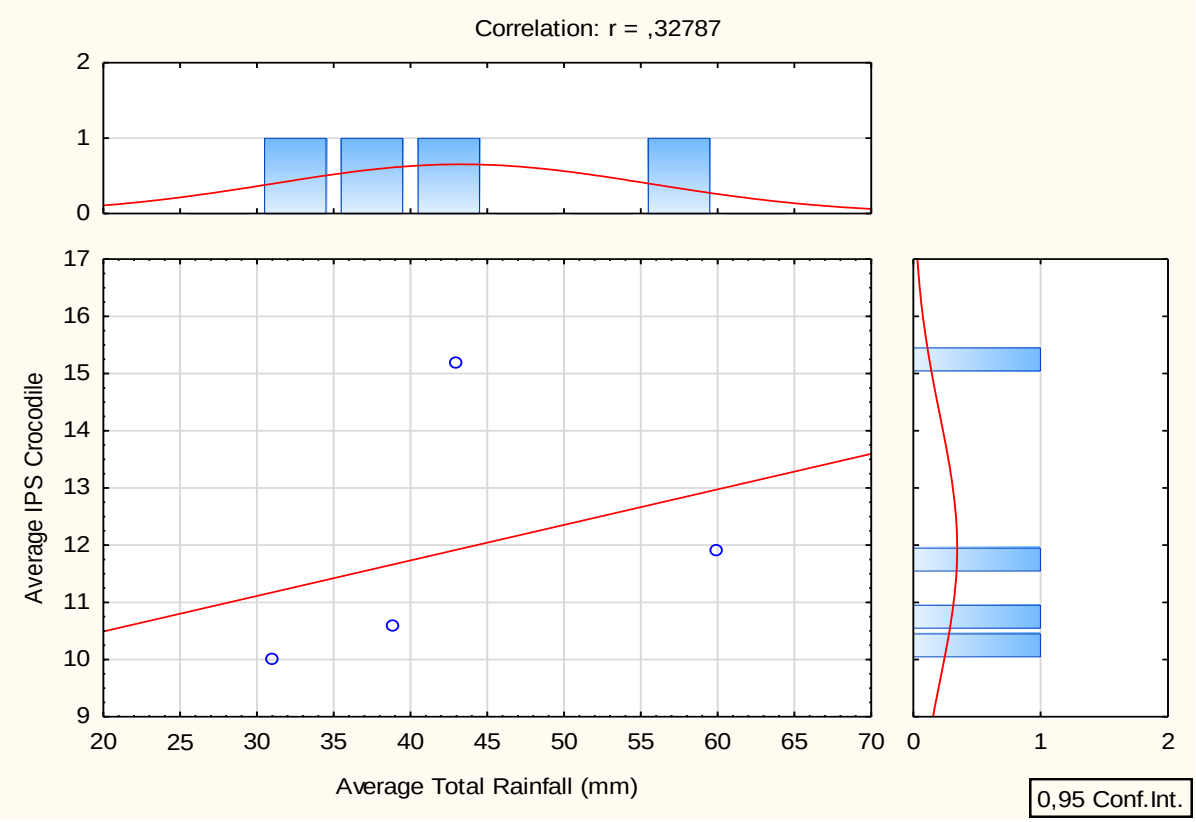

Figure 46: Correlation between the average IPS score for each year (2018 to 2021) in the Crocodile River and the average total rainfall for each respective year. Data points, from left to right, resemble IPS scores and average total rainfall from 2018 to 2021 respectively. (1st – 2018; 2nd – 2019; 3rd – 2020; 4th - 2021).

3.3.3.2 Sabie River

Sekurukwane

This site had high abundances of *Nitzschia* spp. during 2018 and 2019, comprising around 50% of the community structure in both years (Table 13). *Gomphonema* spp. and *Nitzschia frustulum* were also present during 2018, and together with *Nitzschia* spp., account for the low IPS score for that year (5.3). *Achnanthidium* spp. were also present during 2018 together with *Ulnaria nyanse*, however, in lower abundance. *Ulnaria nyanse* is commonly found in meso- to eutrophic conditions (Hustedt, 1937; Hustedt, 1957).

From 2018 to 2019, *Nitzschia* spp. remained abundant, however, *Encyonopsis leei* var. *sinensis, Achnanthidium rivulare* and *Cymbella turgidula* all increased in abundance in 2019. These species together represented less than 12% of the community composition, and because

of the high prevalence of *Nitzschia* spp., the water quality remained poor although *E. leei* var. *sinensis* and *C. turgidula* typically prefer lower electrolyte levels and little organic material (Hustedt, 1957; Weber, 1970; Taylor *et al*., 2007b). However, the IPS still increased from 5.3 to 6.8 (Table 9) from 2018 to 2019 because of the higher abundance of the latter taxa.

Nitzschia spp. were still abundant during 2020, although lower in number than in 2018 and 2019. Other taxa including *Melosira varians, Encyonema minutum* and *Navicula* spp. increased in abundance (Table 13). *Melosira varians* is common in eutrophic waters, it can also be particularly abundant in brackish conditions (Hustedt, 1937; Jørgensen, 1952; Hustedt 1957; Cholnoky, 1968). *Encyonema minutum*, however, prefers lower electrolyte content and oligotrophic conditions similar to *Achnanthidium* spp. and *Cymbella turgidula*, which were also present. This explains the increase in the IPS score from 6.8 in 2019 to 9.0 in 2020 (Table 9).

During 2021, *Nitzschia* spp. abundance decreased significantly. *Achnanthidium crassum, Navicula* spp. and *Navicula vandamii* all increased in abundance (Table 13). *Achanthidium crassum* cannot tolerate high levels of pollution and occurs in waters with moderate electrolyte content. *Navicula vandamii,* however, is often found in waters with higher electrolyte content and is abundant in eutrophic conditions (Taylor *et al*., 2007b). The high presence of *A. crassum* and the low presence of *Nitzschia* spp. explain the increase in water quality from poor (IPS - 9) to moderate (IPS - 14.8) in 2021 (Table 9 & Figure 47).

The diatom community structures at this site was mostly comprised of *Nitzschia* spp. and *Gomphonema* spp. during 2018, these taxa were common in waters with high electrolyte content and meso- to eutrophic states. As mentioned, electrolyte content and nutrient concentrations increase under low flow conditions, which correlates with the low seasonal rainfall experienced during 2018. As the average seasonal rainfall increases from 2018 to 2021, the diatom communities in this site change towards one comprised of taxa associated with moderate to low electrolyte content and meso- to oligotrophic states, which indicates a dilution effect. Additionally, taxa inlcuding *Cymbella turgidula, Achnanthidium minutissimum* and *Encyonopsis* var. *sinensis* indicate little to no organic pollution. The change in diatom community structure from 2018 to 2021 therefore reflects the increase in water quality caused by the increased discharge, linked to seasonal rainfall.

Tinga

A rather even diatom species distribution was present in the community found at this site during 2018. *Navicula* spp.*, Cymbella turgidula, Achnanthidium* spp.*, Planothidium rostratum* and *Encyonopsis leei* var. *sinensis* all occured in similar abundance, not varying by more than 5% (Table 13).

Encyonopsis leei var. *sinensis*, *Cymbella turgidula* and *Achnanthidium* spp. occured in oligo- to mesotrophic conditions with lower electrolyte content (Hustedt, 1957; Weber, 1970; Taylor *et al*., 2007b). *Planothidium rostratum* similarly occurs in low to moderate electrolyte content and often occurs in circumneutral to alkaline waters (Taylor *et al*., 2007b). *Navicula* as a particularly diverse genus does, however, have a wider ecological range (Coquyt & Taylor, 2016) and therefore this in turn leads to lower IPS scores. Nevertheless, the water quality for this site is considered mesotrophic during 2018 (IPS – 13.6) (Table 9). The community structure became less even in 2019, with *E. leei* var. *sinensis* and *Navicula* spp. having higher abundances than other taxa - *Achnanthidium* spp. and *P. rostratum*. The higher abundance of *E. leei* var. *sinensis* in 2019 compared to 2018, raises the IPS score from 13.6 to 14.7, which is on the border of meso-oligotrophic (IPS – 15) (Figure 47).

During 2021, *Achnanthidium* spp. were higher in abundance with *A. minutissimum* well represented. *Encyonopsis leei* var. *sinensis* was also high in abundance with 19% of the community composition (Table 13). *Cymbella turgidula* and *Achnanthidium crassum* were also present, however, in lower abundance. All taxa present prefer lower electrolyte content and low nutrient conditions and consequently the IPS score was higher. The water quality for this site during 2021 is considered oligotrophic, with an IPS score of 17.1 (Table 9 & Figure 47).

The diatom communities at this site were comprised of species occurring in meso-oligotrophic states and moderate to low electrolyte content across all years. This suggests the drought years of 2018 and 2019 did not have a substantial impact on the water quality and that the discharge was sufficient to prevent eutrophication. The water quality did increase from 2018 to 2021 as reflected by the high abundances of *Achnanthidium* spp. and *Achnanthidium minutissimum*. These taxa are firmly attached to their substrate and favour high stream velocities and low nutrient content. The presence of these taxa suggest a further dilution effect caused by the increased discharge linked to higher seasonal rainfall. Additionally, the taxa occurring in greatest abundance, such as *Cymbella turgidula, Achnanthidium* spp. and *A. minutissimum* indicate little to no organic pollution.

Sand

The IPS scores for the Sand River are not illustrated in Figures 47 and 48. The site was only sampled during 2018 and 2021 and this would have distorted the results on the IPS graphs. However, the IPS for the Sand River during 2021 was 8.7 which indicated eutrophic conditions (Table 9). This score was due to the presence of *Nitzschia* spp. and *A. dulcis* which have very low IPS sensitivity (s) and indicator (v) values. *Cocconeis placentula* also does not significantly contribute to a high IPS score as it is found in waters having meso- to eutrophic conditions with moderate to low electrolyte content. The stream depth at this site was extremely shallow and therefore the discharge in terms of volume is low. A lower volume of water does not influence water quality negatively, however, if industrial or domestic effluent is discharged into a river with low water volume, any consituents in the effluent would not be diluted sufficiently to avoid a degredation in water quality. Therefore, the poor water quality during 2021 is not surprising.

Antholysta

The diatom community at this site changed little between 2018 and 2019, additionally, the community had a relatively even distribution of taxa. In both years, *Encyonopsis leei* var. *sinensis* and *Achnanthidium* spp. were in higher abundance compared to other taxa e.g., *Cymbella tumida* and *Cymbella turgidula* (Table 13). All of these taxa occurred in greatest abundance in oligo-mesotrophic conditions with moderate to low electrolyte content; *Cymbella tumida* can only tolerate low salinity (Hustedt, 1957; Foged, 1964). Consequently, their abundances were similar. *Navicula* spp. were also encountered during 2018. *Navicula microlyra* was present in 2019 and absent during 2018. The community structure for 2018 and 2019 indicate moderate and good quality respectively with IPS = 14.6 and IPS = 15.5 (Table 9 & Figure 47).

During 2020, the community shifted in composition. *Achnanthidium* spp.*, Achnanthidium minutissimum* and *Achnanthidium crassum* were higher in abundance (Table 13). *Ulnaria nyanse* and *Cymbella turgidula* shared similar abundances, *U. nyanse* was not present during previous years. This species is found in meso- to eutrophic conditions, however, with the presence of the other taxa, the IPS score (16.2) indicated good water quality.

Ulnaria nyanse was only present in low abundance during 2021 and did not represent more than 5% of the community structure. *Cymbella tumida*, *Cymbella turgidula* and *Envyonopsis leei* var. *sinensis* increased in abundance and indicated a return to oligo– mesotrophic conditions (Taylor *et al*., 2007b). *Cocconeis placentula* was also present, where it was not encountered

during the previous year's sampling, this taxon indicates mesotrophic conditions. The shift in community structure from 2020 to 2021 indicated a decrease in water quality from olig-mesotrophic to mesotrophic conditions (IPS = 14.5) (Table 9 & Figure 47).

The diatom communities, across the study period, were again comprised of taxa occurring in moderate to low electrolyte content, meso- to oligotrophic conditions and low organic content. Taxa such as *Achnanthidium* spp. and *Achnanthidium minutissimum* were present during 2018 and 2019, these taxa are commonly found in high stream velocities, which would suggest the discharge during the drought years was still sufficient to maintain good water quality. A decrease in the inferred water quality was observed for 2021, this was due to the presence of *Cocconeis placentula* which was not encountered in previous years sampled, this taxon prefers meso- to eutrophic conditions with moderate to low electrolyte content. This suggests that the impact of the drought experienced was not as severe in terms of eutrophication, increased ionic compound and organic material.

Lubye-Lubye

The taxon highest in abundance at this site during 2018 was *Encyonopsis leei* var. *sinensis*. This species is found in waters with lower electrolyte content as well as oligo- mesotrophic conditions (Taylor *et al*., 2007b). Other taxa including *Navicula microlyra*, *Nitzschia frustulum* and *Cymbella turgidula* have similar abundances (Table 13). The ecology of *N. microlyra* is largely unknown, however, it was described by Cholnoky (1959) from a small wetland near the shore of the Kleinmond lagoon in Bettie's Bay, South Africa, and is therefore thought to occur under high salt concentrations. *Cymbella turgidula* typically occur in oligo- to mesotrophic conditions with lower electrolyte content (Hustedt, 1957; Weber, 1970) while *Nitzschia frustulum* can tolerate fluctuations in osmotic pressure and occurs in waters with elevated nutrients (Taylor *et al*., 2007b; Simonsen, 1962). The water quality as indicated by the diatom community was good and in a mesotrophic state (IPS = 15.3) (Table 9 & Figure 47).

During 2019, more than 50% of the community was represented by *Encyonopsis leei* var. *sinensis* and *Cymbella kolbei*. Both taxa occur in lower electrolyte content, however, the latter occurs in higher abundance in oligotrophic conditions. *Nitzschia frustulum* and *Cymbella turgidula* remained similar in abundance, while *Navicula microlyra* decreased in abundance (Table 13). Consequently, the high abundance of *C. kolbei* and *E. leei* var. *sinensis* contributed to the higher IPS score of 16.8.

Nitzschia frustulum was not found at this site during 2021. Other taxa including *Achnanthidium crassum* and *Achnanthidium minutissimum* increased in abundance together with other *Achnanthidium* spp. *Encyonopsis leei* var. *sinensis* and *Cymbella turgidula* still remained present in lower abundances. Consequently, the IPS score was high (16.6) indicating good water quality (Table 9 & Figure 47).

The diatom community structure at this site, across all years, is comprised of taxa that occur in moderate to low electrolyte content and meso- to oligotrophic states. However, *Cymbella kolbei*, present during 2019, is strongly associated with oligotrophic conditions and cannot tolerate organic pollution. The discharge of the Sabie River at this site during 2018 and 2019 seemed sufficient to maintain good water quality, through dilution of nutrients and ionic compounds. During 2021, taxa that occur in higher stream flow velocities such as *Achnanthidium* spp., *Achnanthidium crassum* and *Achnanthidium minutissimum* increased in abundance, indicating on higher stream discharge. The increase in water quality for this site can, therefore, be attributed to an increased stream discharge, which is linked to the higher average seasonal rainfall.

Sabiepoort

The community structure during 2018 and 2019 was comprised of species preferring elevated electrolyte content and higher nutrients. *Nitszchia* spp. were particularly abundant with 80% and 65%, respectively, during 2018 and 2019 (Table 13). Other taxa present during 2018 were *N. frustulum, Gomphonema lagenula* and *Gomphonema parvulum*. All these taxa prefer elevated electrolyte content and can tolerate high levels of organic pollution (Taylor *et al*., 2007b), however, Cholnoky (1962a) considered *G. parvulum* to be only tolerant of low salt concentrations and also requires fluctuating nitrogen concentrations to develop optimally. In more recent literature, e.g. Taylor et al (2007b), this taxon is described as occurring under elevated electrolyte content and higher trophic levels. Consequently the water quality for this site is considered bad with an IPS score of 2.1 (Table 9 & Figure 47). During 2019, an increase in the abundance of *Cocconeis placentula* and *Encyonema minutum* was evident, this, however, did not raise the IPS score significantly and was also consequently classified as highly eutrophic (IPS = 3.7) (Figure 47).

The community was more or less evenly distributed during 2021, aside from a higher abundance of *Sellaphora seminulum* (Table 13). This species occurs in high electrolyte content and can tolerate substantial levels or pollution (Taylor *et al*., 2007b). *Nitzschia dissipata* was

also present, this species prefers elevated electrolyte content (Taylor *et al*., 2007b), however, it's exclusively associated with high calcium and magnesium content and not with sodium and chloride content. *Cocconeis placentula* also occurs in abundances similar to *S. seminulum*. *Navicula rostellata* can tolerate higher nutrient levels, however, cannot tolerate more than moderate amounts of pollution. The presence of *S. seminulum* and *N. rostellata* indicates higher nutrient content, and the presence of *C. placentula* and *N. dissipata* indicate moderate water quality. The IPS score for this site in 2021 is 9.4, indicating poor water quality (Table 9 & Figure 47).

During 2018 and 2019, the diatom community composition was comprised of species that occur in elevated electrolyte content and high nutrient concentrations. Additionally, all taxa present, except *Nitzschia dissipata*, can tolerate elevated levels of organic pollution. *Gomphonema parvulum*, *Sellaphora seminulum, Nitzschia frustulum* and *Navicula rostellata* are indicators of organic pollution, however, the latter species cannot tolerate high concentrations of organic substances. Therefore, although the water quality was poor, it is most likely due to organic enrichment and not due to the impact of the recent drought. *Nitzschia dissipata* and *Navicula rostellat*a, present during 2021, can tolerate increased nutrient levels but not more than a moderate amount of organic pollution. The improvement in water quality from 2018 to 2021 was possibly linked to the flushing of organic material linked to the increase seasonal rainfall.

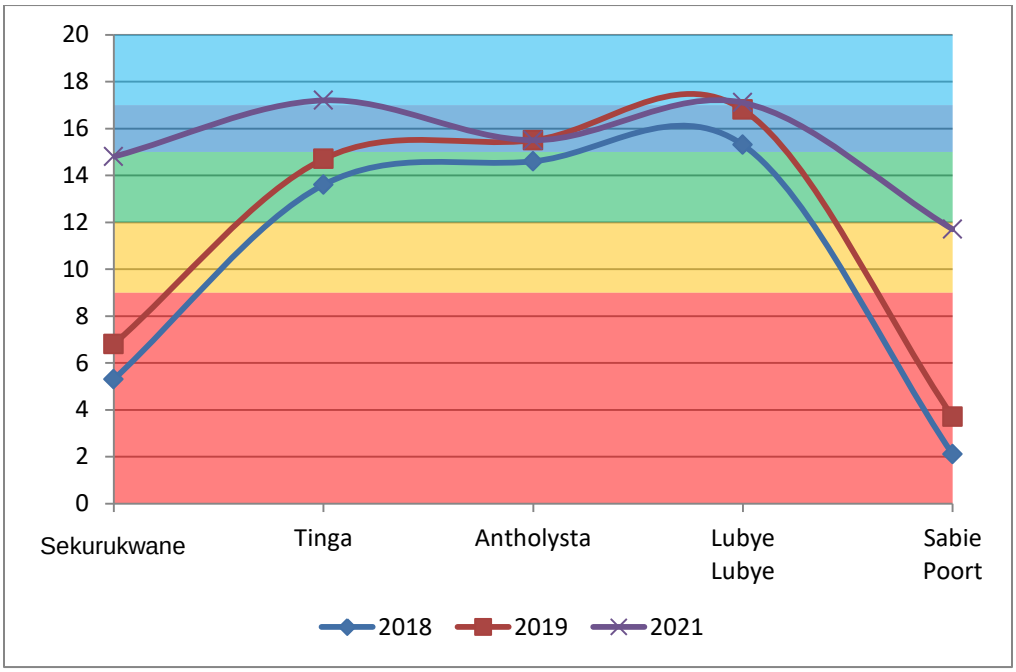

Figure 47: IPS Scores for sites in the Sabie River from 2018 to 2021, not including 2020.

Summary

During 2018 and 2019, the Sekurukwane and Sabiepoort sites were dominated by *Nitzschia* spp., other taxa including *Gomphonema* spp. and *Nitzschia frustulum* were also present. These taxa are associated with increased nutrient concentrations and elevated organic content. During 2020, the Sekurukwane site was similarly dominated by *Nitzschia* spp as was the case in in 2018 and 2019. However, the abundance was lower in 2020 (Table 13). In 2021 the Sekurukwane site was dominated by *Achnanthidium crassum*, *Navicula* spp. and *Achnanthidium* spp*. Achnanthidium crassum* and *Achnanthidium* spp. cannot tolerate organic pollution and occur in high abundance in nutrient poor water with high stream velocities. The Sabiepoort site also experienced a shift in the community structure. Most of the *Nitzschia* spp. were succeeded by *Sellaphora seminulum*, *Nitzschia dissipata* and *Cocconeis placentula*. *Sellaphora seminulum* can tolerate high levels of organic pollution, however, *N. dissipata* and *C. placentula* cannot tolerate organic pollution and occur in waters with moderate electrolyte content. This indicates an increase in water quality for these sites. Additionally, the diversity at the Sabiepoort site for 2021 was the highest enumerated in the present study. A total of 50 taxa were counted and identified from a valve count of 400.

Other sites (Tinga, Antholysta and Lubye-Lubye) had higher abundances of species such as *Encyonopsis leei* var. *sinensis*, *Cymbella turgidula*, *Achnanthidium* spp., *Cymbella tumida* and some *Navicula* spp. during 2018 and 2019. (Table 13). Most of these taxa occur in oligo- to mesotrophic conditions with low to moderate electrolyte content. During 2021 these sites were similarly dominated by *Achnanthidium* spp., *Encyonopsis leei* var. *sinensis*, *Achnanthidium minutissimum* and *C. turgidula* (Table 13). *Achnanthidium minutissimum* and *Achnanthidium* spp. are commonly associated with high stream velocities and low nutrient content and therefore the higher abundance of these taxa suggest an increase in stream discharge caused by the increased average seasonal rainfall.

The discharge of the Sabie River during 2018 and 2019 seemed sufficient to prevent the concentration of nutrients, organic material and pollutants within the system for most sites sampled. The diatom communities at the Sekurukwane and Sabiepoort sites during 2018 and 2019 indicate high nutrient content and increased organic pollution, however, with the increase in seasonal rainfall, the diatom communities shifted from those dominated by taxa tolerant of organic pollution to a more even distribution of taxa. Overall, the water quality in the Sabie River improved from 2018 to 2021 due to the increased seasonal rainfall, and the diatom community composition changes reflect this change (Figures 48 and 49).

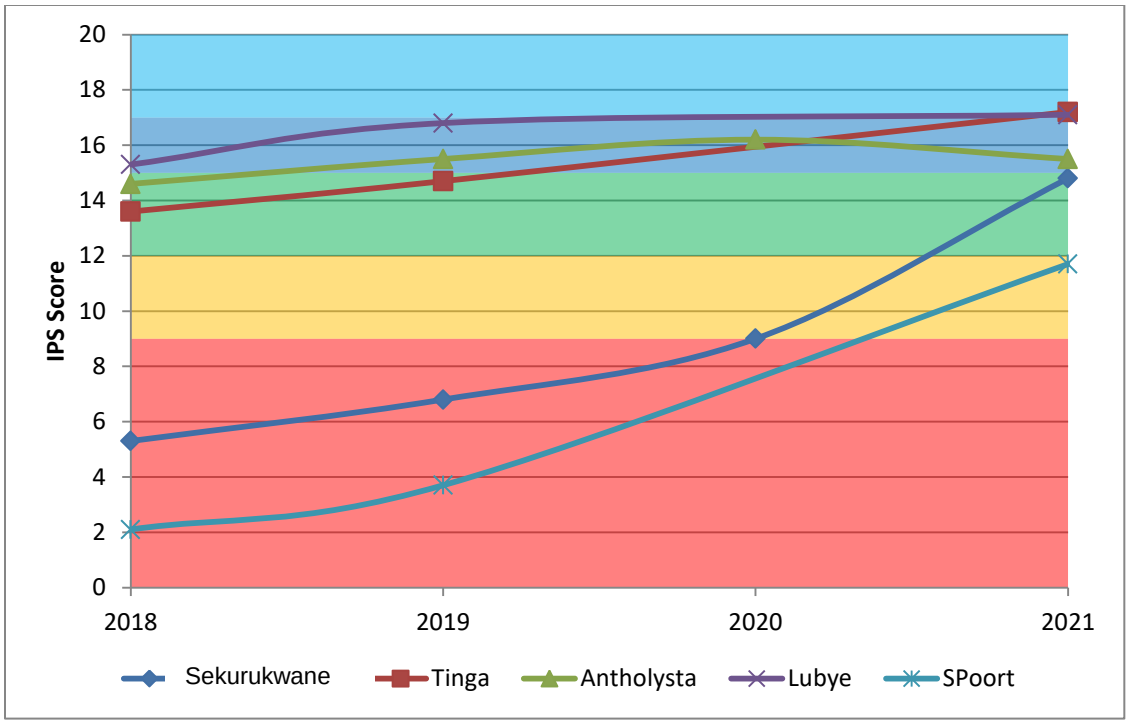

Figure 48: Changes in IPS score for sites in Sabie River from 2018 to 2021.

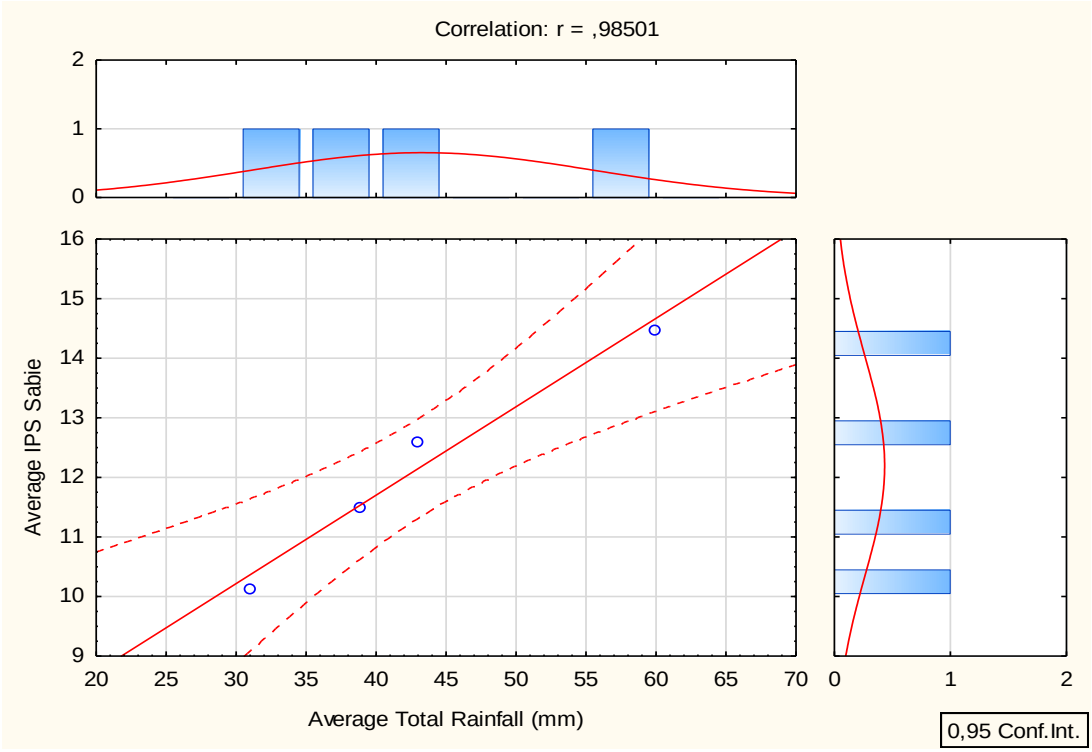

Figure 49: Correlation between the average IPS score for each year (2018 to 2021) in the Sabie River and the average total rainfall for each respective year. Data points, from left to right, resemble IPS scores and average total rainfall from 2018 to 2021 respectively. (1st – 2018; 2nd – 2019; 3rd – 2020; 4th - 2021).

3.3.3.3 Olifants River

Mamba

This site was dominated by *Nitszchia* spp. (76%) in 2018. This taxon, can in general tolerate high levels of pollution and higher electrolyte levels to a greater extent than other genera found in this study. *Navicula* spp. were also present during 2018 with 16%, 5% of which was accounted for by *Navicula cryptotenelloides* (Table 12). This species occurs in meso- to eutrophic waters (Taylor *et al*., 2007b). Consequently the IPS for this site was low (3.0) due to this high abundance of the taxa mentioned, indicating eutrophic, impacted conditions (Table 9). During 2019, *Cocconeis placentula* considerably increased in abundance (Table 12) which indicates a slight improvement in water quality. *Nitzschia frustulum* was still present which consequently lowered the IPS score. The water quality therefore increased from eutrophic (IPS = 3.0) to meso-eutrophic (IPS = 10.0) (Table 9 and Figure 50) from 2018 to 2019.

During 2021, *Nitzschia* spp. dominated this site (80% relative abundance), other taxa including *Gomphonema* spp. and *Achnanthidium* spp. were also present, however, in lower abundances (Table 12). The IPS value was therefore low (3.1) indicating eutrophic, impacted conditions (Figure 50).

The community structure at this site does not reflect an improvement in water quality from 2018 to 2021 as expected from the increased average seasonal rainfall. As mentioned in Section 2.1 the average rainfalls for the Olifants and Letaba rivers were lower compared to the other rivers in this study. A lower dilution was therefore expected, however, a temporal increase in water quality was still expected, which was not the case. The high abundance of one single taxa, *Nitzschia* spp., that can tolerate high degrees of pollution and electrolyte content, indicated a severely degraded ecological state.

Balule

During 2018 this site had a more evenly distributed community with *Nitzschia* spp. (30%), *Cocconeis placentula* (29%) and *Hippodonta* spp. (14%) (Table12). The presence of *C. placentula* indicates a slight increase in the water quality for this site, however, the higher abundance of *Nitzschia* spp. lowers the score and therefore the site during 2018 is considered eutrophic with IPS = 8.7 (Table 9 and Figure 50). *Hippodonta* spp. were found in a range of waters ranging from oligo- to eutrophic and electrolyte-poor to electrolyte-rich (Taylor & Cocquyt, 2016). During 2019 and 2021 the abundance of *C. placentula* greatly decreased to 4%

and 3%, respectively, compared to 2018 (29%) (Table 12). *Nitzschia frustulum* (47%) and *Nitzschia* spp. (32%) had similar abundances in 2019 and therefore the IPS was low at 4.8, indicating eutrophic conditions.

Nitzschia spp. dominated this site with 76% of the community structure during 2021 *Gomphonema* spp. and *Cocconeis placentula* had decreased abundances (7% and 3% of the community structure, respectively) (Table 12). The inferred water quality during 2021 is therefore low (IPS = 3.5) and indicates eutrophic, impacted conditions (Table 9). The shift in community structure from 2018 to 2021 at this site indicates a decrease in water quality over the study period (Figure 51).

Similar to the Mamba site, this site was dominated by *Nitzschia* spp. across all years sampled, however, the higher abundance of *Cocconeis placentula* during 2018 compared to 2019 and 2021 indicate meso- to eutrophic conditions with moderate electrolyte content. Increases in taxa that occur in such conditions were expected in accordance with the increased rainfall. However, this was not the case and taxa preferring high electrolyte content became more abundant from 2018 to 2021. This site did, therefore, not experience an improvement in water quality across years sampled

Confluence

The Confluence site had the best water quality of the Olifants River across all years, however, similar to the Mamba and Balule sites, a decrease in water quality was evident across time (Figure 50 & 51). *Cocconeis placentula* and *Cocconeis pediculus* occurred in high abundance at this site during 2018, the former represent 69% of the community while the latter represent 10% (Table 12). The complete dominance of *Cocconeis placentula* in relation to other taxa results in an IPS score of 14.9 (Table 9), since this taxon is found in waters with moderate electrolyte content and mesotrophic conditions (Taylor *et al*., 2007b). *Rhoicosphenia abbreviata* can, however, tolerate pollution well but does not occur in high abundance (10%). In 2019 *R. abbreviata*, the dominant species of 2018, had decreased in relative abundance. Other taxa including *Epithemia sorex* (34%) and *Nitzschia frustulum* (22%) had increased in abundance (Table 12), this explains the decrease in water quality score from IPS 14.9 to IPS 14, the quality remained in the mesotrophic range.

During 2021, the community composition again shifted where *Nitzschia* spp. increased in abundance to 30% and *Cocconeis placentula* increased to a higher abundance (26%) (Table 12). *Achnanthidium* spp. (15%) were also present at this site, however, the high

abundance of *Nitzschia* spp. indicates a further decrease in water quality from moderate (IPS = 14) to poor (IPS = 10) (Table 9 & Figure 50).

Unlike the Mamba and Balule sites, *Nitzschia* spp. did not dominate this site. Other taxa such as *Cocconeis placentula, Cocconeis pediculus, Epithemia sorex* and *Achnanthidium* spp. were more abundant, these taxa collectively indicate moderate electrolyte content and mesotrophic conditions, which marks an improvement in water quality with distance downstream. *Nitzschia* spp. was, however, encountered during 2019 and increased in abundance in 2021. This marks a decrease in water quality since these taxa occur in greater abundance under high electrolyte content and eutrophic conditions. The increase in average seasonal rainfall did not appear to have an impact on the water quality at this site, although water quality did improve from the previous sites.

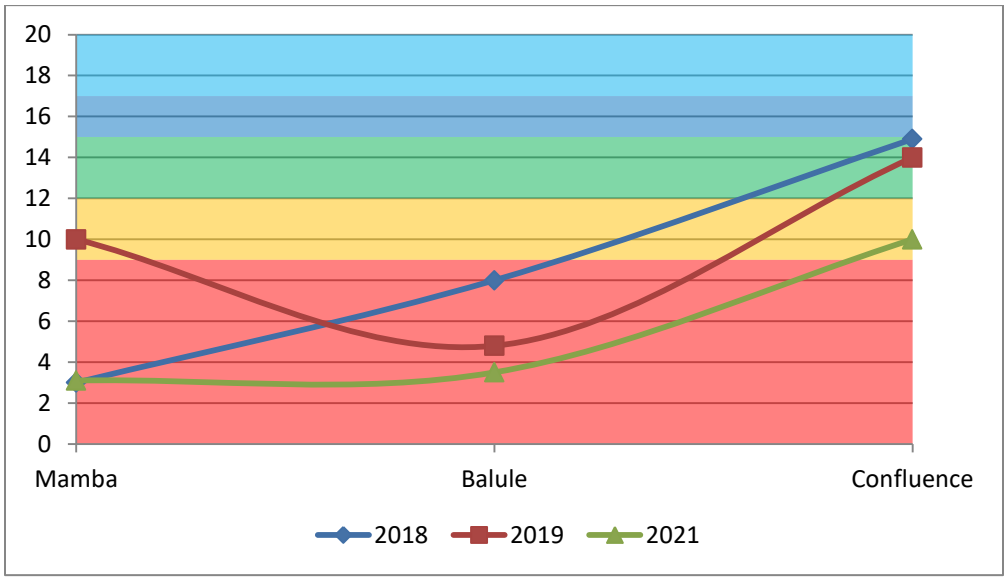

Figure 50: IPS scores for sites in the Olifants River from 2018 to 2021.

Summary

From 2018 to 2021 an overall decrease in water quality was observed for all sites. The Mamba and Balule sites remained eutrophic, while the confluence site decreased from mesotrophic in 2018 to meso-eutrophic in 2021 (Figure 51). Although the water quality showed an improvement with distance downstream (Figure 50), a general decrease in water quality was observed from 2018 to 2021.

The Olifants River was dominated by *Nitzschia* spp., *Nitzschia frustulum* and *Cocconeis placentula* (Table 12). These taxa prefer elevated electrolyte content and higher nutrients, however, *C. placentula* cannot tolerate electrolyte content above 800 µS/cm. *Nitzschia frustulum* can tolerate great fluctuations in osmotic pressure and *Nitzschia* spp. are generally known to be pollution tolerant. Consequently, the inferred water quality was very poor. The Olifants River had the poorest water quality of all rivers in the park throughout the study period and sites. *Nitzschia* spp. similarly dominated the community during 2021, with by far the greatest abundance of taxa in all of the sites sampled. This wass the only river in the study that experienced a decrease in water quality from 2018 to 2021. The average rainfall for the Olifants River was lower compared to the Sabie, Crocodile and Luvuvhu rivers. However, an improvement in temporal water quality was still expected in accordance to the higher average seasonal rainfall experienced from 2018 to 2021, but this was not the case (Figure 52). It is known that this river is subject to effluent discharges from the Palabora mining company located near the eastern perimeter of the park and is a source of point pollution. The impact of such sources is usually alleviated during increased discharge, however, this was not the case and water quality decreased. This decrease in water quality may be attributed to surface pollution from diffuse sources, caused by intense rainfall, however, the Crocodile River, which is also subject to anthropogenic impact (agriculture) did not follow a similar trend. It was therefore difficult to determine the reason for the temporal decrease in water quality despite the increased seasonal rainfall. The diatom community structures did, however, reflect a spatial improvement in water quality which suggests a recovery of the system with distance downstream.

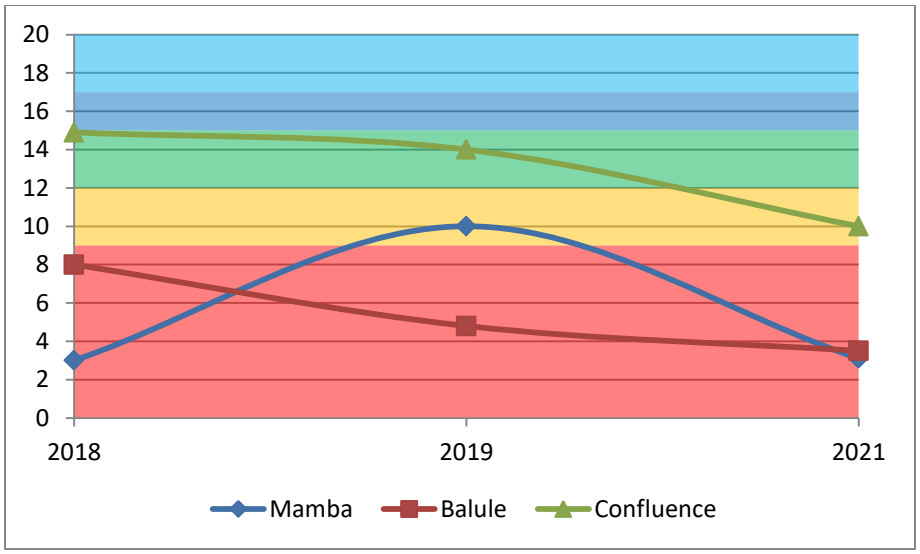

Figure 51: Annual changes in site specific IPS scores in the Olifants River from 2018 to 2021.

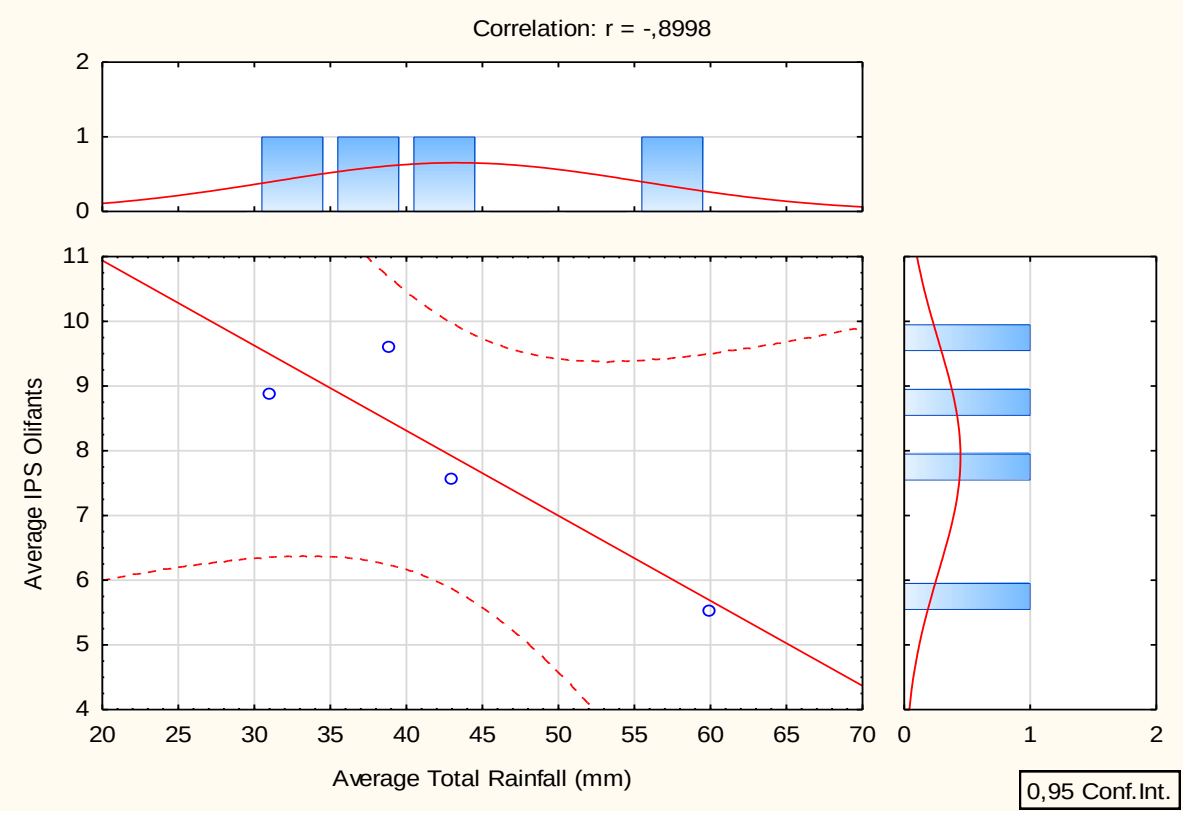

Figure 52: Correlation between the average IPS score for each year (2018 to 2021) in the Olifants River and the average total rainfall for each respective year. Data points, from left to right, resemble IPS scores and average total rainfall from 2018 to 2021 respectively. (1st – 2018; 2nd – 2019; 3rd – 2020; 4th - 2021).

3.3.3.4 Letaba River

Lonely Bull

During 2018, this site was dominated by a high abundance of *Nitzschia* spp. (73%). *Cocconeis placentula* and *Tabularia fasciculata* were also present, each representing 10% of the community (Table 11). The high abundance of *Nitzschia* spp. led to an extremely low IPS score of 2.6 (Table 9). *Tabularia fasciculata* can similarly tolerate high levels of pollution and electrolyte content (Taylor *et al*., 2007b).

During 2019, the community shifted towards a higher abundance of *Cocconeis placentula* (73%) and a decreased abundance of *Nitzschia* spp. (16%) (Table 11). The decrease in *Nitzschia* spp. and the increase in *C. placentula* were the reasons for the IPS score increase from 2.6 to 10.9 (Figure 53).

Interestingly, *Encyonopsis leei* var. *sinensis* was present with 2% abundance during 2019. Although this is relatively low, it is the only site within the Letaba River where this species was found. This taxon has progressively been detected in more locations around South Africa, originally described from China (Taylor *et al*., 2007b), it has considerably increased in abundance within South African rivers.

During 2020, *Cocconeis placentula* was dominant, other taxa including *Tabularia fasciculata*, *Gomphonema parvulum* and *Nitzschia* spp. were also present in higher abundance (Table 11). *Rhopalodia gibba* was also abundant during 2020 in the rapids and run biotopes, it occurs in flowing or standing water and prefers moderate to high electrolyte content (Taylor *et al*., 2007b). The IPS was consequently meso-eutrophic at 11.2 (Table 9)

Cocconeis placentula occurred in high abundance during 2021 (81%), compared to 2019 (73%). *Nitzschia* spp and *Gomphonema parvulum* were also present, however, at relatively low abundances, 6% and 3%, respectively. This explains the increase in IPS from 11.2 to 12.6 and consequently considered mesotrophic (Figure 53).

This site saw a shift in the diatom community structure from 2018 to 2021. During 2018, *Nitzschia* spp. occured in higher abundance than other taxa present by a large degree. *Nitzschia* spp. are common under eutrophic states with elevated electrolyte content. These conditions were related to droughts, where a lack of high seasonal rainfall prevents flushing and can lead to higher concentrations of nutrients and ionic compounds (Van Vliet & Zwolsman, 2008; Nosrati, 2011). From 2019 to 2021, this site saw a high abundance of *Cocconeis*

placentula, which increased with time. *Cocconeis placentula* is common under meso- to eutrophic conditions with moderate electrolyte content, and cannot tolerate more than moderate levels of organic pollution. The shift in diatom community structure indicated a decrease in electrolyte content and a decrease in trophic state, from eutrophic to mesotrophic (Figure 53 & 54). The increased seasonal rainfall therefore aided in the dilution of ionic compounds, nutrient concentrations and organic compounds, thereby causing a temporal increase in water quality.

Klipkoppies

The community structure present at the Klipkoppies site also changed across time. During 2018, interestingly, *Cocconeis placentula* was not present during the count. Other taxa including *Cymbella turgidula* (22%), *Nitzschia* spp. (20%) and *Navicula cryptotenella* (9%) are present (Table 11). *Cymbella turgidula* prefers low to moderate electrolyte content and oligo-mesotrophic states. *Navicula cryptotenella* occurs in oligo- to eutrophic conditions, it also occurs in a range of electrolyte content, but decreases in abundance in extremely low or extremely high electrolyte content (Taylor *et al*., 2007b). The presence of these species together with the presence of *Nitzschia* spp. indicates poor water quality for 2018 with an IPS score of 10.2 (Table 9).

During 2019 and 2021, the community was dominated by *Cocconeis placentula* with 88% and 92%, respectively. Other taxa such as *Nitzschia* spp., *Gomphonema parvulum* and *Kolbesia ploenensis* were also present, however, in much lower abundance compared to *C. placentula* (Table 11). This community structure explains the stable moderate IPS scores 14.1 and 14.2 for 2019 and 2021 (Figure 53 & 54).

This site experienced a shift in the community structure from 2018 to 2021, in 2018 a more even distribution of taxa was observed, however, the high abundances of *Nitzschia* spp. and *Navicula cryptotenella* indicate elevated electrolyte content and high nutrients. During 2019 and 2021 *Cocconeis placentula* occured in far greater abundance than *Nitzschia* spp. and other taxa present. This taxon cannot tolerate more than moderate levels of organic pollution and occur in moderate to low electrolyte content. The shift in the community structure would therefore suggest a dilution of ionic compounds and a lower level of organic pollution caused by the increased average seasonal rainfall.

Confluence

The Confluence site experienced a more radical shift in community structure composition from 2018 to 2021. During 2018, *Epithemia sorex* was present in high abundance (58%) together with *Cocconeis placentula* (11%) (Table 11). The former taxon occured in moderate to high electrolyte content and is typically tolerant of brackish conditions (Taylor *et al*., 2007b). *Nitzschia* spp. were also present with 10.4% relative abundance together with *Achnanthidium saprophilum.* The community structure for this site during 2018 indicates moderate water quality with IPS = 13.3 (Table 9).

During 2019, *Nitzschia* spp. dominated the site (91%), *Cocconeis pediculus* and *Gomphonema parvulum* were also present (Table 12). This explains the extremely low IPS score (1.6) for this site (Table 9). During 2021, however, *Cocconeis placentula* occured in high abundance (53%) together with *Kolbeisa ploenensis* (16%), *Nitzschia* spp. decreased in abundance and represented less than 10% of the community structure. The radical shift from 2019 to 2021 explains the change in IPS scores from 1.6 to 12.7 (Table 9 & Figure 54).

Although the diatom community has shifted radically from 2018 to 2021, the taxa present were all associated with moderate to high electrolyte content and meso- to eutrophic states. This suggests little impact from the increased seasonal rainfall from 2019 to 2021, the inferred water quality substantially increased, which indicated the increased average seasonal rainfall had aided in the dilution of ionic compounds and nutrients in the system.

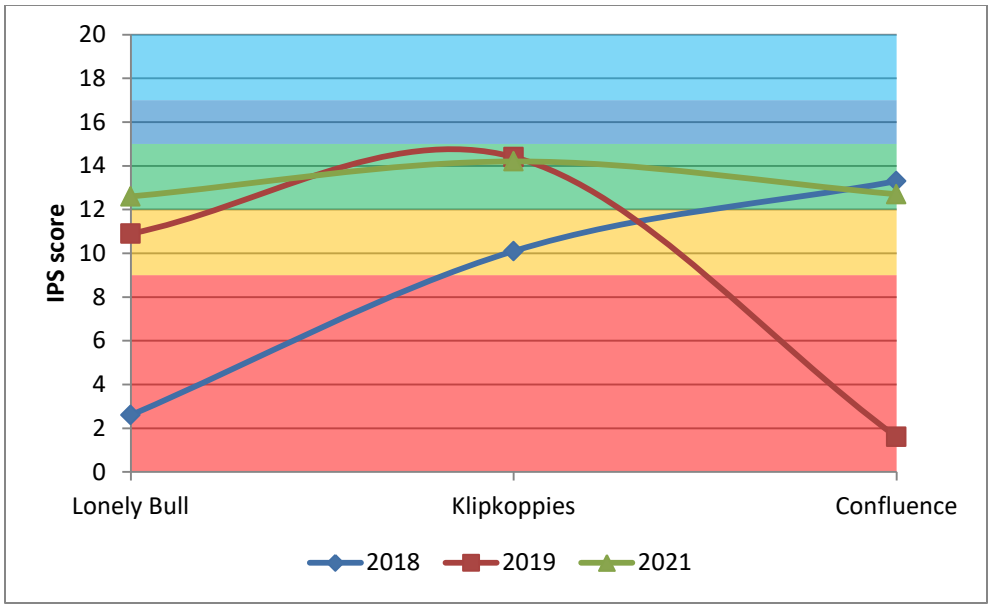

Figure 53: IPS Score change with in terms of flow direction from 2018 to 2021 in the Letaba River.

Summary

A general increase in water quality was observed across all years for all sites in the Letaba River. During 2018 the diatom community in the river was dominated by taxa such as *Nitzschia* spp., *Cocconeis placentula, Epithemia sorex* and to a lesser degree *Cymbella turgidula* (Table 11). The former three taxa are tolerant of elevated nutrients and higher electrolyte content. In 2019 the community was similarly dominated by the previously mentioned taxa. However, *C. placentula* increased in abundance during 2019 (Table 11) and dominated two of the sites (Lonely Bull and Klipkoppies). The remaining site, Confluence, was dominated by a 91% abundance of *Nitzschia* spp. This explained the sharp drop in the IPS score for 2019.

During 2020, *Cocconeis placentula* dominated all biotopes at the Lonely Bull site. However, the abundances were lower than in 2018 and a more evenly spread community composition was observed (Table 11). The 2018 community composition was similar to that of 2020 for the same site, however, the evenness of taxa was higher. During 2021, *C. placentula* dominated by a large degree. This taxon occurs in meso- to eutrophic conditions and moderate EC. The water quality is therefore considered moderate across all sites in 2021.

Overall the water quality for the Letaba River improved temporally and spatially. Taxa comprising the diatom communities of the Lonely Bull and Klipkoppies sites were mostly *Nitzschia* spp. During 2018, *Cocconeis placentula* did occur in high abundance at the confluence site. From 2019 to 2021, however, *C. placentula* occured in high abundance across

all sites where *Nitzschia* spp. decreased in abundance, except at the confluence site during 2019, which had a complete dominance of *Nitzschia* spp. The increased abundance of *C. placentula* and decreased abundance of *Nitzschia* spp., over time, indicates a change in trophic state from eutrophic to mesotrophic as well as a decrease in the amount of ionic compounds present. These changes indicate a possible dilution effect caused by the increased seasonal rainfall, none of the sites had poor water quality in 2021 as opposed to 2018 and 2019. It is clear that this river experienced an improvement in water quality due to the increased seasonal rainfall events of 2020 and 2021 (Figure 54 & 55).

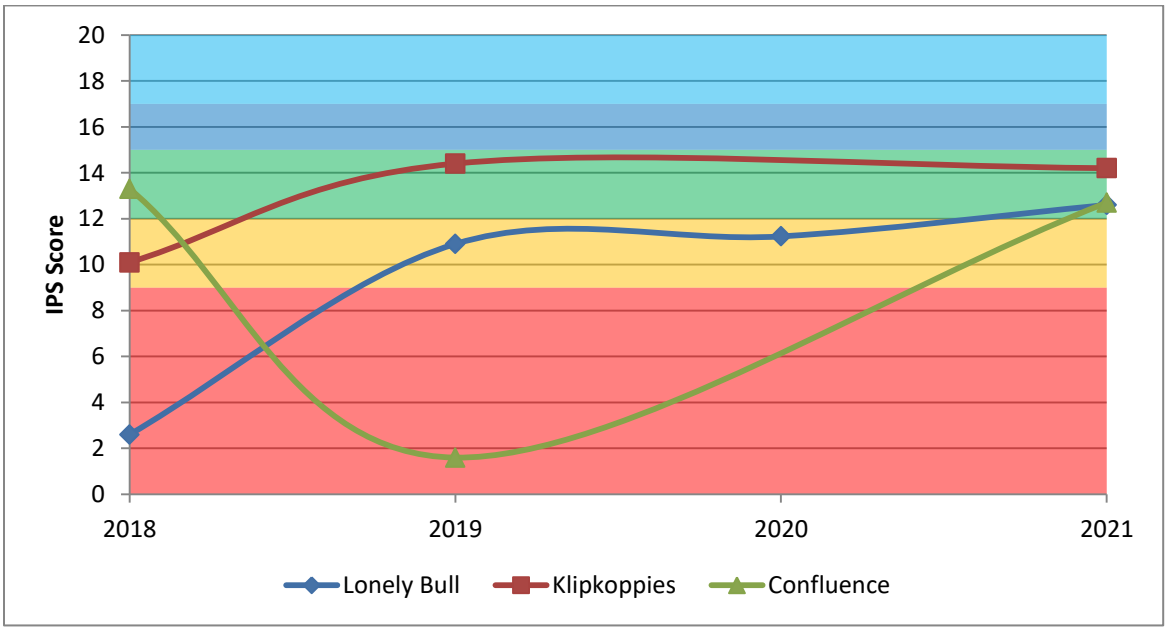

Figure 54: Annual changes in IPS scores for sites in the Letaba River from 2018 to 2021.

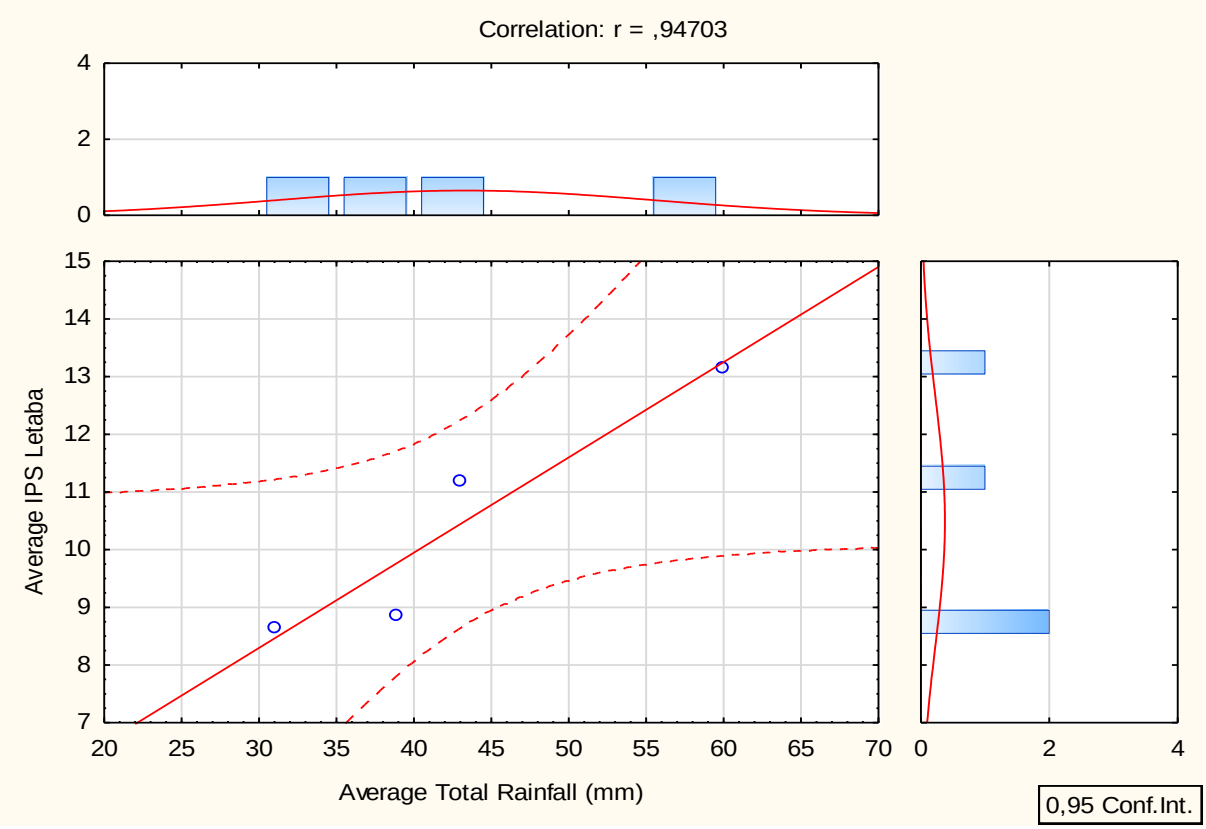

Figure 55: Correlation between the average IPS score for each year (2018 to 2021) in the Letaba River and the average total rainfall for each respective year. Data points, from left to right, resemble IPS scores and average total rainfall from 2018 to 2021 respectively. (1st – 2018; 2nd – 2019; 3rd – 2020; 4th - 2021).

3.3.3.5 Luvuvhu River

Dongadzhiva

This site had little alteration in the diatom community structures over time. During 2018 and 2019, the community was dominated by *Achnanthidium* spp. and *Encyonopsis leei* var. *sinensis* (Table 10). Both taxa are associated with oligo-mesotrophic conditions and low to moderate electrolyte content. *Fragilaria* spp. were also present during 2018, whereas *Encyonopsis krammeri* increased in abundance from 2018 to 2019. *Encyonopsis krammeri* occurs in oligotrophic conditions with low electrolyte content (Taylor *et al*., 2007b). The shift in the community structure from 2018 to 2019 indicates an improvement in water quality (IPS = 16.5 to IPS = 17.3) (Table 9 and Figure 56), although both years had oligo-mesotrophic to oligotrophic conditions, respectively, and high water quality.

During 2020 and 2021, the community was comprised of a higher abundance of *Achnanthidium* spp., especially *Achnanthidium minutissimum* (Table 10), in both years these taxa collectively comprised more than 60% of the community composition. The latter is indicative of high water quality, since it commonly occurs *en masse* in oligotrophic, electrolyte-poor rivers (Taylor & Cocquyt, 2016). Taxa such as *Navicula* spp. and *Brachysira vitrea* were also present during 2020, the former has a wide ecological range while the latter occurs in oligo- to mesotrophic conditions with low electrolyte content (Taylor *et al*., 2007b). Therefore, the water quality during 2020 is considered good and within a meso-oligotrophic state (IPS = 16.8). During 2021, *Achnanthidium minutissimum* had a very high abundance (62%), *Encyonopsis leei* var. *sinensis* was also present together with *Cymbella kolbei* (Table 10). *Cymbella kolbei* occurs in oligotrophic conditions with low electrolyte content (Cholnoky, 1962a). The inferred water quality for 2021 at this site was therefore extremely high (IPS = 18.4) (Table 9)

During 2018 when drought conditions were experienced, the community structure was comprised of species occurring in meso- to oligotrophic conditions with moderate to low electrolyte content. The presence of these species indicated maintenance of sufficient discharge to aid in dilution and removal of nutrients and organic material. The rainfall for the Luvuvhu River is on average higher compared to the Letaba and Olifants rivers, the high lying area near Punda-Maria creates updrafts increasing higher rainfall near this area.

From 2018 to 2021, as the average seasonal rainfall increased, further dilution and flushing effect were expected. This is supported by the change in diatom community structure. During 2019, *Encyonopsis krammeri* became more abundant, this taxon is associated with oligotrophic, electrolyte-poor conditions, and so the increase in the abundance of this taxon marks a decrease in trophic state and electrolyte content. The further increase in *Achnanthidium* spp. and *Achnanthidium minutissimum* during 2021 marks an increase in stream velocity and a further decrease in nutrient concentration, ionic compounds and organic material. During 2021, the high water quality was maintained, and slightly improved due to the presence of *Cymbella kolbei*, this taxon occurs in high abundance in oligotrophic, electrolyte-poor conditions and so its presence indicates on a further improvement in water quality. The increased seasonal rainfall, therefore, aided in the improvement in water quality due to seasonal flushing and dilution of constituents such as nutrients, organic substances and ionic compounds.

Xindzivhani

During 2018, *Achnanthidium* spp. and *Fragilaria* spp. were present together with *Gomphonema venusta* and *Encyonopsis leei* var. *sinensis* (Table 10). *Gomphonema venusta* occurs in oligotrophic conditions with low electrolyte content (Taylor *et al*., 2007b), similar to the ecological preferences for other taxa present. *Fragilaria* spp. can however tolerate a wider trophic range and elevated electrolyte content. This explains the meso-oligotrophic state ascribed to this site during 2018 (IPS = 15.6) (Table 9). The shift in the inferred water quality from 2018 (IPS 15.6) to 2019 (IPS 16.6) is due to the remaining presence of *Achnanthidium* spp. as well as the high abundance of *C. turgidula* (26%), which was absent during 2018 (Table 10). This, together with the increased abundance of *Encyonopsis leei* var. *sinensis,* suggests an improvement in water quality at this site. *Achnanthidium rivulare* and *Encyonopsis krammeri* were also present at low abundance.

The diatom community was comprised of a high abundance of *Cocconeis placentula* during 2020, where it was not recorded during the previous years sampled. *Achnanthidium* spp. and *Achnanthidium minutissimum* were also relatively abundant, comprising 15% and 13% of the community structure respectively (Table 10). *Gomphonema venusta* was also present together with *Navicula zanoni*. The latter is a common sub-tropical species that generally associated with low nitrogen content (Cholnoky, 1960a; 1960b; 1962a; 1962b) while the former is common in oligotrophic conditions with low electrolyte content (Taylor *et al*., 2007b). The overall community structure therefore represents meso-oligotrophic conditions (IPS = 16.8). During 2021, the site saw a decrease in the abundance of *C. placentula* and a shift to the dominance of *Achnanthidium* spp. and in particular *A. minutissimum* (Table 10). *Fragilaria capucina* and *Encyonopsis leei* var. *sinensis* were also present. The former three species occurs in oligo- to mesotrophic waters with low to moderate electrolyte content and consequently explains the increase in IPS from 16.8 to 18.0 (Table 9).

Similar to the Dongadzhiva site, the community structures during drought years were comprised of taxa occurring in moderate to low electrolyte content and meso-oligotrophic conditions. This indicates that the stream discharge was still sufficient at this site to maintain good water quality and aid in the removal of excess nutrients. Similar conditions remained during 2019, however, an increase in the abundance of *Cymbella turgidula* together with the high abundance of *Achnanthidium* spp. marks an increase in water quality in terms of electrolyte content and trophic state. As mentioned, *Achnanthidium* spp. were generally associated with higher stream discharges and low nutrient and organic content. A general increase in the abundance of this

taxon from 2018 to 2021 suggests an increase in stream discharge related to the increased average seasonal rainfall. *Cocconeis placentula* occurred in high abundance during 2020, and is indicative of moderate water quality, however, this species is prostrate and can attach well to its substrate and therefore withstand higher stream velocities to some degree.

Mutale (outpost)

During 2018 the community composition at this site was comprised of *Navicula* spp., *Fragilaria* spp., *Cymbella turgidula* and *Nitzschia* spp. Both *Navicula* spp. and *Fragilaria* spp. include species occurring across wide ecological ranges of trophic levels and electrolyte content (Taylor *et al*., 2007b). *Cymbella turgidula* similarly occurs in oligo- to mesotrophic conditions with moderate to low electrolyte content. The presence of *Nitzschia* spp. during 2018 indicates poor water quality and explains the low IPS score of 11.6. During 2019, a greater abundance of *C. placentula* (30%) and *Achnanthidium* spp. (18%) were encountered in relation to other taxa present including *Nitzschia* spp. (6%) and *Navicula cryptotenella* (5%) (Table 10). This indicates an improvement in water quality. The inferred water quality for 2019 is mesotrophic with IPS = 13.8 (Table 9).

During 2020, this site was dominated by *Cocconeis* spp., especially *Cocconeis pediculus* and *Cocconeis placentula*. Both taxa occur in meso- to eutrophic conditions, where the former can also extend into brackish conditions. However, the presence of *Cocconeis placentula* var. *lineata* and *Achnanthidium* spp. indicate better water quality with lower nutrient concentrations. *Gomphonitzschia ungeri* was also present at this site (Table 10). This species is sub-tropical and rather rare in South Africa (Cocquyt and Taylor, 2016). This community structure changes from 2019 to 2020 indicating an increase in water quality for this site. The inferred water quality is meso-oligotrophic with IPS = 15.0 (Table 9).

Cocconeis spp. were present in high abundance during 2021, however, *Cocconeis placentula* dominated with 54% of the community composition (Table 10). Other taxa inlcuding *Achnanthidium* spp. (11%), *Gomphonema venusta* (4%), *Achnanthes* spp. (5%) and *Gomphonema pumilum* var. *rigidum* (5%) were also present. The former two taxa share similar ecological ranges and are associated with low electrolyte content, and cannot tolerate pollution (Taylor *et al*., 2007b). The latter two taxa are associated with elevated electrolyte content (Taylor & Cocquyt, 2016), *G. pumilum* var. *rigidum* can also occur in waters with higher nutrient content (Taylor *et al*., 2007b). The shift in community structure correlates with the water quality for this site during 2021 (IPS = 16.4).

The presence of *Navicula* spp. and *Nitzschia* spp. at this site during 2018 indicate poor water quality. The former taxa have a wide ecological range and can occur in eutrophic conditions. The latter taxa are associated with increased nutrient concentration, increased electrolyte content and increased levels of pollution. This site is not located in the Luvuvhu River, but rather is a nearby tributary of the Mutale River. The discharge of the Mutale River may be weaker than the discharge of the Luvuvhu River, since it is a tributary thereof and of smaller stream order. During 2019, taxa such as *Achnanthidium* spp. and *Cocconeis* spp. increased in abundance. *Cocconeis placentula* can attach firmly to a substrate and can withstand higher stream velocities although not as well as *Achnanthidium* spp due to their larger cell size. During 2020, these taxa also occurred in high abundance, however, other *Gomphonema* spp. were also present. These taxa build mucilage stalks on which they position themselves to better compete in their environment. However, these taxa do not build such stalks in high stream velocities. Additionally, these stalks are only constructed when the community has reached a climax state (Patrick, 1977).

Bobomane

This site had species that occur in moderate electrolyte content such as *Tabularia fasciculata* and *Cocconeis placentula*. However, *Nitszchia frustulum* and *Achnanthidium saprophilum* were also present (Table 10), these taxa are common in elevated electrolyte content and higher trophic levels. The latter species can tolerate increased levels of organic pollution which suggests a decrease in water quality. The inferred water quality is consequently poor during 2018 with IPS = 10.7 (Table 9).

In 2019 *Geissleria decussis* increased in abundance together with *Cocconeis placentula* (Table 10). The former species is found in eutrophic conditions with elevated electrolyte content, it can, however, not tolerate high levels of pollution (Taylor *et al*., 2007b). *Cymbella kolbei* was also present at this site, which greatly increased the IPS score for this site. This site experienced an increase in water quality, as indicated by IPS scores, from 2018 to 2019 although still moderate (IPS = 10.7 to IPS = 13.4).

The taxa present at this site all indicate moderate to poor water quality. *Geissleria decussis* is common in waters with high electrolyte content. Additionally, *Achnanthidium* spp. were not encountered at this site where it was encountered at previous sites during 2018 and 2019. The diatom community structure therefore suggests a higher electrolyte content and nutrient

concentration at this site, however, the presence of *Cymbella kolbei* during 2019, suggests an increase in water quality from 2018 to 2019 in terms of trophic status.

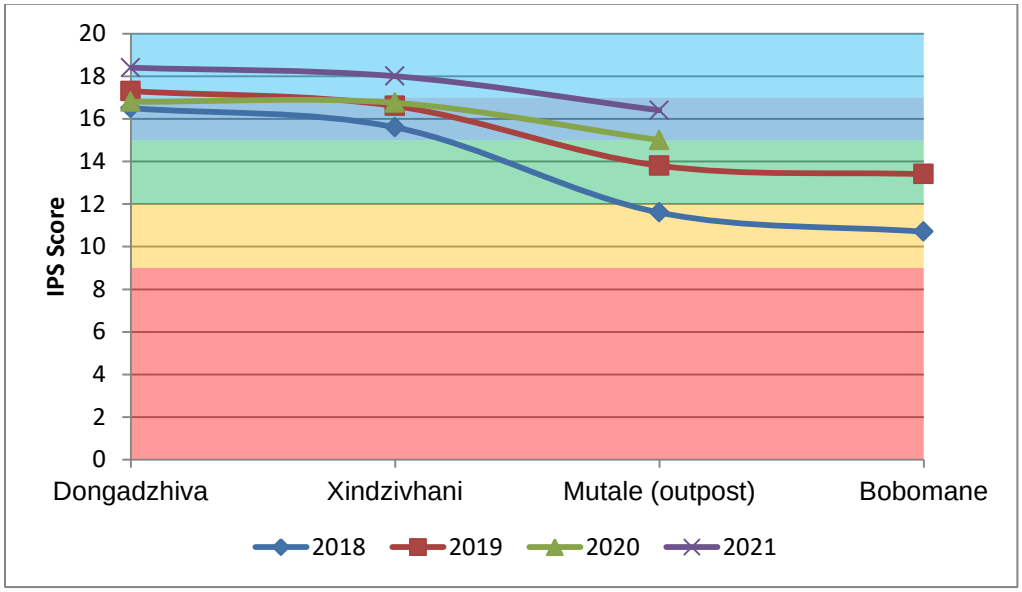

Figure 56: IPS score profile for sites along the Luvuvhu River from 2018 to 2021.

Summary

During 2018 and 2019, the diatom communities in the Luvuvhu River were, in part, comprised of species that are able to tolerate elevated nutrient content such as *Tabularia fasciculata*, *Nitzschia frustulum* and *Achnanthidium saprophilum*, present at the Bobomane site during 2018 (Table 10). Other species present during 2019 that occur in elevated EC and higher trophic levels were *Cocconeis placentula* and *Geissleria decussis*. EC was also higher across all sites during 2018 and 2019 than in 2021 (Tables 2 and 3).

The diatom communities present during 2020 and 2021 were almost entirely comprised of species that occur in oligo- to mesotrophic conditions as well as low to moderate electrical conductivities including *Achnanthidium minutissimum* and *Encyonopsis leei* var. *sinensis* (Table 8). The EC, even when high in 2018 and 2019, was not as high as the EC for other Rivers such as the Olifants and Crocodile rivers.

According to the current study, the Luvuvhu River is one of the healthiest Rivers in the KNP. Of the 14 sites sampled in this river across the study period, only two sites, Mutale and Bobomane, experienced poor water quality in 2018 and moderate water quality in 2019 (Figure 57). All remaining sites have been classified as having high water quality (10 sites). A temporal increase

in water quality was observed as explained for the individual sites. However, an immediate deterioration in spatial water quality was evident (Figure 56). These decreases in water quality scores was associated with the increased abundances of *Cocconeis placentula*, *Nitzschia spp., Navicula* spp. and *Geissleria decussis* at sites further downstream. This suggests an increase in the trophic state and electrolyte content as the water flows from Dongadzhiva to Bobomane. The Luvuvhu River was the only river in the study that experienced a spatial decrease in water quality, this in contrast to the expected flushing effect.

The autecology of diatoms has therefore successfully been used to indicate water quality for the Luvuvhu River in terms of trophic level, electrolyte content and levels of organic pollution. The river maintains moderate to low trophic levels and contains little organic substances. Additionally, water quality during droughts years, where water quality constituents are more concentrated and eutrophic conditions are more common, is generally lower. As high rainfall events of 2020 and 2021 were experienced, the water quality improved (Figure 58).

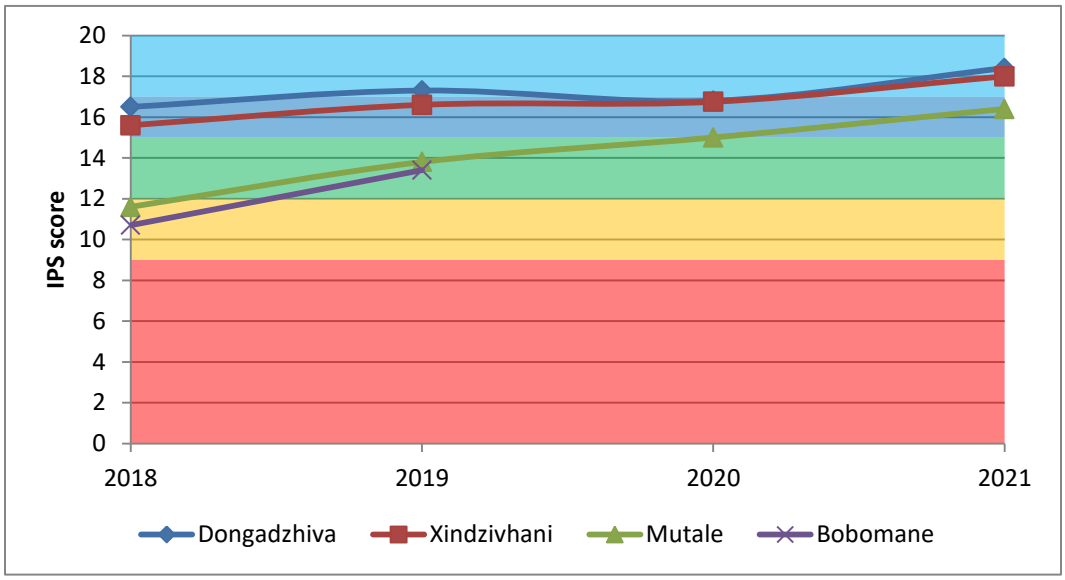

Figure 57: Annual changes in IPS scores for sites specifically in the Luvuvhu River.

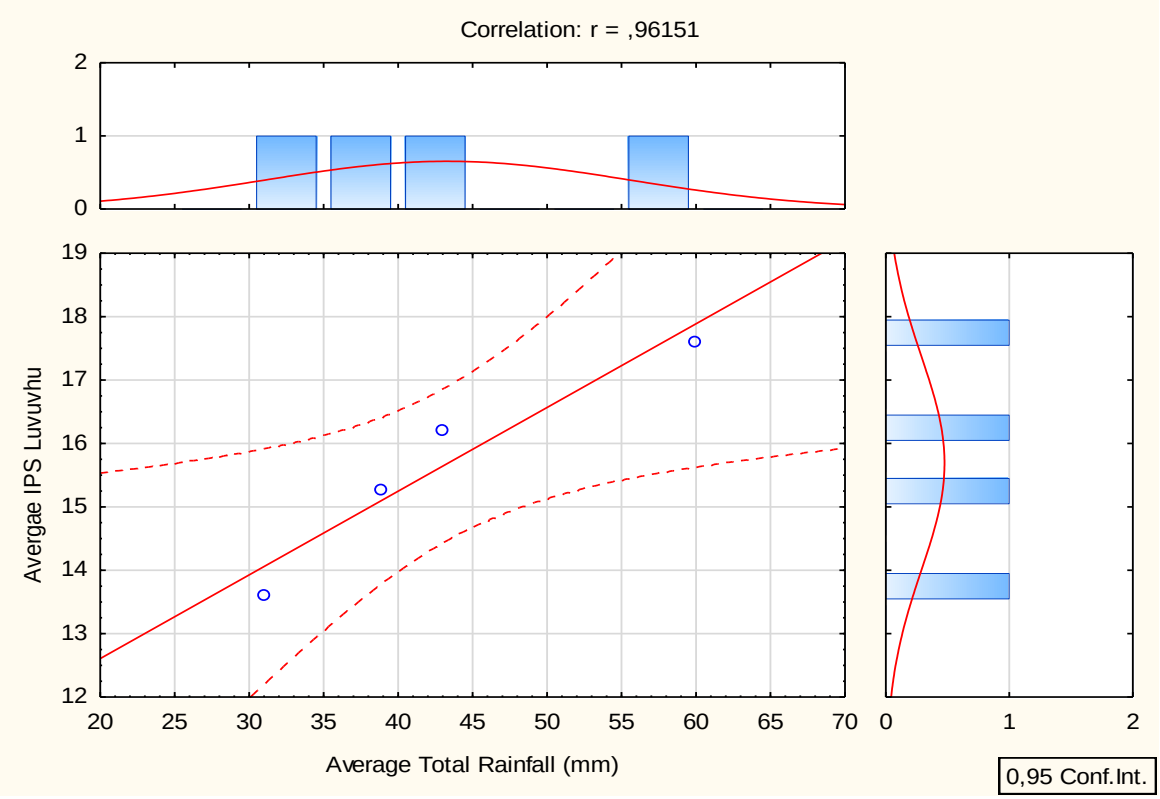

Figure 58: Correlation between the average IPS score for each year (2018 to 2021) in the Luvuvhu River and the average total rainfall for each respective year. Data points, from left to right, resemble IPS scores and average total rainfall from 2018 to 2021 respectively. (1st – 2018; 2nd – 2019; 3rd – 2020; 4th – 2021).

Table 9: Diatom index scores for sites and rivers during 2021. Refer to Table 1 for colour codes.

		GDI				IPS				BDI				%PT			
River	Site	2018	2019	2020	2021	2018	2019	2020	2021	2018	2019	2020	2021	2018	2019	2020	2021
Sabie	Sekurukwane	7.2	7.4	10.1	14.6	5.3	6.8	9.0	14.8	13.3	16.4	14.7	15.5	7.7	0.8	1.6	1.8
	Tinga	14.3	14.1	-	17.2	13.6	14.7	-	17.1	13.8	13.3	-	15.9	1.3	1.8	-	0.5
	Sand	9.6	-	-	-	13.5	-	-	8.7	12.2	-	-	-	7.9	-	-	-
	Antholysta	16.4	16.2	15.6	15.5	14.6	15.5	16.2	14.5	13.3	13.0	15.7	14.0	2.2	2.5	3.0	0.8
	Lubye-Lubye	13.4	15.3	-	17.1	15.3	16.8	-	16.6	11.5	14.5	-	16.2	15.5	11.6	-	0.8
	Sabiepoort	2.3	4.8	-	11.7	2.1	3.7	-	9.4	7.0	10.2	-	9.2	8.7	4.5	-	43.4
Crocodile	Nsikazi	11.5	7.6	-	-	12.1	8.1	-	-	15.2	14.1	-	-	0.5	8.8	-	-
	Malelane	10.7	12.2	-	9.1	10.4	13.5	-	8.9	13.5	15.0	-	14.0	14.4	0.0	-	12.0
	Marula	6.7	10.2	12.9	12.3	5.5	10.0	15.2	13.0	12.8	14.0	15.3	15.2	1.2	6.5	0.3	0.3
	Nkongoma	11.7	11.0	-	11.3	12.1	10.8	-	13.9	14.0	13.7	-	14.4	4.5	5.7	-	6.0
Olifants	Mamba	3.2	7.3	-	3.1	3.0	10.0	-	3.1	13.5	10.4	-	14.0	0.7	32.5	-	0.0
	Balule	8.4	3.0	-	3.5	8.7	4.8	-	3.5	13.8	5.4	-	12.8	2.5	48.5	-	0.5
	Confluence	12.6	12.0	-	9.6	14.9	14.0	-	10.0	14.9	9.8	-	14.5	1.5	24.4	-	0.8
Letaba	Lonely Bull	3.2	10.6	11.0	11.9	2.6	10.9	11.2	12.6	8.8	14.8	12.2	14.7	1.2	0.0	8.2	4.2
	Klipkoppies	12.0	12.4	-	12.5	10.1	14.1	-	14.2	12.4	15.2	-	15.1	2.8	0.2	-	2.0
	Confluence	14.9	1.9	-	10.8	13.3	1.6	-	12.7	11.5	11.7	-	13.8	0.7	3.2	-	12.0
Luvuvhu	Dongadzhiva	16.2	17.2	16.4	17.2	16.5	17.3	16.8	18.4	20.0	20.0	20.0	19.8	0.3	0.0	0.8	0.2
	Xindzivhani	15.5	17.4	15.5	17.0	15.6	16.6	16.8	18.0	13.1	16.3	17.8	19.2	0.2	0.5	2.0	0.0
	Mutale (Outpost)	12.0	13.4	14.1	14.3	11.6	13.8	15.0	16.4	12.5	14.4	15.4	15.7	3.0	4.5	3.3	0.0
	Bobomane	10.8	13.2	-	-	10.7	13.4	-	-	10.3	14.5	-	-	15.5	0.0	-	-

Chapter 4: Conclusions and recommendations

The Kruger National Park is large protected area that hosts many species of endemic and endangered wildlife as well as conserving a range of habitat types. The rivers that flow through the park are of utmost importance with regard to water security. Although these rivers are protected within the park, they are not exempt from upstream impacts such as point and non-point sources of pollution. This has been recognised by the park and various management protocols have been set in place to ensure the water that flows within these rivers is of suitable quality for use by terrestrial flora as well as the biota within. The River Eco-status Monitoring Programme (REMP), which replaced the RHP in 2016, is implemented within the KNP and involves, in part, the use of bioindicator organisms to infer the water quality for these rivers; the REMP is a component of the National Aquatic Ecosystem Health Monitoring Programme (NAEHMP).

Five perennial rivers flow through the KNP and are distributed across the entire park from north to south. The Crocodile River marks the southern boundary of the KNP and subject to agricultural impacts on its southern banks, where the area is not well protected. The Luvuvhu River forms the northern boundary of the park and is generally known to be a healthy system with little anthropogenic impact. The remaining three perennial rivers are the Sabie, Olifants and Letaba rivers. The Sabie is located north of the Crocodile River and is subject to little anthropogenic impact in its headwaters. The origin of the Sabie River is not far from its entrance into the park and most of the river flows within a protected area, therefore, the Sabie River is generally a healthy system. Unlike the Sabie, the Olifants River originates much further away and is, therefore, subject to greater anthropogenic impact as it flows from its point of origin until it enters the park. The Olifants River is subject to industrial pollution and organic enrichment, therefore, monitoring the health of the Olifants river within the KNP is important to provide feasible management protocols to mitigate the impacts from pollution. The Letaba River is located not far from the Olifants River and is in a generally healthier state. This river is not subject to much anthropogenic impact, and joins the Olifants River within the park, near its eastern boundary.

These rivers are also subject to natural impacts such as drought and floods. These phenomena can alter the concentration of constituents in the water through a change in stream discharge. During drought years when rainfall is low, the surface water contribution is diminished and

groundwater contribution maintains flow. Low flow conditions are known to concentrate constituents such as ionic compounds and nutrients, thereby increasing the risk of eutrophication. Flooding on the other hand is linked to higher rainfall and generally mitigates the effect of drought through a flushing of the system as flood pulses become more frequent and intense. Extreme rainfall can, however, contribute to pollution of rivers by flushing an increased amount of constituents from diffuse sources into the water, thereby increasing the nutrient and organic load. Seasonal flooding is therefore a regular occurring phenomenon that helps maintain a healthy river state, however, seasonal flooding can also compromise the health of a river when intensity and frequency of rainfall is high.

The aquatic biota within rivers are well adapted to seasonal flooding and employ various strategies to survive such conditions, however, when seasonal flooding disappears and leads to drought or when seasonal flooding becomes more intense due to high rainfall frequency, the biotic communities are adversely affected and in turn ecosystem function is compromised. Monitoring the water quality in these conditions is, therefore, important.

The biomonitoring tools used by KNP scientific services include many indicator groups among which fish and macroinvertebrates are widely used. Diatoms also form part of these biomonitoring tools but have not been as extensively used to monitor water quality changes in the park. Diatoms are excellent indicators of specific water quality change and adhere to a many criteria that other bioindicator organisms do not, such as their ubiquitous nature, their fast generation times, the low cost of sampling and the ease of use. Additionally, diatoms respond predictably and accurately to a wide range of pollutants, and are sensitive to water quality change.

Diatoms were used to infer the water quality for the five perennial rivers within the KNP from 2018 to 2021. Within this time frame, a general increase in the total annual rainfall and total average annual rainfall was experienced during the phase shift of El Niño toward La Niña. El Niño is known to create drought across South Africa due to low annual rainfall. La Niña, in turn, leads to increased annual rainfall and can create flood risks. The inter-annual flow regime for rivers in the KNP is largely determined by seasonal rainfall which is in turn affected by El Niño and la Niña as described above.

The effect of this increase in seasonal rainfall was determined by using diatoms as indicators of water quality change. The chosen diatom index for this study was the Indice de Polluosensibilité Spécifique (IPS). The calculation of this index is based on the autecological preferences of

diatom taxa to ionic composition, trophic state and organic enrichment. Seasonal flooding aids in the removal of harmful substances and pollutants and promotes a healthier ecosystem function; harmfull substances may include heavy metals and herbicides that were not included in the study. Therefore, a change in ionic composition, organic material and trophic state occurs in response to seasonal flooding. The IPS index was used infer and demonstrate water quality change in response to the increased average seasonal rainfall for the five perennial rivers in the park over the study period.

The inferred water quality generally increased in response to the higher seasonal rainfall. However, the profile followed by each river differs from the others. The rivers that are generally known to be healthy, such as the Luvuvhu and Sabie rivers experienced a greater increase in temporal water quality. During drought years, stream flow was still sufficient to maintain healthy water quality. As the average seasonal rainfall increased, the rivers showed a further increase in water quality. The most notable change in the diatom community structures for these rivers was the increasing abundance and diversity of *Achnanthidium* spp. These taxa are strongly associated with fast-flowing well oxygenated water, and thus an increase in the abundance of these taxa indicates an increase in stream discharge. The Sabie River showed an increase in spatial water quality (upstream to downstream) from the first site sampled (Sekurukwane) to the second last site sampled (Lubye-Lubye), from that point up to the last site (Sabiepoort) a severe deterioration in water quality was experienced across all years, this did improve over time but requires further study as this may indicate pollution or organic enrichment within this stretch of water. The Luvuvhu River experienced a spatial decrease in water quality, this river is subject to little or negligible anthropogenic impact and implies a different source of concern in terms of the decrease in water quality, possibly originating within the park. The Letaba River experienced an increase in temporal and spatial water quality and was dominated by a single taxon, *Cocconeis placentula*. The prevalence of this species increased from 2018 to 2021, where it replaced more pollutant tolerant taxa present in previous years. This river experienced the greatest overall improvement in water quality.

The remaining rivers, Crocodile and Olifants, did not experience similar increases in temporal and spatial water quality compared to the Sabie, Luvuvhu and Letaba rivers. The Crocodile River did show a temporal increase in water quality, however, during 2020, the Marula site was dominated by a 91% relative abundance of *Cocconeis placentula*. Spatially, the water quality changed between sites and did not generally improve downstream. Water quality generally decreased between the second and third sites and increased towards the fourth. The third site

was located across from a protected game reserve and, therefore, the water quality at this site was expected to be high. This suggests a possible impact from this area that caused a decrease in the water quality.

The water quality of the Olifants River is a great cause for concern. Although this river is subject to greater pollution than other rivers in this study, this is the only river that experienced a temporal decrease in water quality in response to the increased annual rainfall. The sources of pollution for the Olifants River are generally industrial and considered point sources of pollution; these sources include but are not limted to untreated wastewater discharge, hospital discharge, mine water discharge and AMD. This type of pollution is generally mitigated in response to increased discharge due to a dilution effect. This did not occur and suggests a different origin for pollution. Increased seasonal rainfall generally increases pollution originating from diffuse sources, the closest source of pollution near the Olifants River is the Palabora mining company, however, these industries are considered point sources of pollution and not diffuse sources. The decrease in temporal water quality is cause for concern and need to be further investigated. The water quality of the Olifants River did, however, improve spatially, which means the river recovers within the park.

Diatoms were therefore successfully implemented to indicate water quality change in response to increased seasonal rainfall, by using the IPS index. This index was not expressly designed for the purpose of determining water quality changes in response to water quantity changes as a result of rainfall, nevertheless some of the data support the project hypothesis. This supports the efficacy of diatoms as bioindicators as they are highly integrated in aquatic systems and food webs. The use of diatoms as indicator organisms is therefore highly recommended within the KNP. The implementation thereof would increase the ease of sampling, since diatom material can be gathered quickly, it would also decrease the cost of monitoring since diatom sampling is cheap compared to extensive chemical analysis. It is well established that diatom communities are correlated with water quality variables and, therefore, the further use of physico-chemical analysis in addition to diatom analysis in the park is redundant, unnecessary and costly. Diatoms can, therefore, form part of the biomonitoring tools used in the KNP. It is, however, as always, recommended that multiple bioindicators be used to infer water quality when possible.

Chapter 5: References

Addo-Bediako, A. & Rasifudi, L. 2021. Spatial distribution of heavy metals in the Ga-Selati River of the Olifants River system, South Africa. *Chemistry and Ecology*, **37**(5):450-463.

Aizebeokhai, A.P. 2009. Global warming and climate change: Realities, uncertainties and measures. *International Journal of Physical Sciences*, **4**(13):868-879.

Alford, J.B. & Walker, M.R. 2013. Managing the flood pulse for optimal fisheries production in the Atchafalaya River basin, Louisiana (USA). *River Research and Applications*, **29**(3):279-296.

Alvarez-Vázquez, L.J., Martínez, A., Vázquez-Méndez, M.E., Pollak, A.W. & Pierce, J.J. 2014. Optimal location of river sampling stations: A case study. In: Fonters, M., Günther, M. & Marheineke, N. eds. *Progress in Industrial Mathematics at ECMI 2012. Mathematics in Industry, Vol 19*. Cham: Springer. pp. 39-45.

Anderson, T.K. & Shepherd, J.M. 2013. Floods in a changing climate. *Geography Compass*, **7**(2):95-115.

Bate, G.C., Adams, J.B. & van der Molen, J.S. 2002. Diatoms as indicators of water quality in South African river systems. WRC Report No 814/1/02. Pretoria: Water Research Commission.

Bate, G.C., Smailes, P.A. & Adams, J.B. 2004. Benthic diatoms in the rivers and estuaries of South Africa. WRC Report No TT234/04. Pretoria: Water Research Commission.

Bertrand, J. 2021. Movements of diatoms VIII: Synthesis and hypothesis. In: Cohn, S., Manoylov, K. & Gordon, R. eds. *Diatom Gliding Motility*. Beverly: Scrivener Publishing LLC. pp. 283-294.

Bohórquez, J., McGenity, T.J., Papaspyrou, S., Garcia-Robledo, E., Corzo, A. & Underwood, G.J.C. 2017. Different types of diatom-derived extracellular polymeric substances drive changes in heterotrophic bacterial communities from intertidal sediments. *Frontiers in Microbiology*, **8**:245.

Britannica. 2013. Lebombo Mountains. https://www.britannica.com/place/Lebombo-Mountains Date of access: 15 Mar. 2022.

Britannica. 2022. Eutrophication. https://www.britannica.com/science/eutrophication. Date of access: 12 Feb. 2022.

Chaplin, M.F. 2001. Water: its importance to life. *Biochemistry and Molecular Biology Education*, **29**(2):54-59.

Ching, C.Y., Lee, H.Y., Toriman, M.E., Abdullah, M., Yatim, B.B. 2015. Effect of the big flood events on the water quality of the Muar River, Malaysia. *Sustainable Water Resources Management*, **1**(2):97-110.

Cholnoky, B.J. 1959. Neue und seltene diatomeen aus Afrika IV. Diatomee aus der Kaap-Proninz. *Österreichischen Botanischen Zeitschrift*, **106**(1/2):1-169.

Cholnoky, B.J. 1960a. Beiträge zur kennntis der diatomeenflora von Natal (Südafrika). *Nova Hedwigia*, **2**(1+2):1-128.

Cholnoky, B.J. 1960b. Beiträge zur kennntis der Ökologie der Diatomeen is dem Swartskops-Bache nahe Port Elizabeth (Südost kaapland). *Hydrobiologia*, **16**(3):229-287.

Cholnoky, B.J. 1962a. Beiträge zur kennntis der Ökologie der diatomeen in Ost-transvaal. *Hydrobiologia*, **19**(1):57-119.

Cholnoky, B.J. 1962b. Ein Beitrag zu der Ökologie der Diatomeen in den Englischen Protektorat Swaziland, *Hydrobiologia*, **20**:309-355.

Cholnoky, B.J. 1962c. Beiträge zur Kennntis der Südafrikanischen Diatomeenflora. diatomeen aus der Kaap-Provinz. *Revista de Biologia*, **3**(1):1-80.

Cholnoky, B.J. 1966. Diatomeenassoziationen aus Einigen Quellen in Südwest-Afrika und Bechaunaland. *Nova Hedwigia*, **21**:163-244.

Cholnoky, B.J. 1968. *Die Ökologie der Diatomeen in Binnengewasser*. Lehre: J. Cramer. p 1-699.

Coffey, R., Paul, M.J., Stamp, J., Hamilton, A. & Johnson, T. 2018. A review of water quality responses to air temperature and precipitation changes 2: Nutrients, algal blooms, sediment, pathogens. *Journal of American Water Resources Association*, **55**(4):844-868.

CEMAGREF. 1982. Etude des méthodes biologiques quantitatives d'appréciation de la qualité des eaux. Rapport Division Qualit6 des Eaux Lyon - Agence Financière de Bassin Rhône-Méditerrané- Corse. Pierre-Bénite.

Cox, E.J. 1996. *Identification of Freshwater Diatoms From Live Material*. London, UK: Chapman & Hall. p 1-158.

Cushing, D.H. 1989. A difference in structure between ecosystems in strongly stratified waters and in those that are only weakly stratified. *Journal of Plankton Research*, **11**(1):1-13.

Dallas, H.F. & Day, J.A. 2004. The effect of water quality variables on aquatic ecosystems: A review. WRC Report No TT 224/04. Pretoria: Water Research Commission.

Dalu, T. & Froneman, P.W. 2016. Diatom-based water quality monitoring in southern Africa: Challenges and future prospects. *Water S.A*., **42**(4):551-559.

De la Rey, P.A., Taylor, J.C., Laas, A., van Rensburg, L. & Vosloo, A. 2004. Determining the possible application value of diatoms as indicators of general water quality: A comparison with SASS 5. *Water S.A.*, **30**(3):325-332.

De Villiers, S. & Mkwelo, S.T. 2009. Has monitoring failed the Olifants River, Mpumalanga? *Water S.A.*, **35**(5):671-676.

Descy, J.P. 1979. A new approach to water quality estimation using diatoms. *Nova Hedwigia*, **64**:305-323.

Dieppois, B., Rouault, M. & New, M. 2015. The impact of ENSO on Southern African rainfall in CMIP5 ocean atmosphere coupled climate models. *Climate Dynamics*, **45**:2425-2442.

Dowrick, S. & Gemmer, N. 1991. Industrialisation, catching up and economic growth: A comparative study across the world's capitalist economies. *The Economic Journal*, **101**(405):263-275.

Du Plessis, A. 2017. *Freshwater Challenges of South Africa and its upper Vaal River: Current state and outlook*. Cham: Springer. p. 1-164.

Dube, K. 2022. Nature-based tourism resources and climate change in Southern Africa. In: Stone, L.S., Stone, M.T., Mogomotsi, P.K. & Mogomotsi, G.E.J. eds. *Protected areas and tourism in Southern Africa: Concervation goals and community livelihoods*. Abington & New York: Routledge. pp. 114-128.

DWAF (Department of Water Affairs and Forestry). 1986. Management of the water resources of the Republic of South Africa. Government printers: Pretoria.

DWAF (Department of Water Affairs and Forestry). 1996a. South African Water Quality Guidelines (2nd ed). Vol 4: Agricultural Use: Irrigation.

DWAF (Department of Water Affairs and Forestry).1996b. South African Water Quality Guidelines. Vol 7: Aquatic Ecosystems.

DWAF (Department of Water Affairs and Forestry). 1996c. South African Water Quality Guidelines (2nd ed), Vol 3: Industrial Use.

DWAF (Department of Water Affairs and Forestry). 1996d. South African Water Quality Guidelines (2nd ed). Vol 6: Agricultural Water Use: Aquaculture.

DWAF Department of Water Affairs and Forestry. 1998. South African National Water Act, Number 36 of 1998. *Government Gazette*. 191182:201, 26 Aug.

Fallon, R.D. & Brock, T.D. 1979. Decomposition of blue-green algal (cyanobacterial) blooms in Lake Mendota, Wisconsin. *Applied and Environmental Microbiology*, **37**(5):820-830.

Field. J.G. & Shillington, F.A. 2005. Variability of the Benguela current system (16,E).In: Robinson, A.R. & Brink, K.H., eds. *The Sea, Ideas and Observations on Progress in the Study of the Seas: The global coastal ocean, interdisciplinary regional studies and syntheses. Part B:The coasts of Africa, Europe, Middle East, Oceania and Polar regions*. Vol 14. Cambridge: Harvard University Press. pp. 835-864.

Foged, N. 1948. Diatoms in water-courses in Funen. *Dansk Botanisk Arkiv*, **12**:1-112.

Foged, N. 1954a. Diatoms from West Greenland. *Meddelelser Om Grønland*, **147**:1-86.

Foged, N. 1954b. On the diatom flora of some Funen lakes. *Folia Limnologica Scandinavica*, **6**:1-75.

Foged, N. 1964. Freshwater diatoms from Spitsbergen. *Tromsø Museums Skrifter*, **11**:1-159.

García-Rodríguez, F., Bate, G.C., Smailes, P., Adams, J.B. & Metzeltin, D. 2007. Multivariate analysis of the dominant and sub-dominant epipelic diatoms and water quality data from South African rivers. *Water S.A.*, **33**(5):653-658.

Gasse, F. 1986. *Bibliotheca Diatomologica: East African diatoms, taxonomy, ecological distribution*. Berlin: J. Cramer Verlag. p. 1-201.

Ger, K.A., Urrutia-Cordero, P., Frost, P.C., Hansson, L., Sarnelle, O., Wilson, A.E. & Lürling, M. 2016. The interaction between cyanobacteria and zooplankton in a more eutrophic world. *Harmful algae*, **54**:128-144.

Gillson, L. & Ekblom, A. 2008. Untangling anthropogenic and climatic influence on riverine forest in the Kruger National Park, South Africa. *Vegetation History and Archaeobotany*, **18**(2):171-185.

Greenfield, R., van Vuren, J.H.J. & Wepener, V. 2012. Heavy metal concentrations in the water of the Nyl River system, South Africa. *African Journal of Aquatic Science*, **37**(2):219-224.

HACH. 2021. DR 3900 Benchtop Spectrophotometer without RFID Technology – Methods/procedures. https://za.hach.com/dr-3900-benchtop-spectrophotometer-without-rfid-technology/product-downloads?id=55240716184 Date of access: 2 Oct. 2021.

Hall, R.I. & Smol, J.P. 1992. A weighted - averaging regression and calibration model for inferring total phosphorus concentration from diatoms in British Columbia (Canada) lakes. *Freshwater Biology*, **27**(3):417-434.

Halpert, M., Barnston, A., L'Heureux, M., Becker, E. 2016. El Niño and La Niña: Frequently asked questions. https://www.climate.gov/news-features/understanding-climate/el-ni%C3%B1o-and-la-ni%C3%B1a-frequently-asked-questions Date of access: 23 April. 2022.

Hamm, C.E., Merkel, R., Springer, O., Jurkojc, P., Maier, C., Prechtel, K. & Smetacek, V. 2003. Architecture and material properties of diatom shells provide effective mechanical protection. *Nature*, **421**:841-843.

Harding, W.R., Archibald, C.G.M., Taylor, J.C. & Mundree, S. 2004. The South African diatom collection: An appraisal and overview of needs and opportunities. WRC Report No. TT242/04. Pretoria: Water Research Commission.

Harding, W.R., Archibald, C.G.M. & Taylor, J.C. 2005. Diatomology in South African biomonitoring: the South African Diatom Collection. *African Journal of Aquatic Science*, **30**(2):221-221.

Harrison, P.J., Khan, N., Yin, K., Saleem, M., Bano, N., Nisa, M., Ahmed, S.I., Rizvi, N. & Azam, F. 1997. Nutrient and phytoplankton dynamics in two mangrove tidal creeks of the Indus River delta, Pakistan. *Marine Ecology Progress Series*, **157**:13-19.

Hasle, G.R. & Fryxell, G.A. 1970. Diatoms: Cleaning and mounting for light and electron microscopy. *Transactions of the American Microscopical Society*, **89**(4):469-474.

Hellebust, J.A. & Lewin, J. 1977. Heterotrophic nutrition. In: Werner, D. ed. *The Biology of Diatoms*. Berkeley: University of California Press. pp. 169-179.

Hoell, A., Funk, C., Zinke, J. & Harrison, L. 2016. Modulation of the Southern Africa precipitation response to the El Niño Southern Oscillation by the subtropical Indian Ocean dipole. *Climate Dynamics*, **48**:2529-2540.

Hustedt, F. 1930. Bacillariophyta. In: Pascher. A. ed. *Die Süßwasser-flora Mitteleuropas*, **2**(10):1-466.

Hustedt, F. 1937 Systematische und ökologische untersuchungen über die diatomeen-flora von Java, Bali und Sumatra nach dem material der Deutschen limnologischen sunda-expedition. *Archiv Für Hydrobiology,* **15**:131-177.

Hustedt, F. 1957. Die diatomeenflora des flusssystems der weser im gebiet der Hamsestadt Bremen. *Abhandlungen Herausgegeben vom Naturwissenschaftlichen Verein zu Bremen*, **34**(3):181-440.

Jørgensen, E.G. 1952. Notes on the ecology of diatom *Navicula acomoda* Hustedt. *Svensk Botanisk Tidskrift*, **49**:189-191.

Junk, W., Bayley, P.B. & Sparks, R.E. 1989. The flood pulse concept in river-floodplain systems. In: ed. Dodge, D.P. Proceedings of the international large river symposium (LARS) *Canadian Journal of Fisheries and Aquatic Sciences,* **106**:110-127.

Kelly, M.G. & Whitton, B.A. 1995. The trophic diatom index: A new index for monitoring eutrophication in rivers. *Journal of Applied Phycology*, **7**:433-444.

Kelly, M.G., Cazaubon, A., Coring, E., Dell'Uomo, A., Ector, L., Goldsmith, B., Guasch, H. Hürlimann, J., Jarlman, A., Kawecka, B., Kwandrans, J., Laugaste, R., Linstrøm, E.A., Leitao, M., Marvan, P., Padisák, J., Pipp, E., Prygiel, J., Rott, E., Sabater, S., van Dam, H. & Vizinet, J. 1998. Recommendations for the routine sampling of diatoms for water quality assessments in Europe. *Journal of Applied Phycology*, **10**:215-224.

Khatri, N. & Tyagi, S. 2014. Influences of natural and anthropogenic factors on surface and groundwater quality in rural and urban areas. *Frontiers in Life Science*, **8**(1):23-39.

Kock, A. 2017. Diatom diversity and response to water quality within the Makuleke Wetlands and Lake Sibaya. Potchefstroom: North-West University. (Dissertation - MSc).

Krammer, K. & Lange-Bertalot, 2004b. Bacillariophyceae: Teil 3: Centrales, Fragilariaceae, Eunotiaceae. eds. Ettl, H., Gerloff, J., Heynig, H. & Mollenhauer, D. *Süsswasserflora von Mitteleuropa, Band 3/2*. Berlin: Spektrum Akademischer Verlag. p. 1-598.

Krammer, K. & Lange-Bertalot, H. 1986. Bacillariophyceae: Teil 1: Naviculaceae. eds. Ettl, H., Gerloff, J., Heynig, H. & Mollenhauer, D. *Süsswasserflora von Mitteleuropa, Band 2/1*. Jena: Gustav Fisher. p. 1-876.

Krammer, K. 2002. *Cymbella*. Lange-Bertalot, H. ed. *Diatoms of Europe*: *Diatoms of the European inland waters and comparable habitats, Vol 3*. Königstein: Koeltz Scientific Books. p. 1-583.

Krammer, K. 2003. *Cymbopleura, Delicata, Navicymbula, Gomphocymbellopsis, Afrocymbella*. ed. Lange-Bertalot, H. *Diatoms of Europe*: *Diatoms of the European inland waters and comparable habitats, Vol 4*. Königstein: Koeltz Scientific Books. p. 1-530.

Krammer, K. & Lange-Bertalot, H. 2004a. Bacillariophyceae: Teil 4: Achnanthaceae, Kritische Erganzungen Zu *Achnanthes* S.L., *Navicula* S.Str., *Gomphonema*. eds. Ettl, H., Gärtner, G., Heynig, H. & Mollenhauer, D. *Süsswasserflora von Mitteleuropa, Band 2/4*. Berlin: Spektrum Akademischer Verlag. p. 1-468.

Krammer, K. & Lange-Bertalot, H. 2007a. Bacillariophyceae: Teil 1: Naviculaceae. eds. Ettl, H., Gerloff, J., Heynig, H. & Mollenhauer, D. *Süsswasserflora von Mitteleuropa*, *Band 2/1*. Germany: Spektrum Akademischer Verlag. p. 1-876.

Krammer, K. & Lange-Bertalot, H. 2007b. Bacillariophyceae: Teil 1: Bacillariaceae, Epithemiaceae, Surirellaceae. eds. Ettl, H., Gerloff, J., Heynig, H. & Mollenhauer, D. *Süsswasserflora von Mitteleuropa, Band 2/2*. Germany, Spektrum Akademischer Verlag. p. 1-610.

Krausmann, F. & Halberl, H. 2007. Land-use change and socioeconomic metabolism: A Macro View of Austria 1830 - 2000. In: Fischer-Kowalski, M. & Halberl, H. eds. *Socioeconomic Transitions and Global Change: Trajectories of societal metabolism and land use*. Edward Elgar. pp. 31-59.

Kröger, N. & Poulsen, N. 2008 . Diatoms: from cell wall biogenesis to nanotechnology. *Annual review of genetics*, **42**(1), 83-107.

Kundzewicz, Z.W. 2008. Climate change impacts on the hydrological cycle. *Ecohydrology & Hydrobiology*, **8**(2-4):195-203.

Lange-Bertalot, H. 1979. Pollution tolerance as a criterion for water quality estimation. *Nova Hedwigia*, **64**:285-304.

Lange-Bertalot, H. & Metzeltin, D. 1996. Indicators of oligotrophy. ed. Lange-Bertalot, H. *Iconographia Diatomologica: Annotated diatom micrographs*. Königstein: Koeltz Scientific Books. p. 1-390.

Lange-Bertalot, H. 2001. *Naviucla* sensu stricto, 10 genera separated from *Navicula* sensu lato, Frustulia. ed. Lange-Bertalot, H. *Diatoms of Europe*: *Diatoms of the European inland waters and comparable habitats, Vol 2*. Königstein: Koeltz Scientific Books. p. 1-526.

Lange-Bertalot, H., Bąk, M., Witkowski, A. & Tagliaventi, N. 2011. Eunotia and some related genera. ed. Lange-Bertalot, H. *Diatoms of Europe*: *Diatoms of the European inland waters and comparable habitats, Vol 6*. Königstein: Koeltz Scientific Books. p. 1-747.

Lange-Bertalot, H., Hofmann, G., Werum, M. & Cantonati, M. 2017. *Freshwater Benthic Diatoms of Central Europe: Over 800 common species used in ecological assessment*. Oberreifenberg: Koeltz Scientific Books. p. 1-942.

Lecointe, C., Coste, M. & Prygiel, J. 1993. “Omnidia”: software for taxonomy, calculation of diatom indices and inventories management. *Hydrobiologia*, **269**:509-513.

Levkov, Z. 2009. *Amphora* sensu lato. ed. Lange-Bertalot, H. *Diatoms of Europe*: *Diatoms of the European inland waters and comparable habitats, Vol 5*. Königstein: Koeltz Scientific Books. p. 1-916.

Loaiciga, H.A., Valdes, J.B., Vogel, R., Garvey, J. & Schwarz, H. 1996. Global warming and the hydrologic cycle. *Journal of Hydrology*, **174**:83-127.

Macdonald, I.A.W. 1988. The history, impacts and control of introduced species in the Kruger National Park, South Africa*. Transactions of the Royal Society of South Africa*, **46**(4):251-276.

MacFadyen , S., Zambatis, N., van Teeffelen, A.J.A., Hui, C. 2018. Long-term rainfall regression surfaces for the Kruger National Park, South Africa: A spatio-temporal review of patterns from 1981 to 2015. *International Journal of Climatology,* **38**:2506-2519.

Malherbe, J., Smit, I., Wessels, K.J. & Beukes, P.J. 2020. Recent droughts in the Kruger National Park as reflected in the extreme climate index. *African Journal of Range & Forage science*, **37**(1):1-17.

Marilainen, J. 1967. The diatom flora and the hydrogen-ion concentration of the water. *Annales Botanici Fennici*, **4**:51-85.

Mathivha, F., Tshipala, N.N. & Nkuna, Z. 2017. The relationship between drought and tourist arrivals: A case study of Kruger National Park, South Africa. *Jàmbá: Journal of Disaster Risk Studies,* **9**(1).

Mgbemene, C.A., Nnaji, C.C. & Nwozor, C. 2016. Industrialization and its backlash: focus on climate change and its consequences. *Journal of Environmental Science and Technology*, **9**(4):301-316.

Miles, J. 2005. R-squared, Adjusted R-squared. In: Everitt, B.S. & Howell, D.C. eds. *Encyclopedia of Statistics in Behavioral Science,* **4**:1655-1657.

Mimikou, M.A., Baltas, E., Varanou, E. & Pantazis, K. 2000. Regional impacts of climate change on water resources quantity and quality indicators. *Journal of Hydrology*, **234**(1-2):95-109.

MIthen, S. & Black, E. 2011. *Water, Life and Civilisation: Climate, environment and society in the Jordan valley*. Cambridge: Cambridge University Press. p. 1-520.

Mnisi, N. 2020. *Water scarcity in South Africa: A result of physical or economic factors?* https://hsf.org.za/publications/hsf-briefs/water-scarcity-in-south-africa-a-result-of-physical-or-economic-factors Date of access: 10 March. 2021.

Morris, R. 2015. Spectrophotometry. *Current Protocols Essential Laboratory Techniques II*, **11**(1):2.1.1-2.1.30.

Mosley, M. 2015. Drought impacts on the water quality of freshwater systems; review and integration. *Earth-Science Reviews*, **140**:203-214.

Murdoch, P.S., Baron, J.S. & Miller, T.L. 2000. Potential effects of climate change on surface-water quality in North America. *Journal of the American Water Resources Association*, **36**(2):347-366.

Musa, R. & Greenfield, R. 2018. Use of diatom indices to categorise impacts on and recovery of a floodplain system in South Africa. *African Journal of Aquatic Science*, **43**(1):59-69.

Neal, C., Jarvie, H.P., Howarth, S.M., Whitehead, P.G., Williams, R.J., Neal, M., Harrow, M. & Wickham, H. 2000. The water quality of the River Kennet: initial observations on a lowland chalk stream impacted by sewage inputs and phosphorus remediation. *The Science of the Total Environment*, **251-252**:477-495.

Neelin, J.D., Battisti, D.S.,Hirst, A.C., Jin, F., Wakata, Y., Yamagata, T. & Zebiak, S.E. 1998. ENSO Theory. *Journal of Geophysical Research*, **103**(C7):14261-14290.

Nhesvure, B. 2020. Impacts of ENSO on coastal South African sea surface temperatures. Cape Town: University of Cape Town. (Dissertation - MSc).

Nicholson, S.E. & Entekhabi, D. 1986. The quasi-periodic behaviour of rainfall variability in Africa and its relationship to the southern oscillation. *Archives for Meteorology, Geophysics, and Bioclimatology, Series A*, **34**:311-348.

Nicholson, S.E. & Selato, J.C. 2000. The Influence of La Niña on African rainfall. *International Journal of Climatology*, **20**:1761-1776.

Nosrati, K. 2011. The effects of hydrological drought on water quality. *Assessment of Water Quality Under Changing Climate Conditions*. Wallingford : IAHS Publishers. **348**:51-57.

Oemke, M.P. & Burton, T.M. 1986. Diatom colonization dynamics in a lotic system. *Hydrobiologia*, **139**:153-166.

Okito, A.M., Oleko, R.W., Madder, Z. & Cocquyt, C. 2021. Epiphytic diatoms on herbarium material from the central forest phytogeographic region of the Democratic Republic of the Congo. *Plant Ecology and Evolution*, **154**(2):245-256.

Oxley, S. 2021. Assessing water quality using benthic diatoms as bioindicators in the Sabie River (Kruger National Park). Johannesburg: University of the Witwatersrand. (Dissertation - MSc).

Parry, M.L., Canziani, O.F., Palutikof, J.P., van der Linden, P.J. & Hanson, C.E., eds. 2007. *IPPC, 2007. Climate Change 2007: Impacts, adaptation and vulnerability*. Cambridge, UK: Cambridge University Press. pp. 1-1976.

Patrick, R. & Reimer, C.W. 1966. The Diatoms of the United States. I. Monographs of the academy of natural sciences of Philadelphia. Pennsylvania: Livingston Publishing Company. p. 1-688.

Patrick, R. 1977. Ecology of freshwater diatoms – Diatom communities. In. Werner, D. ed. *The Biology of Diatoms, Vol 13*. Berkeley: University of California Press. pp. 284-332.

Philander, S.G. & Rasmusson, E.M. 1985. The southern oscillation and El Niño. *Advances in Geophysics*, **28**:197-215.

Pienaar, U. de. V. 1982. *The Kruger Park saga*. Skukuza: National Paarks Board of South Africa.

Prygiel, J., Carpentier, P., Almeida, S., Coste, M., Druart, J.C., Ector, L., Guillard, D., Honeré, M.A., Iserentant, R., Ledeganck, P., Lalanne-Cassou, C., Lesniak, C., Mercier, I., Moncaut, P., Nazart, M., Nouchet, N., Peres, F., Peters, V., Rimet, F., Rumeau, A., Sabater, S., Straub, F., Torrisi, M., Tudesque, L., van der Vijver, B., Vidal, H., Vizinet, J. & Zydek, N. 2002. Determination of the biological diatom index (IBD NF T 90-354): results of an intercomparison exercise. *Journal of Applied Phycology*, **14**:27-39.

Qi, J., Deng, L., Song, Y., Qi, W & Hu, C. 2022. Nutrient thresholds required to control eutrophication: Does it work for natural alkaline lakes? *Water*, **14**(17):2674.

Quiring, S.M. 2009. Monitoring drought: An evaluation of meteorological drought indices. *Geography Compass*, **3**(1):64-88.

Raymond, P.A. & Saiers, J.E. 2010. Event controlled DOC export from forested watersheds. *Biogeochemistry*, **100**(1-3):197-209.

Reid, M.A., Tibby, J.C., Penny, D. & Gell, P.A. 1995. The use of diatoms to assess past and present water quality. *Australian Journal of Ecology*, **20**(1):57-64.

RHP (River Health Programme). 2005. State-of-Rivers report: Monitoring and managing the ecological state of rivers in the Crocodile (West) Marico water management area. Pretoria: Department of environmental Affairs and Tourism.

Riddell, E.S., Govender, D., Botha, J., Sithole, H., Petersen, R. & Shikwambana, P. 2019. Pollution impacts on the aquatic ecosystems of the Kruger National Park, South Africa. *Scientific African*, **6**:1-12.

Roeder, D.R. 1977. Relationships between phytoplankton and periphyton communities in a central Iowa stream. *Hydrobiologia*, **56**(2):145-151.

Round, F.E., Crawford, R.M. & Mann, D.G. 1990. *The Diatoms: Biology morphology and the genera*. Cambridge: Cambridge University Press. p.1-747.

Round, F.E. 1991. Diatoms in river water-monitoring studies. *Journal of Applied Phycology*, **3**:129-145.

Round, F.E. 1993. *A Review and Methods for the Use of Epilithic Diatoms for Detecting and Monitoring Changes in River Water Quality*. Methods for the examination of water and associated materials. London: HMSO publication. p. 1-65.

Roy, C. & Reason, C. 2001. ENSO related modulation of coastal upwelling in the eastern Atlantic. *Progress in Oceanography*, **49**(1-4):245-255.

Rutherford, M.C. & Westfall, R.H. 1986. *Biomes of Southern Africa - an objective categorization*. Memoirs of the botanical survey of South Africa (no 54). Botanical Research Institute: Pretoria, South Africa. p. 1-98.

Sarthou, G., Timmermans, K.R., Blain, S. & Tréguer, P. 2005. Growth physiology and fate of diatoms in the ocean: A review. *Journal of Sea Research*, **53**(1-2):25-42.

Scheele, M. 1952. Systemische-ökologische untersuchungen uber due diatomeenflora der Fulda. *Archiv fur Hydrobiologie*, **46**:305-423.

Schober, P., Boer, C. & Schwarte, L.A. 2018. Correlation Coefficients: Appropriate use and interpretation. *Anesthesia & Analgesia*, **126**(5):1763-1768.

Schoeman, F.R. 1976. Diatom indicator groups in the assessment of water quality in the Jukskei-Crocodile River system (Transvaal, Republic of South Africa). *Journal of the Limnological Society of Southern Africa*, **2**(1):21-24.

Schoeman, F.R. 1979. Diatoms as indicators of water quality in the upper Hennops River. *Journal of the Limnological Society of Southern Africa*, **5**(2):73-78.

Shikwambana, P., Taylor, J.C., Govender, D., Botha, J. 2021. Diatom responses to river water quality in the Kruger National Park, South Africa. *Bothalia*, **5**(1).

Simonsen, R. 1962. Untersuchungen zur systematik und ökologie der bonden diatomeen der westlichen Ostsee. *Internationale Revue der Gesamten Hydrobiologie und Hydrographie*, **35**:267-285.

Simonsen, R. 1987a. *Atlas and Catalogue of the Diatom Types of Friedrich Hustedt, Vol 1*. Berlin & Stuttgart: J. Cramer Verlag. p. 1-525.

Simonsen, R. 1987b. *Atlas and Catalogue of the Diatom Types of Friedrich Hustedt, Vol 2*. Berlin & Stuttgart: J. Cramer Verlag. p. 1-597.

Simonsen, R. 1987c. *Atlas and Catalogue of the Diatom Types of Friedrich Hustedt, Vol 3*. Berlin & Stuttgart: J. Cramer Verlag. p. 1-619.

Sládeček, V. 1973. System of water quality from the biological point of view.*Achieves für Hydrobiology*, **7**(1):1-128.

Sládeček, V. 1986. Diatoms as indicators of organic pollution. *Acta Hydrochimica et Hydrobiologica*, **14**(5):555-566.

Smakhtin, V.U. 2001. Low flow hydrology: A review. *Journal of Hydrology*, **240**(3-4):147-186.

Sohoulande, D.D.C. & Singh, V.P. 2015. Impact of climate change on the hydrologic cycle and implications for society*. Environment and Social Psychology*, **1**(1):36-49.

Soria, M., Leigh, C., Datry, T., Bini, L.M. & Bonada. 2017. Biodiversity in perennial and intermittent rivers: A meta-analysis. *Oikos*, **126**(8):1078-1089.

Steffens, F.E. 1993. Geostatistical estimation of animal abundance in th Kruger National Park, South Africa. In: Soares, A. ed. *Geostatistics Tróia '92. Quantitative Geology and Geostatistics, Vol 5*. Dordrecht: Springer. pp. 887-897.

Stevenson, R.J. & Pan, Y. 2001. Assessing environmental conditions in rivers and streams with diatoms. In: Stoermer, E.F. & Smol, J.P. eds. *The Diatoms: Applications for the environmental and earth sciences*. Cambridge: Cambridge University Press. pp. 11-40.

Talbot, C.J., Bennett, E.M., Cassell, K., Hanes, D.M., Minor, E.C.,Paerl, H., Raymond, P.A., Vargas, R., Vidon, P.G., Wollheim, W. & Xenopoulos, M.A. 2018. The impact of flooding on aquatic ecosystem services. *Biogeochemistry*, **141**(3):439-461.

Tallaksen, L.M. & Van Lanen, H.A.J. 2004. Introduction. In: Tallaksen, L.M. & van Lanen, H.A.J. eds. *Hydrological Drought: Processes and estimation methods for stream flow and groundwater*. Amsterdam: Elsevier. pp. 3-15.

Taylor, J.C. 2004. The Application of diatom-based pollution indices in the Vaal Catchment. Potchefstroom: North-West University. (Dissertation - MSc).

Taylor, J.C., Harding, W.R. & Archibald, C.G.M. 2007a. A methods manual for the collection, preparation and analysis of diatom samples: Version 1. WRC Report TT 281/07. Pretoria: Water Research Commission.

Taylor, J.C., Harding, W.R. & Archibald, C.G.M. 2007b. An illustrated guide to some common diatom species from South Africa . WRC Report TT 282/07. Pretoria: Water Research Commission.

Taylor, J.C. & Cocqyut, C. 2016. Diatoms from the Congo and Zambezi basins - Methodologies and identification of the genera. Vol 16. Abc Taxa.

Ter Braak, C.J.F. 1987. Unimodal modals to relate species to environment. Netherlands: Landouwuniversiteit, Generaal Foulkesweg. (Thesis - PhD).

Ter Braak, C.J.F & Prentice, I.C. 1988. A theory of gradient analysis. *Advances in Ecological Research*, **18**:271-317.

Ter Braak, C.J.F. & van Dam, H. 1989. Inferring pH from diatoms: A comparison of old and new calibration methods. *Hydrobiologia*, **178**:209-223.

Ter Braak, C.J.F, Verdonschot, P.F.M. 1995a. Canonical correspondence analysis and related multivariate methods in aquatic ecology. *Aquatic Sciences*, **57**(3):255-289.

Ter Braak, C.J.F. 1995b. Ordination. In: Jongman, R.H.G., Ter Braak, C.J.F. & van Tongeren, O.F.R. *Data Analysis in Community and Landscape Ecology*. Cambridge: Cambridge University Press. pp. 91-274.

Thommason, K. 1925. Methoden zur untersuchung der mikrophyton der limnischen litoral und profundalzone. Abderhalden Handbuch der Biologischen Arbeitsmethoden Abt. ix, Teil 2, 1. Berlin.

Tornés, E., Acuña, V., Dahm, C.N. & Sabater, S. 2015. Flood disturbance effects on benthic diatom assemblage structure in a semiarid river network. *Journal of Phycology*, **51**(1):133-143.

Van Vliet, M. & Zwolsman, G. 2008. Impact of summer droughts on the water quality of the Meuse River. *Journal of Hydrology*, **353**(1):1-17.

Vildirim, S. 2020. P value - Explained. https://towardsdatascience.com/p-value-explained-c7f5547c0562. Date of access: 5 March 2022.

Viljoen, M. 2015. The Kruger National Park: Geology and Geomorphology of the Wilderness. In: Grab, S. & Knight, J. eds. *Landscapes and Landofrms of South Africa- An overview*. Cham: Springer. pp. 111-120.

Von Stosch, H.A. 1974. Pleurax, seine synthese und seine verwendung zur einbettung und darstellung det zellwande von diatomeen, peridineen und anderen algen, sowie fur eine neue methode zur electivfarbung von dinoflagellaten-penzern. *Archiv fur Protistenkunde*, **116**:132-141.

Walker, N.D. 1990. Links between South African summer rainfall and temperature variability of the Agulhas and Benguela Current systems. *Journal of Geophysical Research*, **95**(C3):3297-3319.

Wang, J., Jiang, X., Zheng, B., Chen, C., Kang, X., Zhang, C., Song, Z., Wang, K., Wang, W. & Wang, S. 2015. Effect of algal bloom on phosphorus exchange at the sediment-water interface in Meiliang Bay of Taihu Lake, China. *Environmental Earth Sciences*, **75**(1):1-9.

Watanabe, T. 1982. Nurnerical assessment of river pollution based on the water quality chart. *Research Report on Environmental Science*, **B121-R-42-10**:92-95.

Watanabe, T. 1990. Numerical simulation of organic pollution in flowing waters. In: *Encyclopaedia of Environmental Control Technology, Vol 4: Hazardous Waste Containment and Treatment*. Houston: Gulf Publishing Company. pp. 251-281.

Weber, C.I. 1970. A new freshwater centric diatom *Microsiphona potamos* gen. et sp. Nov. *Journal of Phycology*, **6**:149-153.

Werner, D. 1977. Silicate metabolism. In: Werner, D. ed. The Biology of Diatoms. Berkeley: University of California Press. pp. 110-142.

Wilhite, D.A. & Glantz, M.H. 1985. Understanding the drought phenomenon: The role of definitions. *Water International*, **10**(3):111-120.

Williams, G.P. 1989. Sediment concentration versus water discharge during single hydrologic events in rivers. *Journal of Hydrology*, **111**(1-4):89-106.

Zambatis, N. 2003. Determinants of grass production and composition in the Kruger National Park. KwaZulu-Natal: University of Natal. (Dissertation - MSc).

Zelinka, M., Marvan, P. 1961. Zur Präzisierung der biologischen klassifikation der reinheit fließender gewässer. *Hydrobiolgia*, **57**:389-407.

Appendix A: Complete species list

Achnanthes Bory de St. Vincent

Achanthes oblongella Oestrup

Achnanthes subhudsonis (Hustedt) H. Kobayasi

Achnanthidium Kützing

Achnanthidium crassum (Hustedt) Potapova & *Ponader*

Achnanthidium eutrophilum Lange-Bertalot

Achnanthidium exiguum (Grunow) Czarnecki

Achnanthidium macrocephalum (Hust.) Round & Bukhtiyarova

Achnanthidium minutissimum (Kützing) Czarnecki

Achnanthidium saprophilum (Kobayasi et Mayama) Round & Bukhtiyarova

Achnanthidium rivulare Potapova &Ponader

Adlafia Moser Lange-Bertalot & Metzeltin

Amphora Ehrenberg & Kützing

Amphora coffeaeformis (Agardh) Kützing

Amphora fontinalis Hustedt

Amphora montana Krasske

Amphora pediculus (Kützing) Grunow

Amphora veneta Kützing

Anorthoneis dulcis Hein

Bacillaria paradoxa Gmelin

Brachysira vitrea (Grunow) Ross

Caloneis Cleve

Caloneis molaris(Grunow) Krammer

Capartogramma crucicula Grunow) Ross

Cocconeis Ehrenberg

Cocconeis pediculus Ehrenberg

Cocconeis placentula Ehrenberg

Cocconeis placentula var.lineata (Ehr.) Van Heurck

Craticula Grunow

Craticula ambigua (Ehrenberg) Mann

Craticula halophila (Grunow ex Van Heurck) Mann

Cyclotella meneghiniana Kützing

Cymbella Agardh

Cymbella bengalensis Grunow
Cymbella bengaliformis Krammer
Cymbella kappii Cholnoky (Cholnoky)
Cymbella kolbei Hustedt
Cymbella subleptoceros Krammer
Cymbella tumida (Brébisson) Van Heurck
Cymbella turgidula Grunow
Cymbella vulgata Krammer
Diadesmis confervacea Kützing
Diatoma vulgaris Bory
Diploneis Ehrenberg Cleve
Diploneis smithii (Brébisson) Cleve
Discostella pseudostelligera (Hustedt) Houk & Klee
Encyonema Kützing
Encyonema mesianum (Cholnoky) D.G. Mann
Encyonema minutum (Hilse) D.G. Mann
Encyonema ventricosum (Agardh) Grunow
Encyonopsis Krammer
Encyonopsis krammeri Reichardt
Encyonopsis leei var. *sinensis* Metzeltin & Krammer
Eolimna Lange-Bertalot & Schiller
Eolimna minima (Grunow) Lange-Bertalot
Eolimna subminuscula (Manguin) Moser & Lange-Bertalot
Epithemia sorex Kützing
Eunotia Ehrenberg
Eunotia formica Ehrenberg
Eunotia minor (Kützing) Grunow
Fallacia Stickle & Mann
Fallacia insociabilis (Krasske) D.G. Mann
Fallacia pygmaea (Kützing) Stickle & D.G. Mann
Fallacia tenera (Hustedt) D.G. Mann
Fallacia umpatica (Cholnoky) D.G. Mann
Fragilaria Lyngbye
Fragilaria biceps (Kützing) Lange-Bertalot (*Ulnaria*)

Fragilaria capucina Desmazieres
Fragilaria capucina var. *vaucheriae* (Kützing) Lange-Bertalot
Fragilaria dilatata (Brébisson) Lange-Bertalot
Fragilaria parasitica var. *subconstricta* Grunow
Fragilaria ulna var. acus (Kützing) Lange-Bertalot (*Ulnaria*)
Fragilaria ulna var. *acus* (Kützing) Lange-Bertalot abnormal form (*Ulnaria*)
Fragilaria ungeriana Grunow
Geissleria Lange-Bertalot & Metzeltin
Geissleria decussis (Oestrup) Lange-Bertalot & Metzeltin
Gomphonema Ehrenberg
Gomphonema affine Kützing
Gomphonema angustatum (Kützing) Rabenhorst
Gomphonema gracile Ehrenberg
Gomphonema insigne Gregory
Gomphonema lagenula Kützing
Gomphonema laticollum Reichardt
Gomphonema minutum Agardh
Gomphonema parvulum Kützing
Gomphonema pseudoaugur Lange-Bertalot
Gomphonema pumilum var. *rigidum* Reichardt & Lange-Bertalot
Gomphonema venusta Passy, Kociolek & Lowe
Gomphonitzschia ungeri Grunow
Gyrosigma Hassall
Gyrosigma acuminatum (Kützing) Rabenhorst
Gyrosigma attenuatum (Kützing) Rabenhorst
Gyrosigma rautenbachiae Cholnoky
Hantzschia amphioxys (Ehrenberg) Grunow
Hantzschia distinctepunctata Hustedt
Hippodonta Lange-Bertalot, Metzeltin & Witkowski
Hippodonta capitata (Ehrenberg) Lange-Bertalot, Metzeltin & Witkowski
Kolbesia ploenensis (Hustedt) Kingston
Lemnicola hungarica (Grunow) Round & Basson
Luticola D.G. Mann
Luticola goeppertiana (Bleisch) D.G. Mann

Luticola mutica (Kützing) D.G. Mann
Melosira varians Agardh
Navicula Bory de St. Vincent
Navicula antonii Lange-Bertalot
Navicula capitatoradiata Germain
Navicula cryptocephala Kützing
Navicula cryptotenella Lange-Bertalot
Navicula cryptotenelloides Lange-Bertalot
Navicula germainii Wallace
Navicula heimansioides Lange-Bertalot
Navicula microcari Lange-Bertalot
Navicula microlyra Cholnoky
Navicula minima Grunow
Navicula notha Wallace
Navicula radiosa Kützing
Navicula riediana Lange-Bertalot & Rumrich
Navicula rostellata Kützing
Navicula schroeteri Meister
Navicula subminuscula Manguin
Navicula tridentula Krasske
Navicula vandamii Schoeman & Archibald
Navicula veneta Kützing
Navicula viridula (Kützing) Ehrenberg
Navicula zanoni Hustedt
Navicymbulla Krammer
Neidium productum (W.M. Smith) Cleve
Nitzschia Hassall
Nitzschia amphibia Grunow
Nitzschia bulnheimiana (Rabenhorst) H.L.Smith
Nitzschia compressa (J.W. Bailey) Boyer
Nitzschia dissipata (Kützing) Grunow
Nitzschia filiformis (W.M.Smith) Van Heurck
Nitzschia frustulum (Kützing) Grunow
Nitzschia intermedia Hantzsch

Nitzschia lancettula O. Müller
Nitzschia liebetruthii Rabenhorst
Nitzschia linearis (Agardh) W.M. Smith
Nitzschia linearis var. subtilis (Grunow)
Nitzschia microcephala Grunow in Cleve & Moller
Nitzschia obtusa var. *kurzii* (Rabenhorst) Grunow
Nitzschia sigma (Kützing) W.M.Smith
Nitzschia umbonate (Ehrenberg) Lange-Bertalot
Nitzschia valdestriata Aleem & Hustedt
Opephora Petit
Pinnularia Ehrenberg
Pinnularia acrospheria W. Smith
Pinnularia subcapitata f. *divergens* Hustedt
Placoneis Mereschkowsky
Placoneis dicephala (W.Smith) Mereschkowsky
Placoneis placentula (Ehrenberg) Heinzerling
Plagiotropis lepidoptera var. *proboscidea* (Cl.) Reimer
Planothidium Round & Bukhtiyarova
Planothidium minutissimum (Krasske) Lange-Bertalot
Planothidium rostratum (Oestrup) Lange-Bertalot
Pleurosigma salinarum (Grunow) Cleve & Grunow
Pleurosira laevis (Ehrenberg)
Psammothidium Bukhtiyarova & Round
Pseudostaurosira parasitica var. *subconstricta* (Grunow) Morales
Reimeria sinuata (Gregory) Kociolek & Stoermer
Reimeria uniseriata Sala, Guerrero & Ferrario
Rhoicosphenia abbreviata (Agardh) Lange-Bertalot
Rhopalodia Müller
Rhopalodia gibba (Ehrenberg) O. Müller
Rhopalodia gibberula (Ehrenberg) O. Müller
Rhopalodia operculata (Agardh) Håkansson
Sellaphora Mereschkowsky
Sellaphora mutatoides Lange-Bertalot & Metzeltin
Sellaphora nyassensis (O. Müller) D.G. Mann

Sellaphora pupula (Kützing) Mereschkowksy

Sellaphora seminulum (Grunow) D.G. Mann

Sellaphora stroemii (Hustedt) D.G. Mann

Seminavis D.G. Mann

Seminavis strigosa (Hustedt) Danieledis & Economou-Amilli

Stauroneis Ehrenberg

Stauroneis anceps Ehrenberg

Surirella Turpin

Surirella angusta Kützing

Surirella robusta Ehrenberg

Tabularia Williams & Round

Tabularia fasciculata (Agardh) Williams & Round

Thalassiosira weissflogii (Grunow) Fryxell & Hasle

Tryblionella Smith

Tryblionella apiculata Gregory

Tryblionella coarctata (Grunow) D.G. Mann

Tryblionella littoralis (Grunow) D.G. Mann

Tryblionella victoriae Grunow

Ulnaria Compère

Appendix B: Micrographs

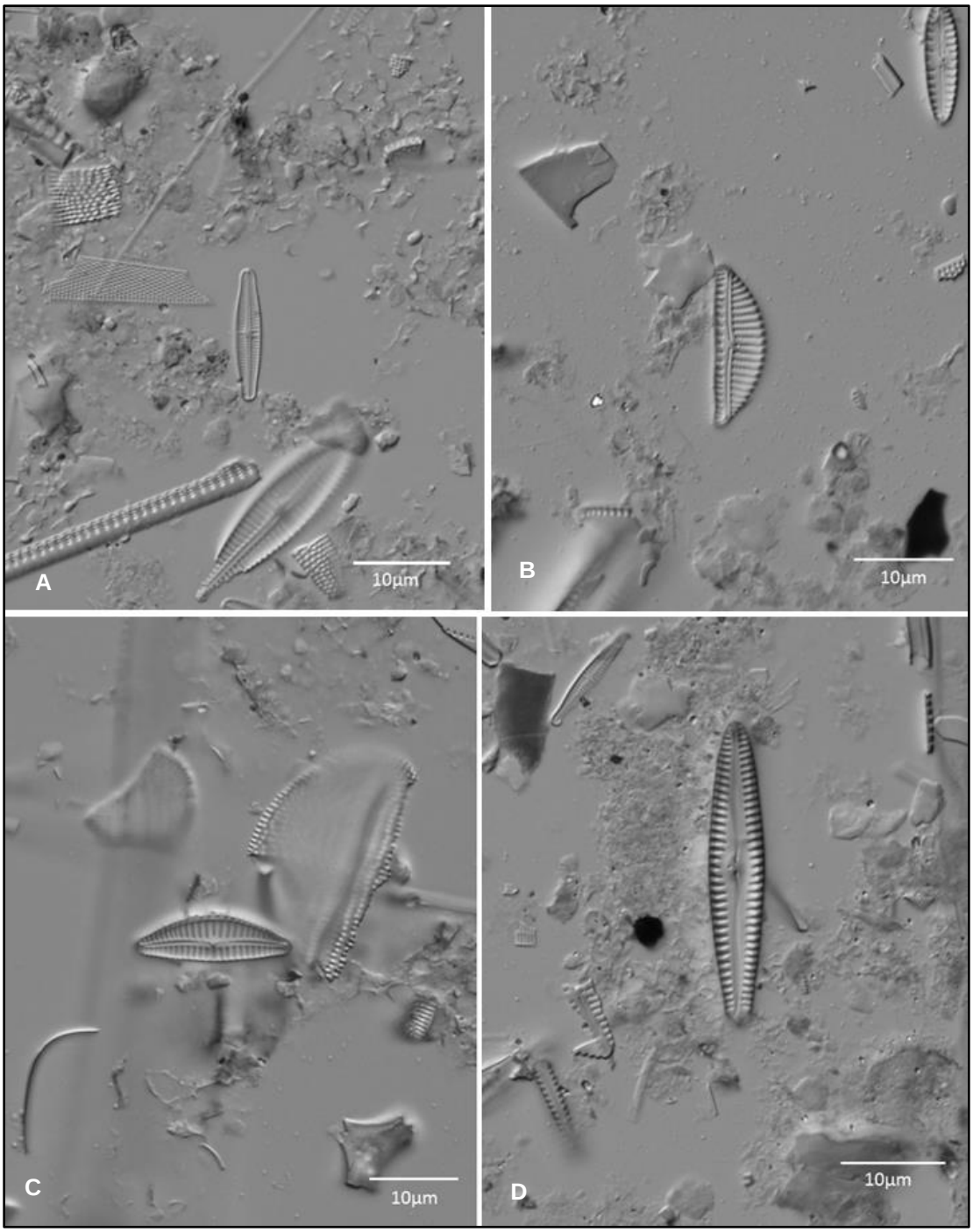

Figure 59: Common oligotrophic species found across all years and sites. A – D. Valve view of cleaned material. **A** - *Achnanthidium minutissimum*. **B** – *Encyonema minutum*. **C** – *Cymbella kolbei*. **D** – *Gomphonema venusta.*

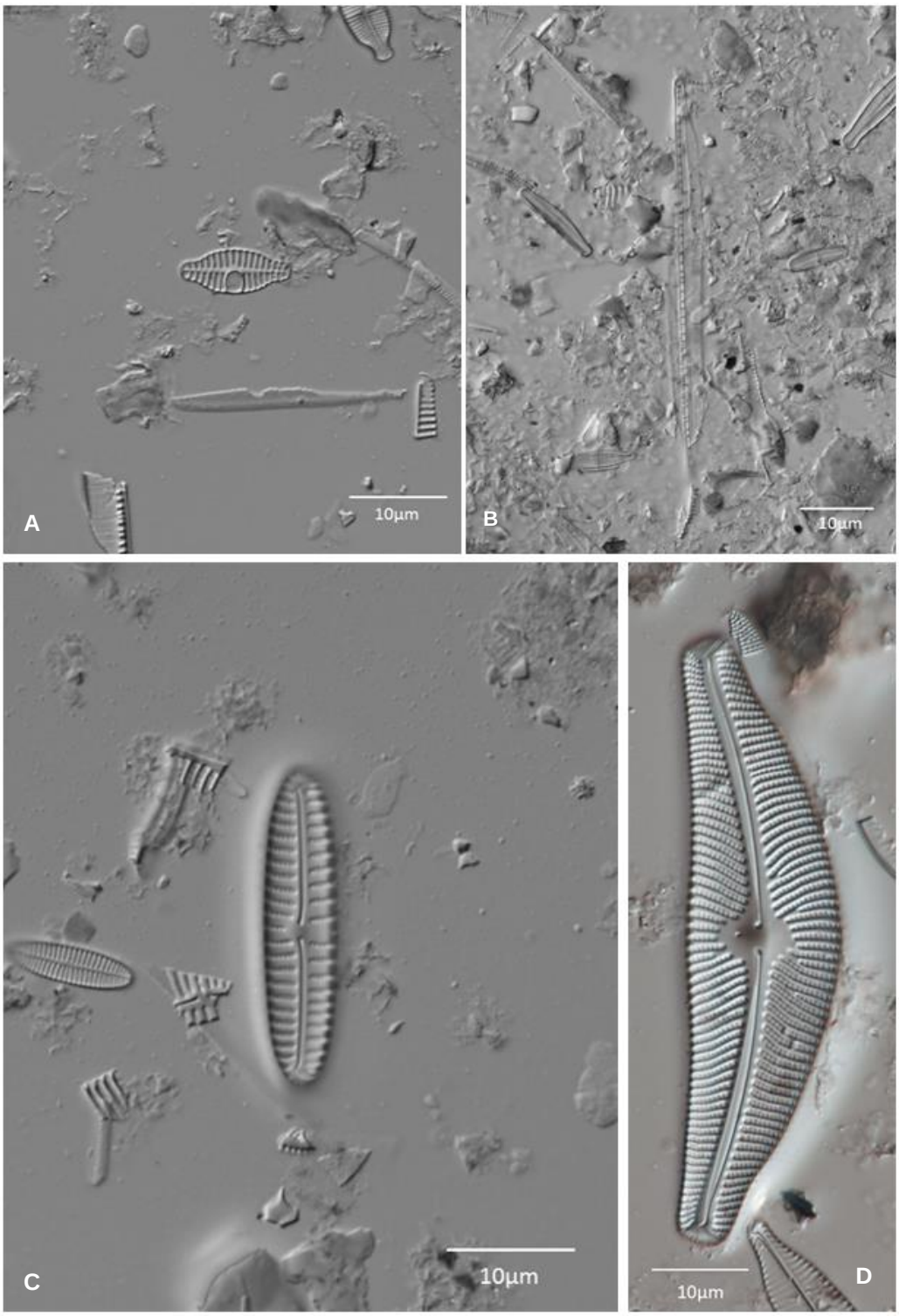

Figure 60: Common oligo- mesotrophic species found across all years and sites. A – D. Valve view of cleaned material. **A** – *Planothidium rostratum*. **B** – *Nitzschia dissipata*. **C** – *Encyonopsis leei* var. *sinensis.* **D** – *Cymbella tumida.*

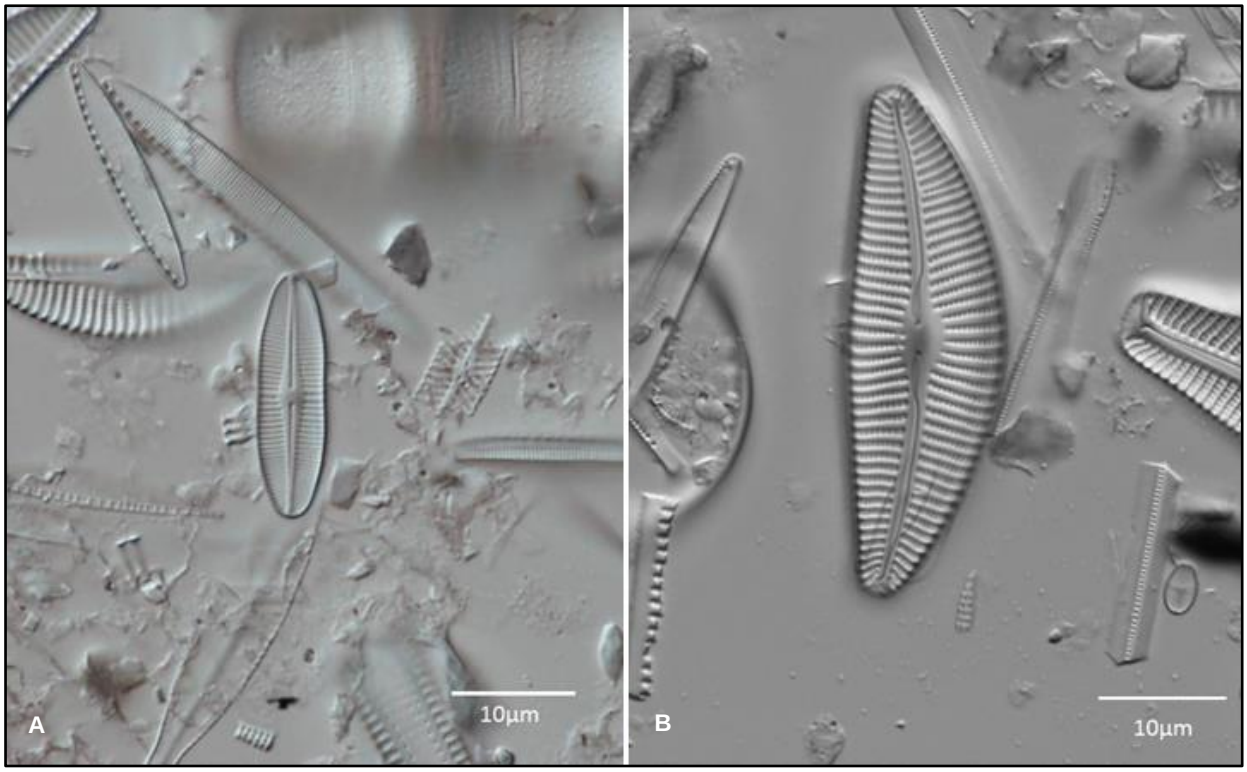

Figure 61: More common oligo- mesotrophic species found across all years and sites. A – B. Valve view of cleaned material. **A** – *Achnanthidium crassum*. **B** – *Cymbella turgidula*.

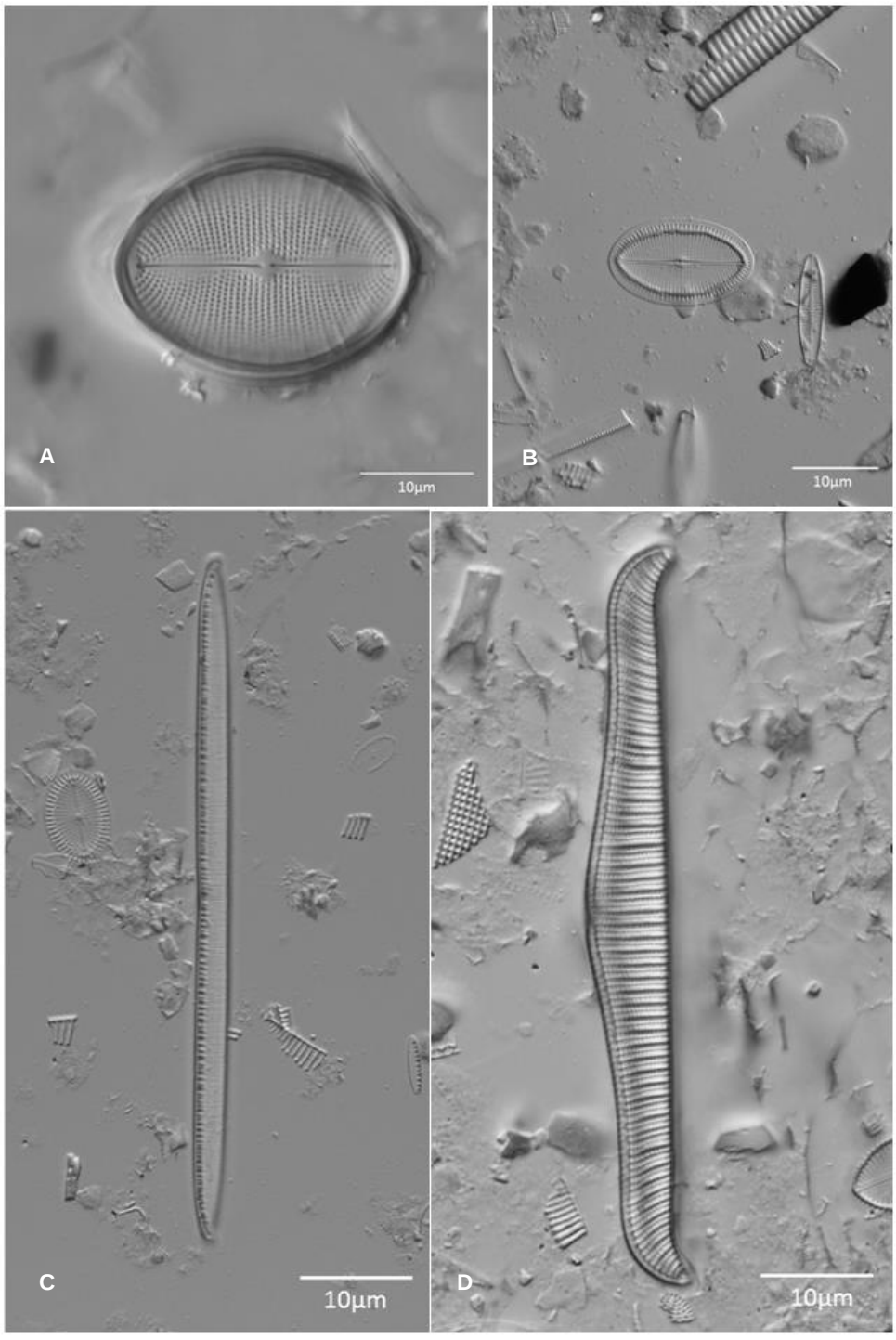

Figure 62: Common meso- to eutrophic species found across all years and sites. A – D. Valve view of cleaned material. **A** – *Cocconeis pediculus*. **B** – *Cocconeis placentula*. **C** – *Nitzschia linearis.* **D** – *Rhopalodia gibba.*

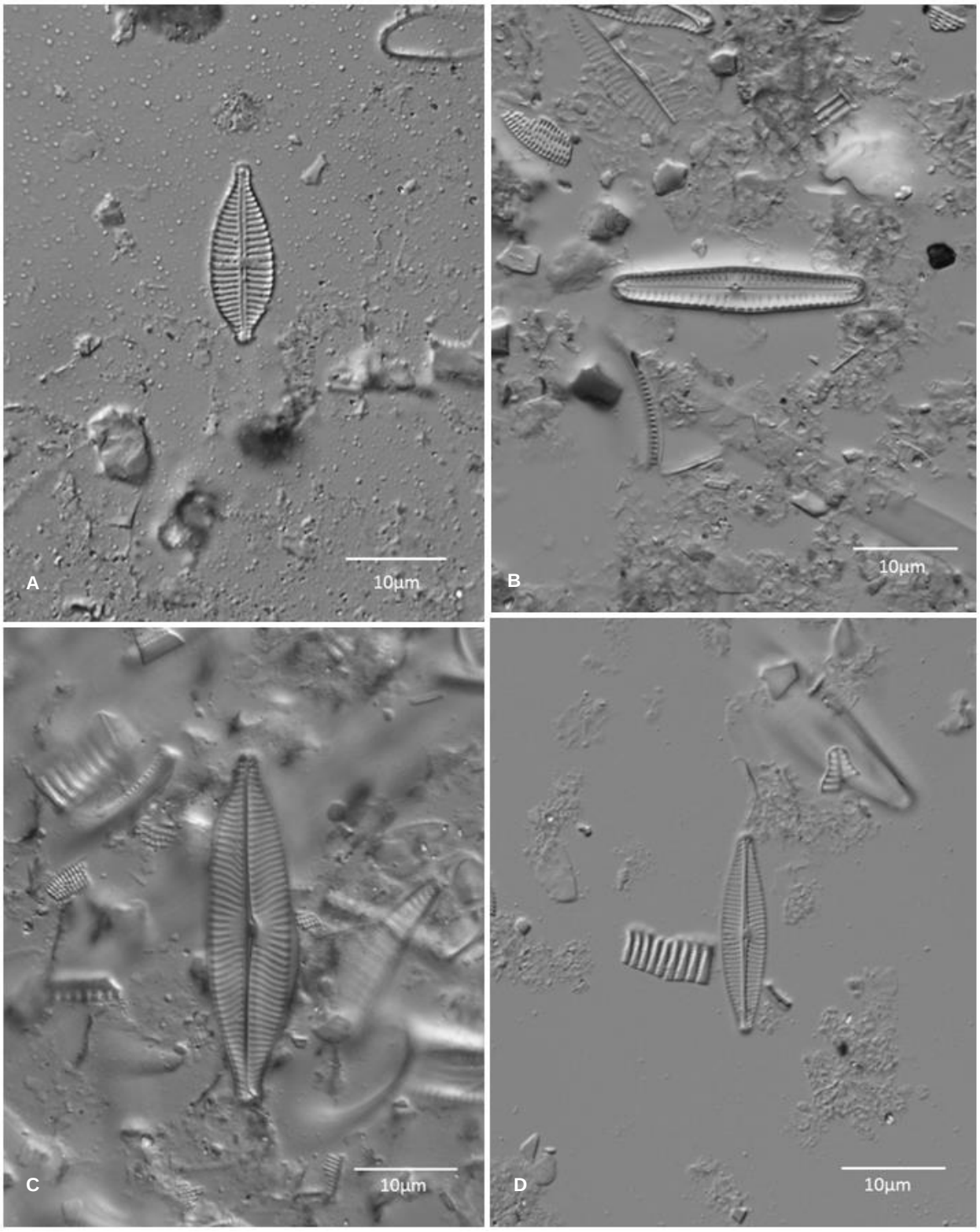

Figure 63: Common eutrophic species found across all years and sites. A – D. Valve view of cleaned material. **A** – *Gomphonema parvulum* var. *lagenula*. **B** – *Gomphonema pumilum* var. *rigidum*. **C** – *Navicula rostellata.* **D** – *Navicula vandamii.*

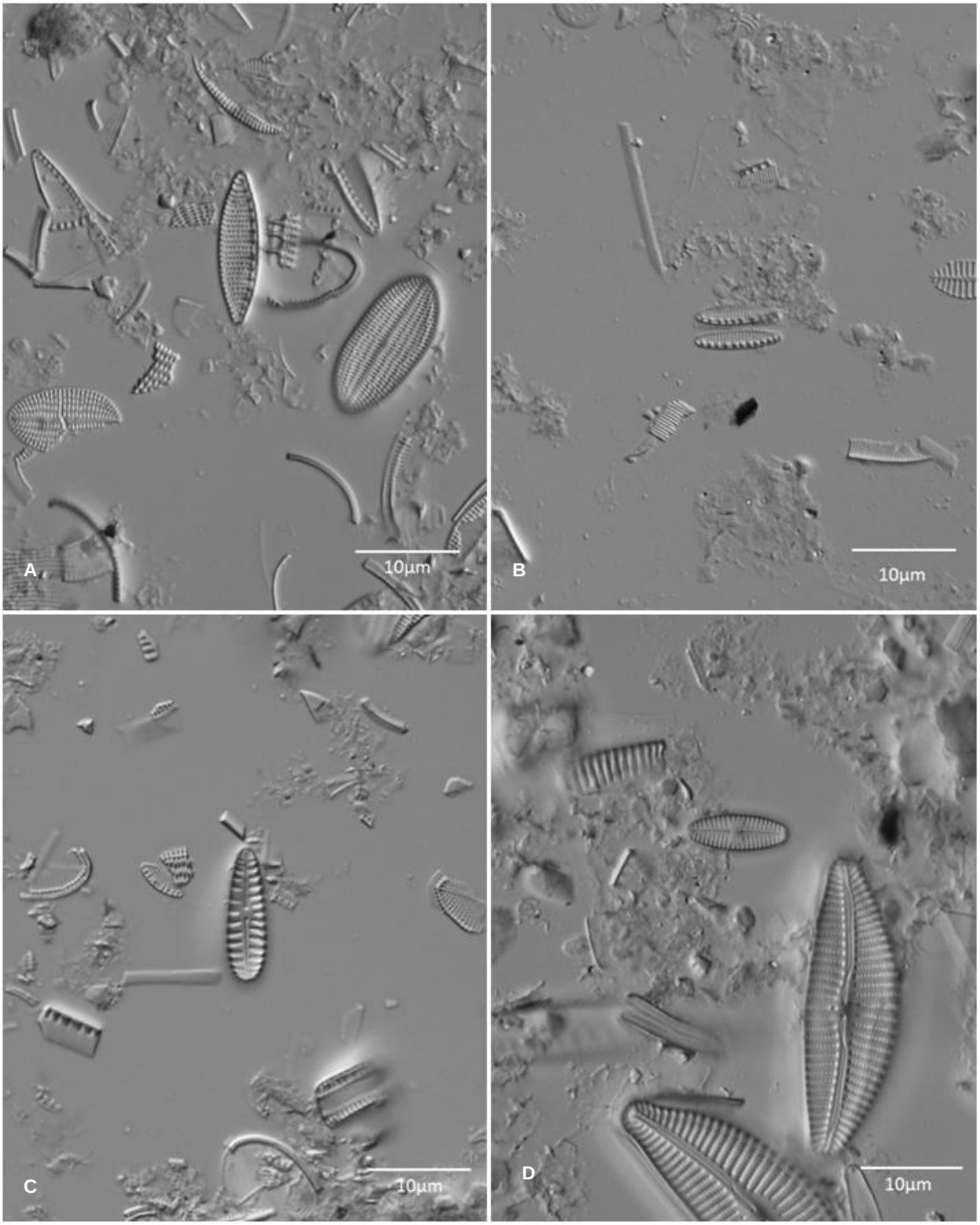

Figure 64: Common eutrophic species found across all years and sites. A – D. Valve view of cleaned material. A – *Nitzschia amphibia*. B – *Nitzschia frustulum*. C – *Rhoicosphenia abbreviata*. D – *Sellaphora seminulum*.

Appendix C: Diatom counts (five most abundant taxa)

Table 10: Top five most abundant diatom taxa corresponding to counts for all sites across all years sampled, Luvuvhu River.

Luvuvhu															
2018				2019				2020				2021			
Site Name	Species	Count	%	Site Name	Species	Count	%	Site Name	Species	Count	%	Site Name	Species	Count	%
Dongadzhiva	*Achnanthidium* spp.	154	39	Dongadzhiva	*Achnanthidium* spp.	150	38	Dongadzhiva	*Achnanthidim* spp.	196	49	Dongadzhiva	***Achnanthidium minutissimum***	**248**	**62**
	Encyonopsis leei var. *sinensis*	72	18,0		*Encyonopsis leei* var. *sinensis*	50	13		*Achnanthidium minutissimum*	59	15		*Achnanthidium* spp.	53	13
	Fragilaria sp.	42	11		*Encyonopsis krammeri*	48	12,0		*Navicula* spp.	35	9		*Encyonopsis leei* var. *sinensis*	19	5
	Encyonopsis krammeri	21	5		*Brachysira vitrea*	46	12		*Brachysira vitrea*	21	5		*Cymbella kappii*	16	4
	Gomphonema venusta	19	5		*Navicula* sp.	38	10		*Encyonopsis leei* var. *sinensis*	7	2		*Gomphonema venusta*	13	3
Xindzivhani	*Achnanthidium* spp.	182	45	Xindzivhani	*Achnanthidium* spp.	131	33	Xindzivhani	*Cocconeis placentula*	75	19	Xindzivhani	*Achnanthidium minutissimum*	165	41
	Fragilaria sp.	66	16		*Cymbella turgidula*	107	26,8		*Achnanthidium* spp.	58	15		*Achnanthidium* spp.	118	29
	Gomphonema venusta	32	8		*Encyonopsis leei* var. *sinensis*	68	17		*Achnanthidium minutissimum*	50	13		*Fragilaria capucina*	22	5
	Encyonopsis leei var. *sinensis*	31	7,7		*Achnanthidium rivulare*	24	6		*Gomphonema venusta*	35	9		*Encyonopsis leei* var. *sinensis*	21	5
	Tabularia faciculata	18	4		*Encyonopsis krammeri*	18	5		*Navicula zanonii*	16	4		*Gomphonema* sp.	16	4
Mutale (Outpost)	*Navicula* spp.	110	28	Mutale (Outpost)	*Cocconeis placentula*	121	30	Mutale (Outpost)	*Cocconeis pediculus*	68	17	Mutale (Outpost)	***Cocconeis placentula***	**215**	**54**
	Fragilaria spp.	77	19		*Achnanthidium* spp.	74	18		*Cocconeis placentula*	66	17		*Achnanthidium* sp.	44	11
	Cymbella turgidula	54	13,6		*Nitzschia* spp.	24	6		*Achnanthidium* spp.	60	15		*Achnanthes* sp.	19	5
	Nitzschia spp.	42	11		*Navicula cryptotenella*	23	5,7		*Cocconeis placentula* var. *lineata*	28	7		*Gomphonema pumilum* var. *rigidum*	19	5
	Cocconeis placentula	21	5		*Fragilaria biceps*	21	5		*Gomphonitzschia ungeri*	24	6		*Gomphonema venusta*	16	4
Bobomane	*Tabularia fasciculata*	64	16,0	Bobomane	*Geissleria decussis*	49	12,3	Xindzivhani (Rapids)	*Achnanthidium minutissimum*	181	45	Bobomane	*N/A*	N/A	N/A
	Cocconeis placentula	37	9,2		*Cocconeis placentula*	48	12,0		*Encyonopsis leei* var. *sinensis*	49	12		*N/A*	N/A	N/A
	Nitzschia frustulum	30	7,5		*Cymbella kolbei*	36	9,0		*Achnanthidium* spp.	33	8		*N/A*	N/A	N/A
	Anorthoneis dulcis	29	7,2		*Nitzschia* spp.	35	8,8		*Fragilaria capucina*	21	5		*N/A*	N/A	N/A
	Achnanthidium saprophilum	27	6,7		*Planothidium rostratum*	25	6,3		*Fragilaria capucina* var. *vaucheriae*	15	4		*N/A*	N/A	N/A

Table 11: Top five most abundant diatom taxa corresponding to counts for all sites across all years sampled, Letaba River.

LETABA															
2018				2019				2020				2021			
Site Name	Species	Count	%	Site Name	Species	Count	%	Site Name	Species	Count	%	Site Name	Species	Count	%
Lonely Bull	*Nitzschia* spp.	293	73	Lonely Bull	***Cocconeis placentula***	**293**	**73**	Lonely Bull (Pool)	***Cocconeis placentula***	**202**	**51**	Lonely Bull	***Cocconeis placentula***	**324**	**81**
	Cocconeis placentula	41	10,2		*Nitzschia* spp.	64	16		*Tabularia fasciculata*	83	21		*Nitzschia* spp.	23	6
	Tabularia fasciculata	40	10		*Encyonopsis leei* var. *sinensis*	10	2,5		*Nitzschia* spp.	30	8		*Gomphonema parvulum*	14	3
	Anorthoneis dulcis	8	2		*Kolbesia ploenensis*	9	2		*Gomphonema parvulum*	16	4		*Navicula rostellata*	7	2
	Gomphonema parvulum	4	1		*Tabularia fasciculata*	8	2		*Kolbesia ploenensis*	16	4,0		*Anorthoneis dulcis*	4	1
Klipkoppies	*Cymbella turgidula*	91	22,8	Klipkoppies	*Cocconeis placentula*	358	88,0	Lonely Bull (Rapids)	***Cocconeis placentula***	**216**	**54**	Klipkoppies	***Cocconeis placentula***	**368**	**92**
	Nitzschia spp.	83	20,8		*Nitzschia* spp.	14	3,4		*Gomphonema parvulum*	52	13		*Nitzschia* spp.	11	3
	Navicula cryptotenella	37	9,3		*Kolbesia ploenensis*	8	2,0		*Tabularia fasciculata*	44	11		*Gomphonema parvulum*	7	2
	Rhopalodia gibba	30	7,5		*Hippodonta* sp.	5	1,2		*Rhopalodia gibba*	27	6,8		*Cocconeis pediculus*	3	1
	Navicula veneta	21	5,3		*Rhopalodia gibba*	3	0,7		*Fragilaria ulna*	15	4		*Gomphonema venusta*	3	1
Confluence	*Epithemia sorex*	235	58,5	Confluence	*Nitzschia* spp.	367	91,3	Lonely Bull (Run)	*Cocconeis placentula*	128	32	Confluence	***Cocconeis placentula***	**211**	**53**
	Cocconeis placentula	48	11,9		*Gomphonema parvulum*	13	3,2		*Nitzschia* spp.	63	16		*Kolbesia ploenensis*	64	16
	Nitzschia spp.	42	10,4		*Cocconeis pediculus*	9	2,2		*Rhopalodia gibba*	56	14		*Nitzschia* spp.	34	9
	Achnanthidium saprophilum	30	7,5		*Cocconeis placentula*	8	2,0		*Epithemia sorex*	45	11		*Nitzschia amphibia*	22	6
	Rhopalodia gibba	18	4,5		*Hippodonta* sp.	3	0,7		*Gomphonema parvulum*	28	7,0		*Sellaphora seminulum*	12	3

Table 12: Top five most abundant diatom taxa corresponding to counts for all sites across all years sampled, Olifants River.

OLIFANTS															
2018				2019				2020				2021			
Site Name	Species	Count	%	Site Name	Species	Count	%	Site Name	Species	Count	%	Site Name	Species	Count	%
Mamba	*Nitzschia* spp.	307	76,2	Mamba	*Cocconeis placentula*	158	39,5	Mamba	*N/A*	N/A	N/A	Mamba	***Nitzschia* spp.**	**321**	**80**
	Navicula spp.	48	11,9		*Nitzschia frustulum*	113	28,3		*N/A*	N/A	N/A		*Gomphonema* spp.	23	6
	Navicula cryptotenelloides	19	4,7		*Nitzschia* spp.	34	8,5		*N/A*	N/A	N/A		*Achnanthidium* spp.	15	4
	Rhoicosphenia abbreviata	11	2,7		*Cocconeis pediculus*	21	5,3		*N/A*	N/A	N/A		*Cocconeis placentula*	10	3
	Cocconeis placentula	4	1,0		*Nitzschia dicompressa*	17	4,3		*N/A*	N/A	N/A		*Navicula rostellata*	9	2
Balule	*Nitzschia* spp.	121	30,0	Balule	*Nitzschia frustulum*	191	47,0	Balule	*N/A*	N/A	N/A	Balule	***Nitzschia* spp.**	**305**	**76**
	Cocconeis placentula	120	29,8		*Nitzschia* spp.	131	32,3		*N/A*	N/A	N/A		*Gomphonema* spp.	28	7
	Hippodonta sp.	57	14,1		*Cocconeis placentula*	19	4,7		*N/A*	N/A	N/A		*Cocconies placentula*	12	3
	Navicula spp.	21	5,2		*Tabularia fasciculata*	15	3,7		*N/A*	N/A	N/A		*Hippodonta* sp.	10	2
	Kolbesia ploenensis	17	4,2		*Cocconeis pediculus*	10	2,5		*N/A*	N/A	N/A		*Achnanthidium* sp.	5	1
Confluence	*Cocconeis placentula*	281	69,7	Confluence	*Epithemia sorex*	139	34,7	Confluence	*N/A*	N/A	N/A	Confluence	*Nitzschia* spp.	119	30
	Cocconeis pediculus	42	10,4		*Nitzschia frustulum*	92	22,9		*N/A*	N/A	N/A		*Cocconies placentula*	103	26
	Rhoicosphenia abbreviata	40	9,9		*Cocconeis placentula*	42	10,5		*N/A*	N/A	N/A		*Achnanthidium* sp.	59	15
	Nitzschia spp.	5	1,2		*Cocconeis pediculus*	30	7,5		*N/A*	N/A	N/A		*Cocconeis pediculus*	56	14
	Nitzschia frustulum	5	1,2		*Rhopalodia operculata*	26	6,5		*N/A*	N/A	N/A		*Gomphonema* spp.	29	7

Table 13: Top five most abundant diatom taxa corresponding to counts for all sites across all years sampled, Sabie River.

SABIE															
2018				2019				2020				2021			
Site Name	*Species*	Count	%	Site Name	Species	Count	%	Site Name	Species	Count	%	Site Name	Species	Count	%
Sekorongwane	*Nitzschia* spp.	179	45	Sekorongwane	***Nitzschia* spp.**	**209**	**52**	Sekorongwane (Rapids)	*Nitzschia* spp.	126	32	Sekorongwane	*Achnanthidium crassum*	133	33
	Gomphonema spp.	61	15,2		*Encyonopsis leei* var. *sinensis*	44	11		*Melosira varians*	81	20		*Navicula* spp.	48	12
	Nitzschia frustulum	30	7		*Achnanthidium rivulare*	35	8,8		*Encyonema minutum*	46	12		*Achnanthidium* spp.	31	8
	Achnanthidium spp.	24	6		*Cymbella turgidula*	19	5		*Achnanthidium* spp.	41	10		*Navicula vandamii*	27	7
	Ulnaria nyanse	18	4		*Navicula* spp.	16	4		*Cymbella turgidula*	24	6		*Nitzschia* spp.	23	6
Tinga	*Navicula* spp.	58	14,5	Tinga	*Encyonopsis leei var. sinensis*	91	22,75	Sekorongwane (Run)	*Nitzschia* spp.	156	39	Tinga	*Achnanthidium* spp.	134	33
	Cymbella turgidula	57	14,25		*Navicula* spp.	77	19,25		*Navicula* spp.	36	9		*Encyonopsis leei* var. *sinensis*	77	19
	Achnanthidium spp.	54	13,5		*Achnanthidium* spp.	57	14,25		*Encyonema minutum*	33	8		*Achnanthidium minutissimum*	59	15
	Planothidium rostratum	42	10,5		*Planothidium rostratum*	50	12,5		*Cymbella turgidula*	26	7		*Cymbella turgidula*	30	7
	Encyonopsis leei var. sinensis	36	9		*Cocconeis placentula*	21	5,25		*Achnanthidium* spp.	24	6		*Achnanthidium crassum*	15	4
Sand	*Anorthoneis dulcis*	219	54,1	Sand	N/A	N/A	N/A	Tinga	N/A	N/A	N/A	Sand	*Nitzschia* spp.	93	23
	Cocconeis placentula	56	13,8		N/A	N/A	N/A		N/A	N/A	N/A		*Anorthoneis dulcis*	84	21
	Nitzschia frustulum	24	5,9		N/A	N/A	N/A		N/A	N/A	N/A		*Cocconeis placentula*	33	8
	Gomphonema venusta	22	5,4		N/A	N/A	N/A		N/A	N/A	N/A		*Planothidium* sp.	20	5
	Planothidium rostratum	18	4,4		N/A	N/A	N/A		N/A	N/A	N/A		*Cymbella turgidula*	17	4
Lubye Lubye	*Encyonopsis leei* var. *sinensis*	113	28,2	Lubye Lubye	*Cymbella kolbei*	126	31,0	Lubye Lubye	N/A	N/A	N/A	Lubye Lubye	*Achanthidium crassum*	98	25
	Navicula microlyra	54	13,5		*Encyonopsis leei* var. *sinensis*	89	21,9		N/A	N/A	N/A		*Achnanthidium minutissimum*	77	19
	Nitzschia frustulum	49	12,2		*Nitzschia frustulum*	41	10,1		N/A	N/A	N/A		*Achanthidium* spp.	74	19
	Cymbella turgidula	43	10,7		*Cymbella turgidula*	35	8,6		N/A	N/A	N/A		*Encyonopsis leei* var. *sinensis*	40	10
	Fallacia umpatica	23	5,7		*Navicula microlyra*	31	7,6		N/A	N/A	N/A		*Cymbella turgidula*	27	7
Antholysta	*Encyonopsis leei* var. *sinensis*	86	21	Antholysta	*Encyonopsis leei* var. *sinensis*	112	28,1	Antholysta	*Achnanthidium minutissimum*	84	21	Antholysta	*Cymbella turgidula*	82	21
	Achnanthidium spp.	64	16		*Achnanthidium* spp.	81	20		*Ulnaria nyanse*	51	13		*Encyonopsis leei* var. *sinensis*	57	14
	Cymbella tumida	57	14		*Navicula microlyra*	51	13		*Cymbella turgidula*	44	11		*Cocconeis placentula*	38	10
	Cymbella turgidula	57	14		*Cymbella turgidula*	44	11		*Achnanthidium crassum*	35	9		*Cymbella* sp.	36	9
	Navicula spp.	29	7,1		*Cymbella tumida*	30	7		*Achnanthidim* spp.	33	8		*Cymbella tumida*	29	7
Sabiepoort	*Nitzschia* spp.	323	80,3	Sabiepoort	*Nitzschia* spp.	264	65,8	Sabiepoort	N/A	N/A	N/A	Sabiepoort	*Sellaphora seminulum*	149	37
	Nitzschia frustulum	31	7,7		*Gomphonema lagenula*	40	10,0		N/A	N/A	N/A		*Nitzschia dissipata*	38	10
	Gomphonema lagenula	23	5,7		*Cocconeis placentula*	26	6,5		N/A	N/A	N/A		*Cocconeis placentula*	35	9
	Gomphonema parvulum	4	1,0		*Nitzschia frustulum*	16	4,0		N/A	N/A	N/A		*Navicula rostellata*	28	7
	Navicula heimansioides	3	0,7		*Encyonema minutum*	14	3,5		N/A	N/A	N/A		*Planothidium rostratum*	18	4

Table 14: Top five most abundant diatom taxa corresponding to counts for all sites across all years sampled, Crocodile River.

CROCODILE															
2018				2019				2020				2021			
Site Name	Species	Count	%	Site Name	Species	Count	%	Site Name	Species	Count	%	Site Name	Species	Count	%
Nsikazi	*Cocconeis placentula*	268	66,0	Nsikazi	*Nitzschia* spp.	119	29,7	Nsikazi	*N/A*	N/A	N/A	Nsikazi	*N/A*	N/A	N/A
	Nitzschia spp.	44	10,8		*Cocconeis placentula*	99	24,7		*N/A*	N/A	N/A		*N/A*	N/A	N/A
	Gomphonema minutum	41	10,1		*Rhoicosphenia abbreviata*	86	21,4		*N/A*	N/A	N/A		*N/A*	N/A	N/A
	Geissleria decussis	12	3,0		*Nitzschia linearis*	35	8,7		*N/A*	N/A	N/A		*N/A*	N/A	N/A
	Navicula cryptotenella	9	2,2		*Navicula cryptotenella*	20	5,0		*N/A*	N/A	N/A		*N/A*	N/A	N/A
Malelane	*Cocconeis placentula*	206	51,2	Malelane	*Cocconeis placentula*	342	82,8	Malelane	*N/A*	N/A	N/A	Malelane	*Cocconeis placentula*	249	62
	Nitzschia spp.	45	11,2		*Nitzschia* spp.	19	4,6		*N/A*	N/A	N/A		*Nitzschia* spp.	85	21
	Eolimna subminuscula	38	9,5		*Encyonopsis leei* var. *sinensis*	11	2,7		*N/A*	N/A	N/A		*Eolimna subminuscula*	26	7
	Gomphonema venusta	30	7,5		*Navicula veneta*	9	2,2		*N/A*	N/A	N/A		*Nitzschia amphibia*	18	5
	Eolimna minima	18	4,5		*Navicula microlyra*	7	1,7		*N/A*	N/A	N/A		*Gomphonema* spp.	8	2
Marula	*Nitzschia* spp.	175	44	Marula	*Cocconeis placentula*	203	51	Marula	*Cocconeis placentula*	364	91	Marula	*Cocconeis placentula*	217	54
	Cocconeis placentula	111	28		*Nitzschia* spp.	52	13		*Gomphonema minutum*	8	2		*Gomphonema*	149	37
	Gomphonema pumilum var. *rigidum*	25	6,4		*Gomphonema venusta*	39	10		*Achnanthidium minutissimum*	5	1,3		*Nitzschia* spp.	22	6
	Navicula viridula	13	3		*Navicula cryptotenelloides*	21	5,2		*Gomphonema pumulum* var. *rigidum*	4	1		*Achnanthidium* spp.	3	1
	Navicula schroeteri	10	2		*Nitzschia amphibia*	15	4		*Kolbesia ploenensis*	4	1		*Navicula schroeteri*	3	1
Nkongoma	*Cocconeis placentula*	245	60,9	Nkongoma	*Cocconeis plecentula*	222	55,4	Nkongoma	*N/A*	N/A	N/A	Nkongoma	*Cocconeis placentula*	197	49
	Anorthoneis dulcis	19	4,7		*Nitzschia* spp.	33	8,2		*N/A*	N/A	N/A		*Anorthoneis dulcis*	86	21
	Gomphonema pumilum var. *rigidum*	17	4,2		*Gomphonema minutum*	32	8,0		*N/A*	N/A	N/A		*Coccoceis pediculus*	26	6
	Nitzschia spp.	17	4,2		*Gomphonema parvulum*	16	4,0		*N/A*	N/A	N/A		*Gomphonema* spp.	21	5
	Navicula vandamii	15	3,7		*Fragilaria biceps*	15	3,7		*N/A*	N/A	N/A		*Nitzschia amphibia*	21	5